Effect of lyophilizate collapse on the stability of protein biopharmaceuticals

Timothy McCoy

University of Limerick
Ollscoil Luimnigh

Effect of Lyophilizate Collapse on the Stability of Protein Biopharmaceuticals

A thesis submitted to the University of Limerick for the degree of Master of Science

By
Timothy R. McCoy

Supervisors
Prof J. Tony Pembroke and Dr Seamus McMonagle

Department of Chemical and Environmental Sciences
University of Limerick

May 2011

DECLARATION

This thesis is a presentation of my original research work. Wherever contributions of others are involved, every effort is made to indicate this clearly, with due reference to the literature and acknowledgement of collaborative research and discussions.

The work was completed under the guidance of Professor J Tony Pembroke and Dr Seamus McMonagle, at the University of Limerick, Ireland, along with Dr. Serguei Tchessalov of Pfizer.

Signed,

_____

Timothy McCoy

In my capacity as supervisor of this candidate's thesis, I certify that the above statements are true to the best of my knowledge.

Signed,

_____

Professor Tony Pembroke

_____

Dr. Seamus McMonagle

TABLE OF CONTENTS

ABSTRACT

Thesis Title: Effect of Lyophilizate Collapse on the Stability of Protein Biopharmaceuticals

Author: Timothy R. McCoy

In recent years, freeze drying of protein preparations above the collapse temperature of amorphous or partially amorphous formulations has been the subject of great interest (Leukel et al. 1998. Effects of Formulation and Process Variables on the Aggregation of Interleukin-6 (IL-6) after Lyophilization and on Storage, Pharm. Dev. Technol., 3(3): 337-346; Pikal, M.J., Shah, S. 1990. The collapse temperature in freeze-drying: dependence on measurement methodology and rate of water removal from the glassy phase. Int. J. Pharm., 62: 165-168; Wang, D.Q. et al., 2003. Effect of Collapse on the Stability of Freeze-Dried Recombinant Factor VIII and α-Amylase. J. Pharm. Sci., 93(5): 1253-1263; Passot, S. et al. 2007. Effect of Product Temperature during Primary Drying on the Long-Term Stability of Lyophilized Proteins. Pharm. Dev. Technol., 12(6): 543-533; Schersch K. et. al. 2010. Systematic Investigation of the effect of Lyophilizate Collapse on Pharmaceutically Relevant Proteins I: Stability after Freeze Drying. J. Pharm. Sci., 99(5): 2256-2277). It is understood that freeze drying in this way would generally result in shorter freeze drying cycles and therefore significant savings in operating costs.

Freeze drying protein preparations above and below the critical temperature was assessed using two model proteins made up of either a mannitol or glycine based formulation in the presence of a variety of other excipients, such as sucrose and NaCl. All bulking agents were crystallized using an annealing step during freezing, as crystalline bulking agents are known to act as structural supports in lyophilized cake during the primary drying step (Shalaev, E. Y.; Franks, F. 1996. Changes in the physical state of model mixtures during freezing and drying: Impact on product quality. Cryobiology. 33: 14-26). Protein X (150kDa proprietary biopharmaceutical) was lyophilized using only a mannitol based formulation while Protein B (Fraction V BSA, 66kDa) was lyophilized in conjunction with one of four formulations which were either mannitol or glycine based.

It was found that freeze drying above the critical temperature resulted in a maximum 7 fold improvement in the degradation (aggregation) rate of BSA when freeze dried in a glycine: sucrose (4%w/v :1%w/v) based buffer and stored for 6 months at 25°C and 60% relative humidity or at 40°C and 75% relative humidity. Other formulations provided varied results and the improvement in protein degradation seemed to be a function of excipient choice when dried below or above the critical temperature of the formulation. Formulations with mannitol: sucrose (4%w/v: 1%w/v) and NaCl seemed to experience improved degradation rates when dried above collapse than when using mannitol alone. Proprietary protein X with a mannitol: sucrose (4%w/v: 1%w/v) based formulation showed comparable degradation (aggregation) rates when dried below and above collapse. It was found that choice of excipients was a key factor in the ability of a protein formulation to dry above the collapse temperature without negatively affecting stability. Overall, the use of glycine: sucrose (4%w/v: 1%w/v) combination as excipients resulted in improved protein stability when dried above the collapse temperature and the presence of sodium chloride also was found to be a factor.

ACKNOWLEDGMENTS

Thank you to my wife Claire and my son Timothy. This has been a long time coming. Thank you to my parents and my sisters for their support throughout my years spent in education.

Thank you to Professor Tony Pembroke and Dr. Seamus McMonagle for their fruitful discussions, and reviews enabling me to get the thesis to this stage. Thanks for the advice and help over the years.

Thanks to Dr. Serguei Tchessalov, who is responsible for a lot of what I know today, for helping me to understand the science of freeze drying and to develop the ability to understand and critically analyze literature and think independently.

Thanks to the staff at Wyeth (Pfizer), many of whom were involved in this project to different extents and include - James Pierce, Steve Raso, Wyeth Grange Castle Analytical Development, Wyeth Grange Castle Process Development, Enda Moran, Jim Roycroft, Michael Jordan, Padraig Landers, Nick Warne and Brendan Hughes.

Thanks you also to Dr. Abina Crean, UCC Pharmacy Department for support and for the provision of the CD instrument enabling me to analyze the protein tertiary structure for all freeze dried formulations.

GLOSSARY

N_{vials}	Number of vials
$T_{product}$	Product temperature (typically measured just above the vial bottom), K
ΔE	Activation Energy
$P_{chamber}$	Chamber pressure, Torr
ρ_{frozen}	Density of frozen material, g/cm^3
$\rho_{solution}$	Density of solution, g/cm^3
R_i	Dry cake resistance at given cycle time, Torr*hr* cm^2/g
S_{out}	External surface of vial, cm^2
d_{out}	External vial diameter, cm
h_{frozen}	Frozen cake height, cm
R	Gas Constant
t_i	Given period of sublimation process time, s
$\frac{dQ}{dt}$	Heat flux from the shelf to the product, cal/s
h_{dry}	Height of dry layer, cm
M_{ice}	Ice mass, g
S_{in}	Internal surface of vial, cm^2
d_{in}	Internal vial diameter, cm
A	Pre-exponential factor (prefactor)
$P_{sublsurf}$	Pressure of water vapour over sublimation surface, Torr
t_{cycle}	Primary drying time, s
$k(T_i)$	Rate constant for the reaction (in this case protein degradation)
T_{shelf}	Shelf temperature (typically inlet temperature of heat transfer liquid), K
$\sqrt{t}$	Square root of time
T_i	Storage Temperature at time i

S_{heat}	Surface of heat conduction, cm^2
$T_{sublsurf}$	Temperature of sublimation surface, K
$\frac{dH}{dT}$	Total Heat Flow (W/g)
K_v	Vial heat transfer coefficient, cal/(s.cm^2.K)
$Cp(\frac{dT}{dt})$	Heat Capacity component (reversing signal) (W/g)
$f(T,t)$	Kinetic component (nonreversing signal) (W/g)
$m_{solution}$	Mass of solution in individual vial, g
$(\frac{(dm_{ice})_{vial}}{dt})_i$	Sublimation rate at given cycle time, g/s
$(m_{ice})_{vial}$	Total amount of ice in individual vial, g
$(V_{fill})_{vial}$	Vial filling volume, mL
λ_{frozen}	Heat conductivity of frozen material (~0.00358 Cal/s.cm.K for 10% solids)
%	Percent
°C	Degree Celsius
A_c	Area exposed to radiation effect
API	Active Pharmaceutical Ingredient
ASTM	American Society for Testing and Materials
B1	Buffer 1- 4% Mannitol 1% Sucrose 100mM NaCl 10mM Tris pH7.0
B2	Buffer 2- 4% Mannitol 1% Sucrose 10mM Tris pH7.0
B3	Buffer 3- 4% Glycine 1% Sucrose 100mM NaCl 10mM Tris pH7.0
B4	Buffer 4- 4% Glycine 1% Sucrose 10mM Tris pH7.0
BSA	Bovine Serum Albumin
c	molar concentration of protein fraction
CD	Circular Dichroism
Da	Dalton
dmol	Deci Moles
DSC	Differential Scanning Calorimetry

e_E	Emissivity for Radiative heat transfer between edge vial and heat source
FDM	Freeze Drying Microscopy
g	gram
HCl	Hydrochloric Acid
HMT (t)	High molecular Weight as a function of temperature
HMW (t_0)	High molecular Weight as a function of temperature at time zero
hrs	hours
IL6	Interleukin 6
IPA	Isopropyl Alcohol
K_c	Heat Transfer from Shelf to Glass
kDa	kilo Dalton
K_g	Heat Transfer due to conduction through gas from shelf to vial bottom
K_r	Radiative Heat Transfer
L	Litre
LDH	Lactose Dehydrogenase
m	metre
mDSC	Modulated Differential Scanning Calorimetry
$mg.mL^{-1}$	milligram per millilitre
mM	millimolar
mT	milliTorr
MTR	Mass Transfer Resistance
NaCl	Sodium Chloride
nm	nano meter (wavelength)
Pch	Chamber Pressure during Primary Drying
pDSC	Powder Differential Scanning Calorimetry
PES	Polyethersulfone
Phe	Phenylalanine
PID	Proportional Integral Derivative
PVP	Polyvinylphenol
RO	Reverse Osmosis
SEC	Size Exclusion Chromatography

SEM	Scanning Electron Microscopy
T_b	Temperature of the bottom of the vial, K
Tc	Collapse temperature of the amorphous phase
Tcrys	Crystallization temperature of the bulking agent
Tg	powder glass transition temperature (lyophilized material)
Tg'	glass transition temperature of the amorphous phase (used when Tc not available)
Tm	Melting temperature
Tp end	Product Temperature at the end of Primary Drying (when thermocouple loses contact with ice)
Tp start	Product Temperature at he beginning of the Primary Drying step
Trp	Tryptophan
Tsh	Shelf Temperature during Primary Drying
T_w	Chamber Wall Temperature, K
Tyr	Tyrosine
UF/DF	Ultra Filtration/ Diafiltration
USP	United States Pharmacopeia
XRD	X Ray Diffraction
ε	Water content, mass of water divided per mass of solution
Δε	Delta Epsilon (CD Calculated Spectrum)
θ	CD Spectra raw signal

Note: 1 mTorr = 1.33μbar

Note: Throughout this thesis, Freeze drying and Lyophilisation are two terms that will be interchangeable. They both mean the same thing for the purpose of this document.

1.0 INTRODUCTION

Freeze-drying (lyophilisation) is a processing step commonly used in the biotechnology industry to stabilize protein formulations as protein drug products are known to be more stable in freeze dried form than in liquid or frozen form (Jennings, 1999). During the freeze drying cycle, the protein formulation is first frozen to separate the solvent (water) from the solutes (protein and excipients) after which the ice is removed under vacuum conditions by a process known as sublimation. Finally, any residual water in the solid matrix may be removed by a process known as desorption. Overall, the freeze drying cycle can be viewed mainly as a three step process: freezing, primary drying and secondary drying (Wang, 2000).

During freezing, the solute concentration changes from a viscous liquid to a brittle glass which contains 20-50% water (Pikal 1990b). This reversible transition is commonly known as the glass transition temperature, which is represented by Tg' (Rey & May, 1999, Wang, 2000). Tg' has been found to correlate strongly with the collapse temperature (Tc) (Pikal & Shah, 1990). There are numerous definitions with respect to the collapse temperature of an amorphous or partially amorphous product. One definition states that the collapse temperature of an amorphous system is the temperature above which the interstitial water in the frozen matrix becomes significantly mobile (Jennings 1999). A second defines collapse as the process by which the structure created during freeze-drying is annihilated with the passage of the subliming interface. Generally, a collapsed drug product is said to have lost its shape by becoming a highly viscous liquid and has poor rehydration or reconstitution characteristics (Tsourouflis et al, 1976).

Literature suggests that the freeze-drying of amorphous or partially amorphous protein formulations above the collapse temperature (Tc) may negatively affect protein drug product stability (Pikal & Shah, 1990; Wang et al., 2003). Collapse has been documented to have many effects on the product including reducing the rate of sublimation by blocking the channels where water can escape (Mackenzie, 1976), causing the product to retain higher moisture (Adams & Ramsey, 1996) and exhibit slower reconstitution due to the reduction in surface area. Collapse is also known to retard secondary drying, resulting in unacceptably high residual moisture levels (Carpenter et al., 1997). Shalaev and Franks (1996) showed that for partially amorphous systems

in which the amorphous content crystallizes during freezing, the crystallized components act as macroscopic support to the remaining amorphous phase, thereby making the amorphous phase viscous flow go undetectable when drying above the collapse temperature. It has also been reported that when collapse occurs during freeze drying, ice crystals appear to dissolve rather than to sublime, resulting in a destruction of the channels and a marked increase in the resistance to vapour flow (Tsourouflis et al., 1976). For partially amorphous systems, Tc is commonly referred to as micro-collapse as the crystalline portion of the product structurally supports the solid content, thereby preventing total collapse when the product temperature exceeds the collapse temperature. Collapse may be avoided by maintaining structural integrity of the freeze concentrate (Mackenzie, 1976; Franks, 1991), which can be achieved by performing sublimation (or primary drying) at a product temperature below that of the collapse temperature.

As primary drying is the most time consuming step in the freeze drying cycle, there is obvious interest in optimising this step to make sure it occurs in the shortest possible time. Over the last number of years, work has been conducted to investigate the effect collapse has on the stability of the protein drug product (Pikal & Shah, 1990; Wang et al., 2003; Passot et al., 2007; Schersch et al., 2010). Shalaev & Franks (1996) have shown that a crystalline bulking agent can provide macroscopic support to the amorphous phase undergoing viscous flow. In support of this, Shalaev & Franks (1996) have shown that sucrose to NaCl weight ratio of 1:1 allows primary drying to be conducted above the collapse temperature without the detection of visual collapse in the product. Therefore, with a judicious choice in formulation excipients, primary drying can be conducted substantially above the collapse temperature without affecting the product.

The stimulus behind the idea of freeze drying above the collapse temperature is the ability to reduce cycle time. This will directly impact the overall processing time and processing cost. The primary drying stage is the longest stage of the lyophilisation process and freeze drying above the collapse temperature will not only result in shorter primary drying time, but also a reduction in the overall lyophilisation cycle time (Passot et al., 2007; Schersch et al., 2010).

2.0 PRINCIPLES OF PROTEIN LYOPHILISATION

The lyophilisation cycle can be broken down into three main steps: Freezing, Primary Drying and Secondary Drying.

1. Freezing transforms the water into ice crystals and the solids into two or more phases; usually a crystalline ice phase and an amorphous freeze concentrate phase containing the active pharmaceutical ingredient (API) and excipients (Jennings, 1999; Pikal et al., 1990a).
2. Primary Drying is the step where the solvent is removed by a process known as sublimation where ice is converted to water vapour. Both a vacuum and an increase in the shelf temperature are required to promote sublimation (Jennings, 1999). The primary drying rate is dependent on the vacuum and temperature setpoints along with an efficient freezing step. Primary drying is completed when all the ice crystals have been removed from the formulation, and the volume occupied by the resulting cake is equivalent to that of the frozen matrix (Pikal et al., 1990a).
3. Secondary drying involves the removal of bound water by a process known as desorption. The remaining water to be removed is usually around 15 – 20% w/w of the solute (Rambhatla et al., 2004). The step involves increasing the temperature parameters to higher setpoints than that of primary drying in order to achieve desorption and achieve minimum moisture content within the Lyophilised cake without reducing the volume of the cake (Jennings, 1999; Roy & Gupta, 2004).

Figure 1 represents a complete lyophilisation cycle plot with labels. This plot is generated by the system, where the raw data can be converted to excel format for further trending and analysis.

Fig.1: Plot of a complete Lyophilisation cycle from loading to secondary drying end. The processing conditions were achieved by loading at a shelf temperature of 20°C, ramping to -45°C and holding for 30 minutes after which a ramp to -20°C to complete annealing. Prior to primary drying, the shelf temperature was lowered to -45°C after which vacuum of 50mT (capacitance manometer) and an increase in shelf temperature to 0°C until hour 30 of the cycle. Secondary drying was conducted by increasing the shelf temperature to 45°C to remove all desorbed moisture.

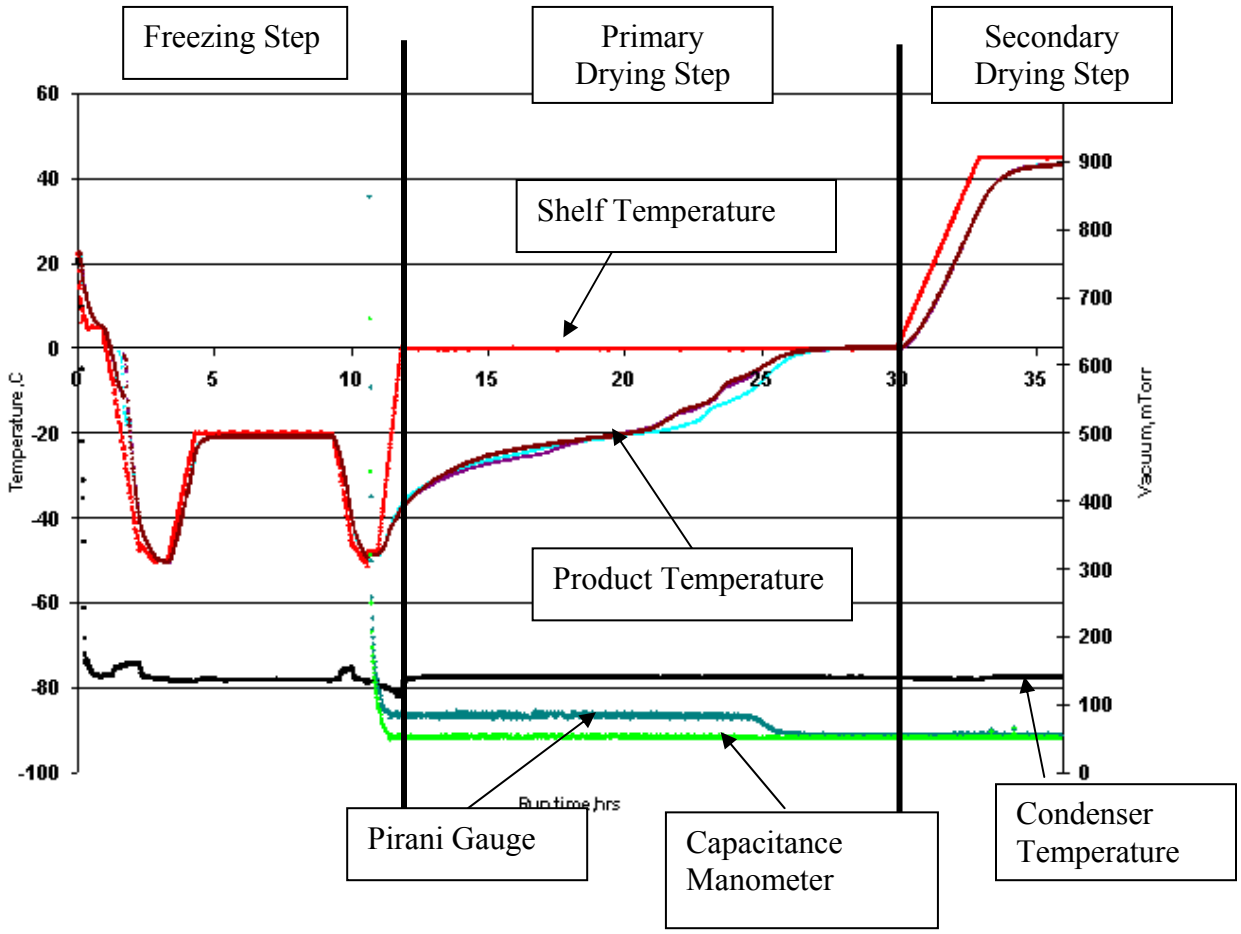

A Freeze dryer or Lyophilizer is made up of the following components (Jennings, 1999):

1. A lyophilizer/ Freeze Drying chamber
2. Condenser
3. Vacuum system
4. Heating and cooling system (Refrigeration)
5. Utilities –Nitrogen & Air for vacuum control, backfill or aeration

The refrigeration heating and cooling system is responsible for the heating and cooling of the heat transfer fluid which flows through the shelves within the chamber depending on step requirements. The heat transfer fluid flows through the shelves achieving the shelf temperature setpoint (Jennings, 1999). The vacuum system is responsible for achieving the vacuum setpoints during primary and secondary drying (Jennings, 1999).

The condenser consists of a condenser coil or plate depending on design, which is cooled to temperatures in the region of -70°C to promote the migration of the vapour from the product on the shelf to the coil (sublimation). The vapour then converts to ice on the cold surface. The condenser temperature is always set lower than that of the lyophilizer shelf temperature during both primary and secondary drying to promote efficient mass transfer of water vapour (Jennings, 1999). The principle operation is based on the fact that as the coil is set at an extremely low temperature, the vacuum pressure at the surface of the coil/ ice would be much lower than the vacuum at the surface of the product in the chamber. This ΔP drives the sublimation process and the condenser coil acts as a vapour trap by directly converting the vapour to ice. Figure 2 illustrates the set up of a basic lyophilizer and condenser system.

Fig. 2: Basic Lyophilizer Equipment system

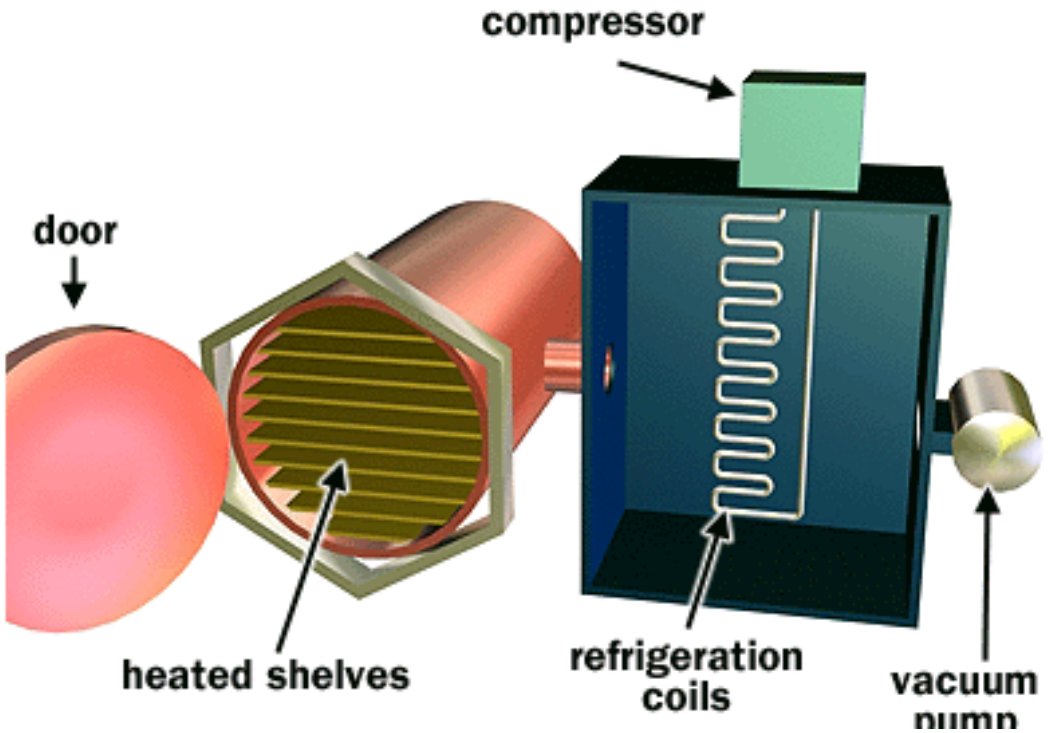

2.1 Freezing

As already mentioned, the principal function of the freezing step is to separate the solvent from the solutes. The solvent (water) will form ice crystals and the solutes (API and excipients) will be confined to the interstitial region between the ice crystals (Jennings, 1999). The freezing step involves the lowering of the shelf temperature of the lyophilizer at a predetermined rate to temperatures as low as -50°C in order to promote ice crystal formation. Faster freezing rates give rise to small ice crystals and slower freezing gives rise to larger ice crystals (Lai & Topp, 1999; Roy & Gupta, 2004). Crystal size is important as a variation in crystal size may negatively impact the primary drying performance. The liquid sample is cooled until pure crystalline ice is formed from part of the liquid and the remainder of the sample is freeze-concentrated into an amorphous or crystalline state where the viscosity is too high to allow further crystallisation (Randolph & Searles, 2002).

The freezing step dictates ice crystal structure (morphology) and size distribution which in turn influences several critical parameters e.g. protein aggregation, primary drying rate, secondary

drying rate, extent of product crystallinity and surface area of the lyophilised product (Searles et al., 2001a). Searles et al. (2001b) reported that the freezing of aqueous protein product by shelf ramp freezing (ramping temperature in a controlled fashion to the target freezing temperature) results in significant heterogeneity in ice crystal formation which affects the primary drying rate.

Less attention has been paid to the freezing conditions and their potential effect on the primary and secondary drying processes and on the characteristics of the finished product during the cycle development stage of the project (Patapoff & Overcashier, 2002). However, optimising the freezing step and achieving optimum crystal structure allows an efficient primary drying step to be developed (Pikal et al., 1990a; Jennings, 1999).

When designing the freezing step, the active ingredient degradative profile must be considered. Extreme temperatures and shear may cause the active ingredient to destabilize. For example, for proteins, extreme temperature and ramp rates may result in denaturation. If extreme temperatures and ramp rates are required for the freezing step, a cyroprotectant may be added as an excipient to the formulation (Pikal et al., 1990a).

The consequences of the extreme temperatures and ramp rates may be significant. Preliminary studies indicate that the freezing method has a significant effect on dried protein stability. The morphology of the product during the freezing step can affect the protein active ingredient. An increased area (fast freezing) correlates with decreased dried product stability for some proteins (Patapoff & Overcashier, 2002; Roy & Gupta, 2004).

2.1.1 Mechanics of Product Freezing

From examining figure 3, it is evident that there are a variety of transitions that may occur when freezing a product formulation that depends on solute concentration and temperature. The phase transition from liquid to ice is known as freezing. The transition from ice to glass is known as the sub ambient glass transition temperature (Tg'). A glass can be defined as non-equilibrium, amorphous, disordered solid of high viscosity and is a function of temperature and solute concentration.

Fig. 3: Phase diagram of a given product of varying solute concentration during the freezing step

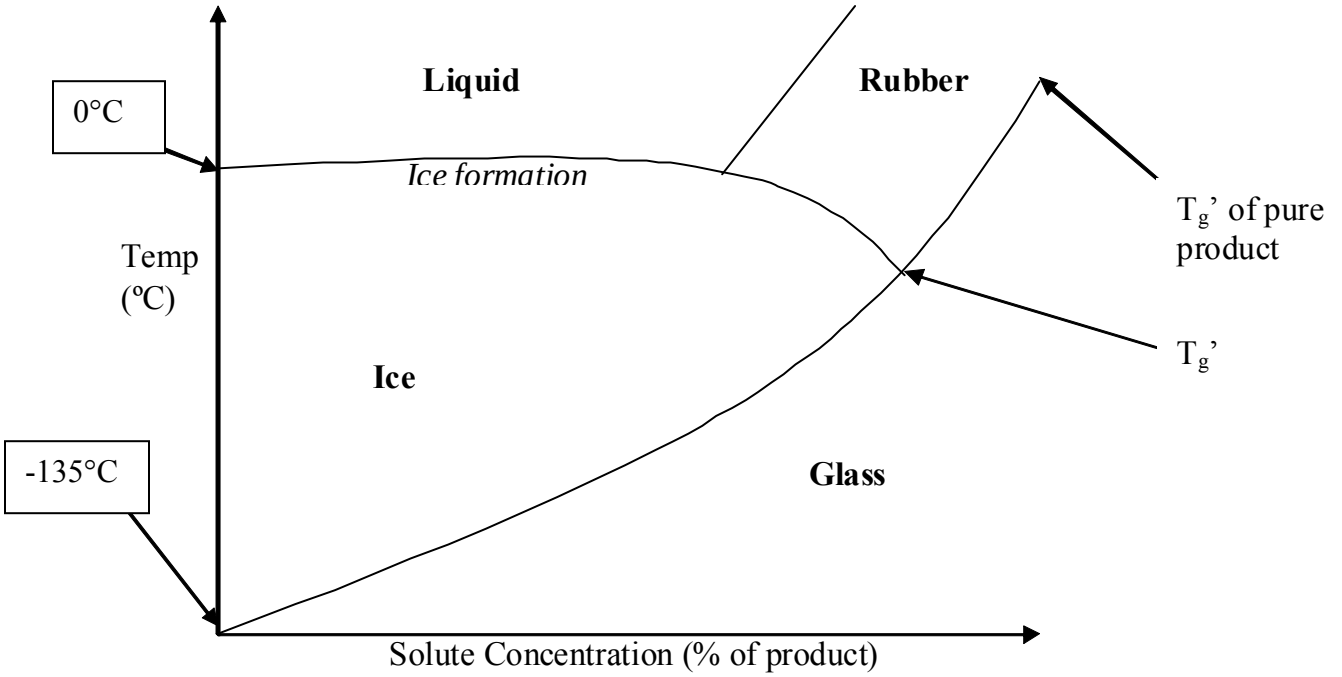

From examining figure 3, it is clear that the Tg' of pure ice is approximately -135°C (Nail et al., 2002). From observing the above figure, as the solute concentration increases, the water volume decreases. Also, as the solute concentration increases, the ice formation temperature decreases.

2.1.2 Nucleation

Crystallisation can be viewed as the consequence of two separate processes – nucleation and supercooling. Crystals arise by a process of nucleation after which crystal growth helps to determine the form of the product (Mackenzie, 1976).

Nucleation occurs when the shelf temperature is decreased over a pre-determined time to temperatures as low as -50°C to ensure that the entire product freezes completely. As the temperature decreases, the liquid cools below the freezing point of the solution: supercooled temperatures range from –10°C to -20°C with ice nucleation (crystallisation) occurring at around -15°C (Patapoff & Overcashier, 2002). Most pharmaceutical manufacturers rely on supercooling because of lack of nucleation centres in the formulation. Nucleation sites include particulate

matter, or imperfections on the side of vials (Patapoff & Overcashier, 2002). Freezing of water in the presence and in the absence of suspended impurities has been studied and found to result in heterogeneous nucleation of ice when suspended impurities were present and homogeneous nucleation in the absence of these impurities (Mackenzie, 1976).

Heterogeneous nucleation is the nucleation of ice crystals on a foreign substance: e.g. the surface of the container, particulate matter present in the water or sites of large molecules (Jennings, 1999). Homogeneous nucleation is the development of a critical sized nucleus through the random aggregation of molecules (Jennings, 1999). Most aqueous product formulations tend to contain some form of impurities, thereby resulting in both heterogeneous and homogeneous nucleation occurring. In this case, the first nucleation event to occur would be heterogeneous nucleation, also known as primary nucleation, followed by homogeneous nucleation, also known as secondary nucleation (Searles et al., 2001a).

2.1.3 Supercooling

Supercooling can be defined as the process of chilling a liquid below its freezing point, without it becoming solid. Typically, pharmaceutical products supercool to roughly -15°C before nucleating (Patapoff & Overcashier, 2002).

Larger ice crystals can be achieved by reducing the degree of supercooling. A high degree of supercooling results in smaller ice crystals. Smaller ice crystals mean a larger number of ice crystals, and therefore a larger surface area (Tang & Pikal, 2004). A high degree of supercooling also results in higher product resistance, a slightly higher product temperature and, a longer primary drying time (Rambhatla et al., 2004). The degree of supercooling is the temperature difference between the thermodynamic or equilibrium ice formation temperature and the actual temperature at which ice begins to form (Tang & Pikal, 2004).

2.1.4 Frozen Matrix

The morphology of the frozen matrix affects the rate of mass transfer of water vapour during sublimation. The vapour channels left by the sublimed ice may resist vapour flow, slowing down the sublimation rate (Patapoff & Overcashier, 2002). Slow rates of primary drying would result in longer primary drying time to eliminate the possibility of collapse (the collapse temperature (Tc) is the temperature at which, when exceeded, the interstitial water in the frozen matrix becomes mobile (Jennings, 1999)) or at which meltback (meltback is the extreme of collapse – gross collapse) occurs (Searles et al., 2001a). The decreased resistance to the mass transfer of water vapour increases the sublimation rate and decreases the primary drying step time while lowering the product temperature (Patapoff & Overcashier, 2002).

Both the length of the freezing step and the rates of cooling during freezing are critical in determining the optimum sublimation rate during primary drying. For fast freezing, small pore sizes and horizontal channels result near the surface of the cake. The channels restrict vapour flow and slow down the rate of sublimation (Patapoff & Overcashier, 2002). This phenomenon is known as mass transfer resistance (MTR) (Pikal et al., 1983). For a given shelf temperature and chamber pressure, a decrease in MTR will increase the sublimation rate (Patapoff & Overcashier, 2002). An increase in mass transfer resistance will decrease the sublimation rate and prolong the sublimation step (primary drying).

2.1.5 Ice Propagation

Ice propagation is the symmetry associated with the formation of ice crystals e.g. vertical or horizontal ice crystal formation. In order to achieve high rates of sublimation during primary drying, vertically structured ice crystals are essential. These ice crystals will minimise mass transfer resistance during primary drying due to the crystals leaving ‘channels’ behind when the ice is being removed, allowing crystals deeper in the cake to be sublimed off with ease, thereby achieving the optimum sublimation rates at any given temperature (Jennings, 1999).

Observations of the lyophilisation of aqueous protein solutions using freeze drying microscopy (FDM) have offered evidence of the formation of channels by ice crystals (Pikal & Shah, 1990).

These channels allow the water vapour to sublime from the lower section of the product, as the sublimation interface in the product proceeds from the surface down to the bottom of the vial.

2.1.6 Interstitial Region

The final frozen matrix will consist of both ice crystals and an interstitial region. The interstitial region is composed of the solutes, such as protein API and excipients, and any uncrystallized water dispersed between the ice crystals. There are two states associated with the interstitial region – amorphous or crystalline states (Jennings, 1999). The amorphous or glassy state is the most common state found in the interstitial region as a result of freezing most formulations (Jennings, 1999). There is evidence that amorphous excipients, such as mannitol or glycine, regularly crystallize in the interstitial region of the frozen matrix during the freezing process (Jennings, 1999; Patapoff & Overcashier, 2002).

2.1.7 Sub ambient Glass Transition Temperature (Tg')

Tg' is a function of the amorphous component of a formulation (Wang, 2000). The product formulation experiences very low temperatures during the freezing step of the lyophilisation cycle (refer to figure 3). For liquid product, the solute concentration of the formulation eventually changes the solution from a viscous liquid to a brittle glass, which contains 20-50% water (Pikal, 1990b). The temperature of this reversible transition is known as the glass transition temperature (Tg'). For a dried material, the powder glass transition temperature is represented by Tg. Likewise, for a frozen material, Tg' represents the glass transition temperature of the frozen state. Tg' is one of the most important parameters for optimisation of a lyophilisation process, as the temperature of the freezing step must be lower than Tg' in order to achieve an optimum freezing step (Wang, 2000). Tg' may be estimated using modulated Differential Scanning Calorimetry (mDSC).

2.1.8 Annealing

Annealing involves holding the product at a temperature above the final freezing temperature for a defined time to crystallize amorphous bulking agents along with promoting homogenous ice

crystal growth (Tang & Pikal, 2004). One of the reasons why annealing is incorporated into the lyophilisation cycle is to overcome heterogeneity in nucleation rates of the protein product (Rambhatla et al., 2004). The annealing step is necessary to allow the crystallisation of crystalline bulking agents, such as mannitol. Failure to crystallize the bulking agent could result in a lower Tg' and thereby compromising the storage stability as the bulking agent may crystallize at certain conditions in the dried state (Tang & Pikal, 2004). Annealing above Tg' results in the homogenous growth of ice crystals, decreasing the product resistance to flow of water vapour and results in shorter primary drying time (Searles et al., 2001b; Pikal et al., 1983).

2.2 Primary Drying

Primary Drying is the second step in the Lyophilisation cycle. In this step, the ice crystals are removed by a process known as sublimation (Wang, 2000). Sublimation is where water is converted from a solid directly to vapour. To achieve this, the temperature is increased from the freezing step temperature and a vacuum is exerted on the system (Xiang et al., 2004). Depending on the nature of the product formulation, the product temperature must remain below Tg' or the collapse temperature (Tc) and the eutectic Tm (Teut) during the majority of primary drying to result in acceptable cake cosmetics at the end of the cycle. Definitions of these temperatures may be found later in sections 2.2.3 and 2.2.4. Due to the low temperature requirement during primary drying, vacuum is required to promote effective sublimation rates (Jennings, 1999). Primary Drying generally removes 90-95% of the moisture by removing all free water (or ice).

The driving forces for sublimation during the lyophilisation cycle are the temperature differential between the heating surface (shelf) and the product (ΔT), and the pressure differential (ΔP) between the product cake surface and the surface of the condenser coil. Both promote high mass transfer rates. The condenser temperature is set at a very low temperature (~-70 ºC) to promote increased rates of sublimation and mass transfer of the water vapour to the condenser (Jennings, 1999). Based on the vapour pressure of ice, the vacuum at the surface of the condenser coil would be lower than that of the cake surface in a given vial in the drying chamber due to the coil temperature, thereby driving sublimation.

2.2.1 Phase Transitions of Water

The triple point of water (figure 4) is the point at which water is readily available in all three phases: solid, liquid and gas. The triple point of water occurs at a pressure of 0.006bar and a temperature of 0.0098°C. Once the pressure drops below this pressure, water is only readily available in two phases, solid and gas, depending on the temperature. It is below the pressure setpoint of 0.006Bar where the sublimation process is conducted.

Fig. 4: Phase Transitions of Water. From the diagram it is clear that at low pressures (vacuum level) it is possible to transfer from the solid phase directly to the vapour phase.

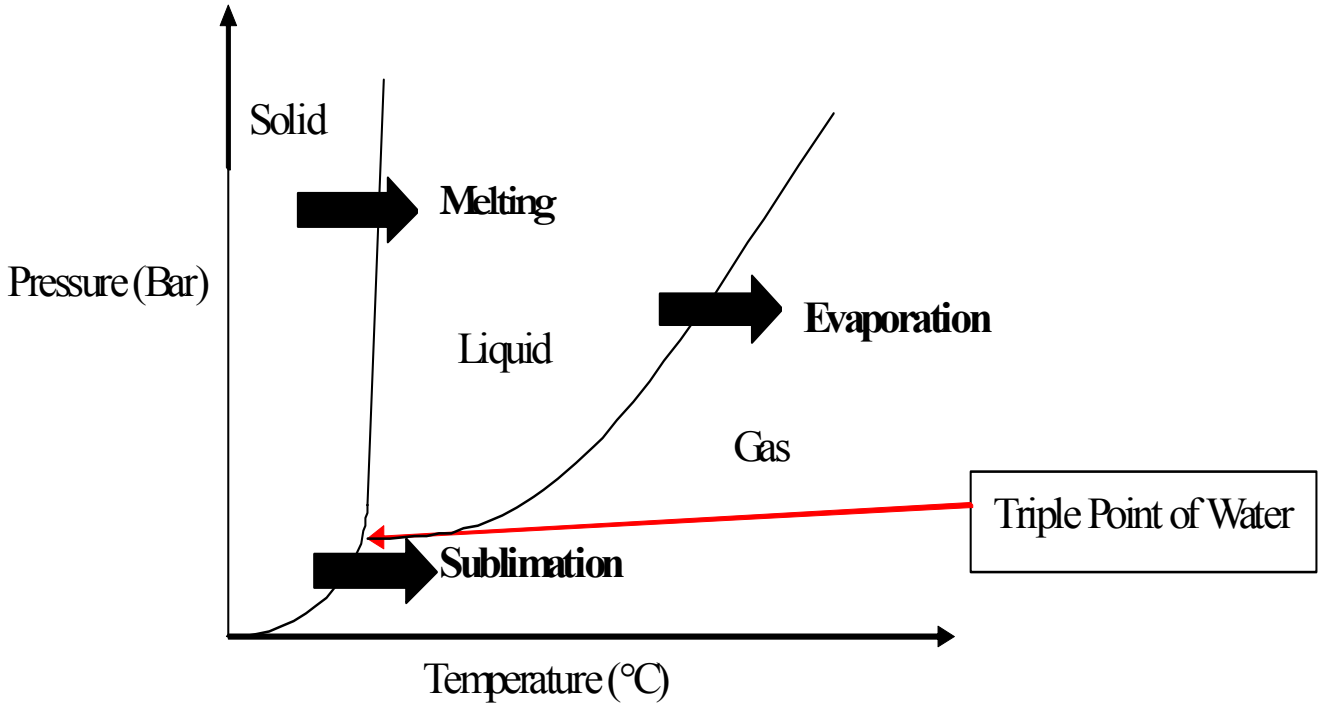

In order for sublimation of ice to occur, the pressure of the chamber must be in the vacuum range. At this point, the product temperature may be increased which will increase the rate of sublimation. This temperature increase is limited to maintenance of the temperature below the critical temperature known as collapse for an amorphous system and eutectic melt for a crystalline system.

2.2.2 Collapse

Collapse consists of the disappearance or annihilation of the freezing pattern with the passage of the subliming interface (Mackenzie, 1976). Possible discolouration of cake can arise with two phases present:

1. A dried upper phase
2. A collapsed lower phase

The collapsed phase is evident by the lack of structure to the cake. Collapse is said to have occurred when the cake volume is less than the frozen matrix. Collapse occurs when the product temperature exceeds Tc of a product formulation. To prevent collapse, the product temperature must be kept lower that this temperature (Wang, 2000). Freeze Drying Microscopy may be used to estimate Tc (Jennings, 1999). Figure 5 illustrates product collapse.

Apart from unacceptable cake appearance, various undesirable properties result from the collapse of the cake during freeze-drying e.g. by clogging the paths where water can escape; collapse can reduce the sublimation rate significantly. The final product tends to retain higher moisture content than a dried product without collapse (Adams & Ramsey, 1996). As already mentioned, collapse has also been found to effect protein stability when protein formulations are freeze dried above Tc (Pikal et al., 2000; Wang et al., 2003).

From examining figure 5, collapse is represented by picture D. However, the sequence of events that occur to collapse the product can be examined by following picture A through D sequentially, where A is the frozen product, B is the formation of a dry layer on the top of the plug, or cake, C is the beginning of micro collapse as the product is drying and D is the final product with evidence of micro collapse.

Fig. 5: Diagrammatic representation of collapse[a]

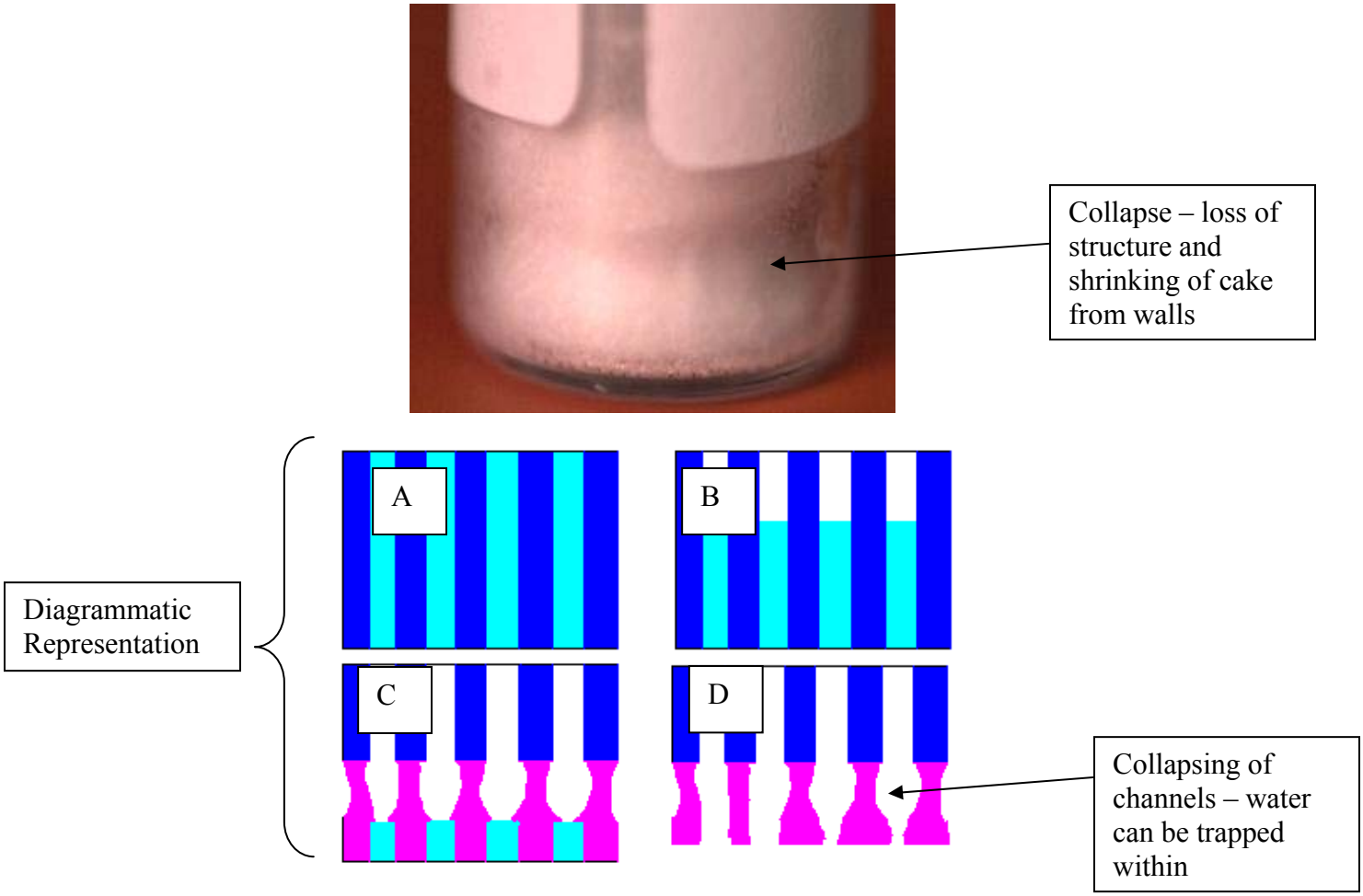

The channels formed by ice crystallization channel collapse within the sample, which interrupts the vapour flow from the lower area of the cake. This causes water to become entrapped, increasing the residual moisture content. It is understood that collapse leads to an increase in moisture content (Pikal & Shah., 1990).

The following schematic (figure 6) also illustrates collapse in pharmaceutical lyophilisation. The sequence of events that occur to collapse the product can be examined by following picture A through F, where A is the frozen product, B is the formation of a dry layer on the top of the plug, or cake, C is the beginning of micro collapse where the product temperature exceeds that of the collapse temperature, D shows evidence of collapse, E illustrated a high degree of collapse (gross

[a] Image courtesy of S Tchessalov, Principal Research Scientist II, Pfizer, Andover, MA

collapse) is being experienced and F shows the gross collapse of the lower section of the cake once all ice is removed from the product. Freeze drying well above the collapse temperature could also result in separation in different parts of the cake.

Fig. 6: Diagrammatic representative of collapse in an amorphous based system[a]

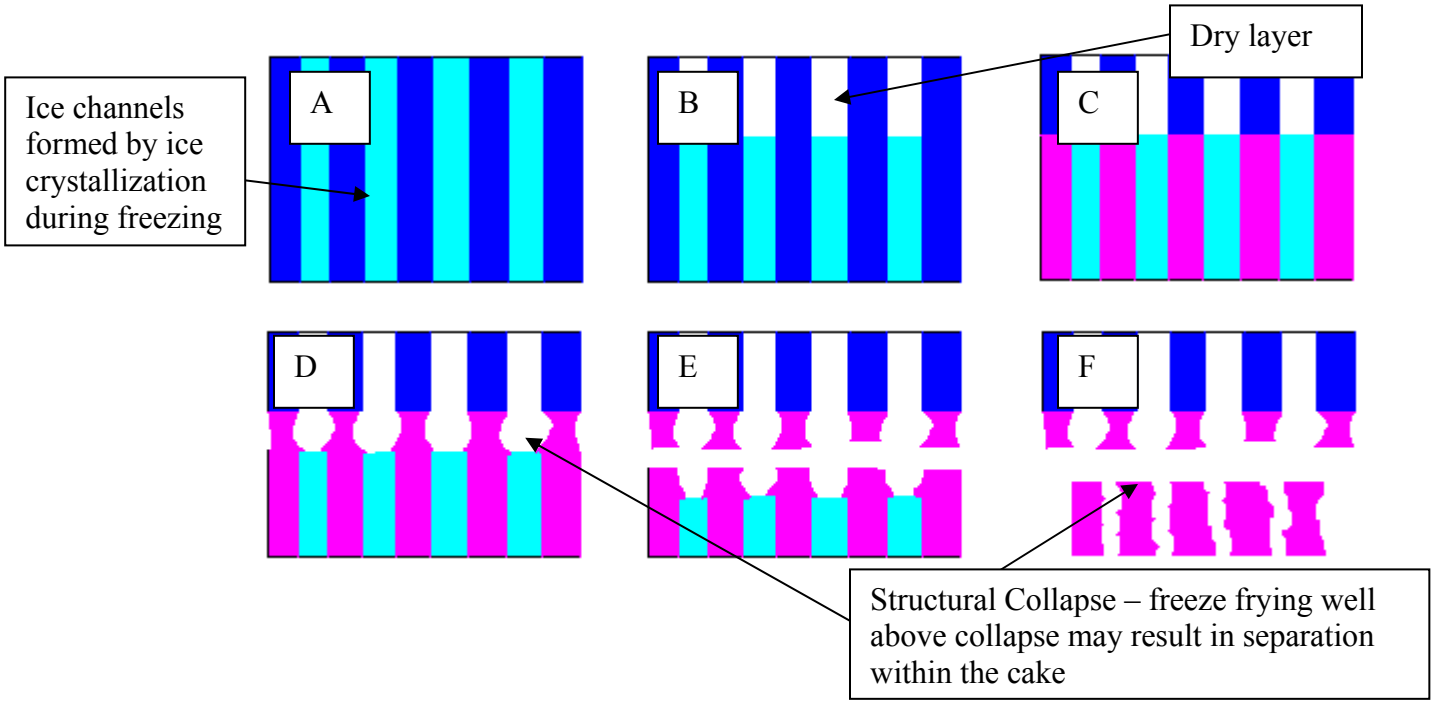

There are numerous variations in the way the collapse temperature is measured. Firstly, the common factor is the fact that the method of choice is freeze-drying microscopy. This consists of placing a small sample, e.g. 5µl, on a stage, in which the sample location may be cooled with liquid nitrogen, heated using a heat exchanger and dried using a vacuum pump. Passot et al. (2007) placed a 5µl sample between two quartz cover slips, separated by a metallic spacer. The sample was frozen below Tg' at 10°C/min and held for 10-20 minutes under vacuum conditions to generate a drying front. The temperature was increased stepwise at 5°C/min up to just prior to where collapse is expected and increased at intervals of 1°C to observe collapse. Each temperature reached was held for a 10 minute isothermal to achieve a drying front.

Meister & Gieseler (2009) equilibrated the sample at 5°C for 1 minute before ramping to -40°C at a rate of 10°C/min. The sample was then held at -40°C for 10 mins. After 8 minutes, the

[a] Image courtesy of S Tchessalov, Principal Research Scientist II, Pfizer, Andover, MA

vacuum was enabled and after the 10 minutes expires, the product was subjected to heat at a rate of 1°C/min through the point of collapse. Nail et al., (1994) reduced the temperature of the sample to -45°C in 3 minutes and then warmed the sample under vacuum conditions to 5°C below the collapse temperature. The sample was then heated at 1°C/minute in stepwise intervals until melting was observed.

The method Passot et al. uses identifies the collapse transition specifically to a given temperature by using isothermal holds, whereas the method Meister & Gieseler (2009) relies on allows for slightly more variation in collapse measurement, which consists of measuring collapse during a heat ramp. The method Meister & Gieseler (2009) use is very similar to the method developed by Nail et al. (1994). Incidentally, the majority of the recent published papers discussing collapse referred to Nail et al. (1994), as the procedure used in the measurement of collapse or eutectic melt.

2.2.3 Collapse Temperature (Tc)

As already introduced, the collapse temperature (Tc) is the temperature at which, when exceeded, the interstitial water in the frozen matrix becomes mobile (Jennings, 1999). Collapse can be in the form of micro or gross collapse. For amorphous and partially amorphous materials, the collapse temperature, measured using freeze drying microscopy, represents the micro collapse temperature as opposed to gross collapse, which is represented by the overall melting temperature, Tm. This thesis discusses collapse throughout and in all cases the text refers to micro collapse unless otherwise specified. Table 1 lists selected compounds and their collapse temperatures (Wang, 2000).

Table 1: Selected Collapse temperatures for selected excipients

Compound	Tc
Sorbitol	-54°C
Sucrose	-31°C
Dextran (10kDa)	-10°C
Hodroxyethyl Starch	-5°C
PEG (6kDa)	-13°C

2.2.4 Meltback

For amorphous and partially amorphous formulations, meltback is the extreme of collapse (gross collapse). The cake is usually shrunk several millimetres away from the walls of container. Occasionally the cake disappears and a small gum like structure is present in the centre of the vial (Jennings, 1999). This occurs when the product temperature exceeds Teut or Tm. mDSC (Jennings, 1999) can be used to measure the Tm. FDM may be used to measure Teut.

Figure 7 shows an example of meltback for a given product. Meltback (also known as gross collapse) is represented by picture D on the diagram. However, the sequence of events that occur in order to collapse the product can be examined by following picture A through D, where A is the frozen product, B is the formation of a dry layer on the top of the plug, or cake, C is the beginning of melt as the product is drying and D is the final product with evidence of gross collapse or melt. This occurs as a result of the product temperature reaching levels above the Tm while there is still ice in the product.

Fig. 7: Example of Meltback[a]

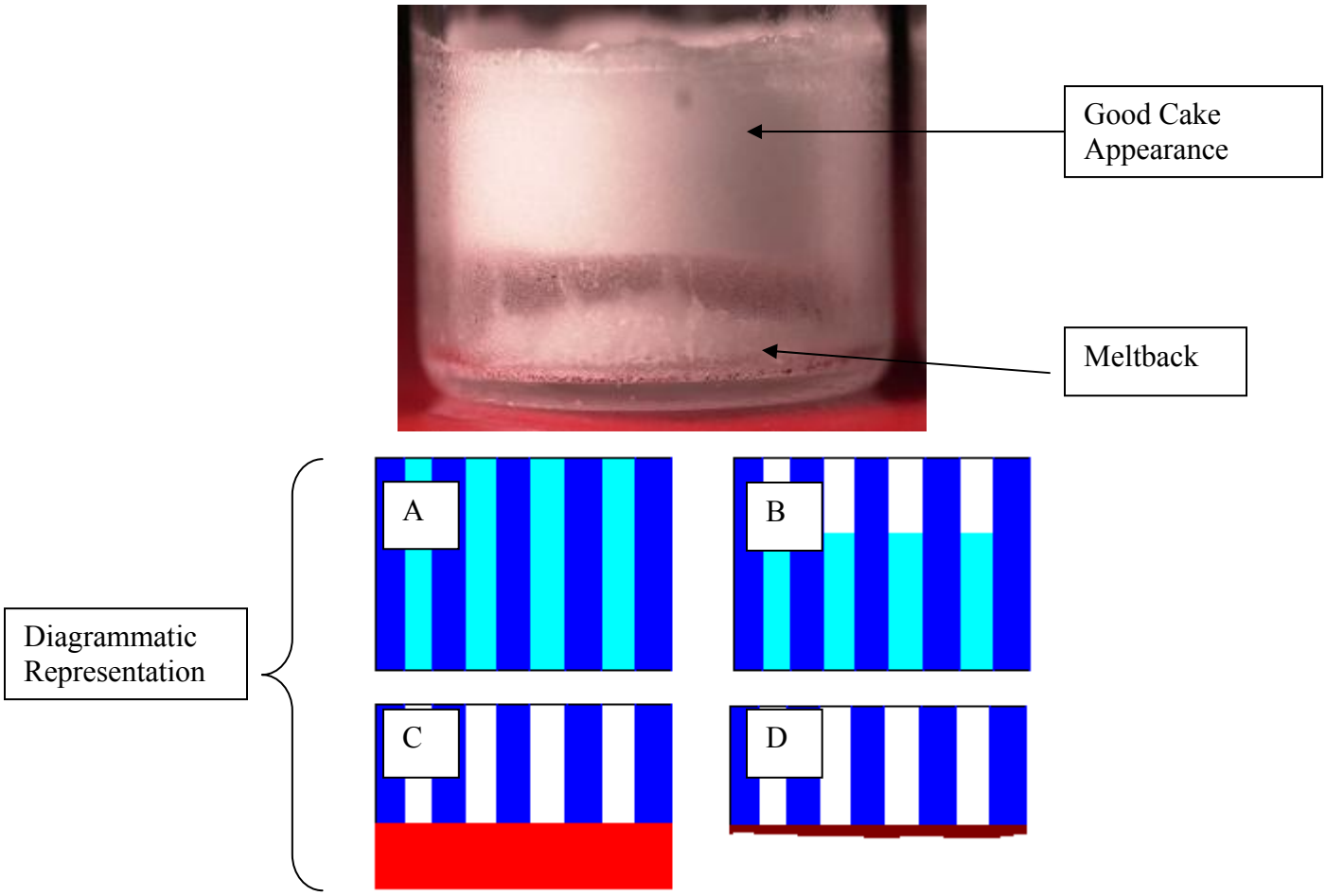

2.2.5 Eutectic Melting Temperature (Tm or Teut)

The eutectic melting temperature, as mentioned, is the Tm of an amorphous or crystalline product formulation. The transition of meltback occurs in the interstitial region of the frozen matrix if this temperature is exceeded. It is important to keep the primary drying temperature below this temperature (Wang, 2000).

2.2.6 Endpoint of Primary Drying

The end of Primary Drying occurs when all the frozen water is removed from the product (Bindschaedler, 1999). Determination of the end point can be carried out in a number of ways:

[a] Image courtesy of S Tchessalov, Principal Research Scientist II, Pfizer, Andover, MA

1. Tproduct converges with Tsh (equilibrium): The product temperature and the shelf temperature converge indicating that there is no ice left in the product (Wang, 2000).
2. Barometric endpoint test (Wang, 2000): The chamber is isolated from the condenser for a short period of time to investigate if the chamber pressure will rise significantly. A significant increase in pressure indicates that there is still moisture remaining in the product. Minor increase indicates the endpoint of the step (Wang, 2000).
3. Vapour pressure (pirani gauge) and absolute pressure (capacitance manometer) converge. This equilibration indicates the endpoint of primary drying (Jennings, 1999). This is understood to be the most effective method of primary drying endpoint determination (Patel et al., 2010).
4. Heat and mass transfer rate measurements. Calculating the rate of heat transfer from the shelf to the vial and mass transfer (sublimation rate) will help to calculate the end point resulted in a more efficient drying process (Jennings & Duan, 1995).

When designing the primary drying step, adding an extra 2-3 hours to the step end point is common practice. This will guarantee that only bound water remains, thus allowing the secondary drying (desorption) step to begin (Wang, 2000).

Figure 8 represents a lyophilisation cycle trend. From examining the trend, it is clear that both the ΔT between Tsh and Tp along with the ΔP between the Pch (manometer) and the pirani gauge (vapour pressure) converge. $\Delta P \approx 0$ indicates the endpoint of primary drying (Patel et al., 2010).

Fig.8: Plot of a complete Lyophilisation cycle from loading to secondary drying end. The processing conditions were achieved by loading at a shelf temperature of 20°C, ramping to -45°C and holding for 30 minutes after which a ramp to -20°C to complete annealing. Prior to primary drying, the shelf temperature was lowered to -45°C after which vacuum of 50mT (capacitance manometer) and an increase in shelf temperature to 0°C until hour 30 of the cycle. Secondary drying was conducted by increasing the shelf temperature to 45°C to remove all desorbed moisture.

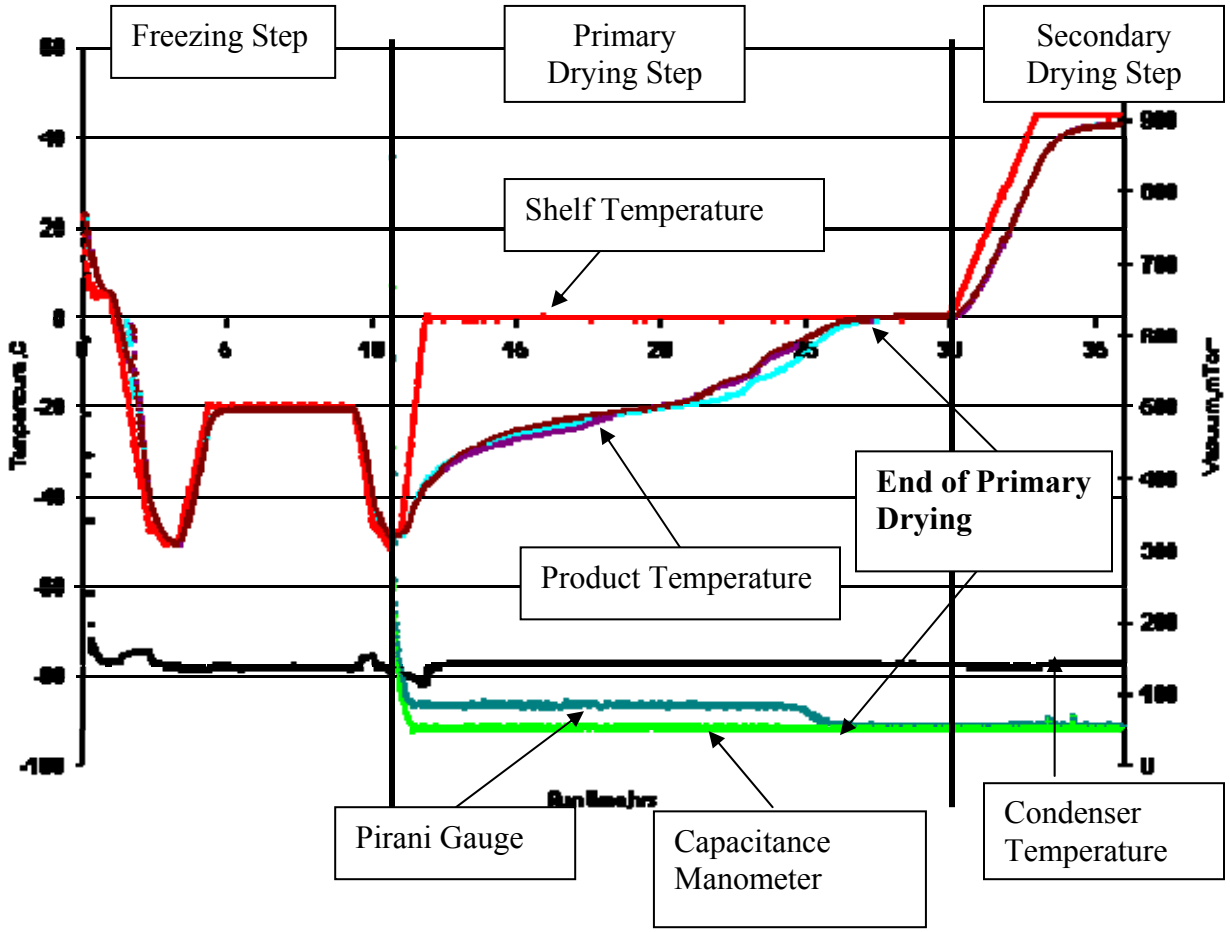

2.2.7 Primary Drying Step Design

The sublimation rate is the variable that must be optimised when designing the primary drying step. The Sublimation rate is dependent on chamber pressure (Pch), condenser temperature (Pcond) and shelf temperature (Tsh) (Jennings, 1999).

A moderate increase in Pch increases the Primary Drying rate (the sublimation rate) when the chamber shelves provide effective heat transfer, leading to a higher product temperature (Tprod) (Bindschaedler, 1999). A chamber pressure of half or a quarter the saturated vapour pressure over ice usually leads to an acceptable sublimation rate (Bindschaedler, 1999).

When determining the optimum sublimation rate, a number of parameters must be taken into account. It is understood that the higher the product temperature during primary drying under a balanced vacuum, the faster the sublimation rate. Likewise, a decrease in product temperature under a balanced vacuum decreases the sublimation rate (Overcashier et al., 1999). However, product temperature can only be increased to a certain level during primary drying. This limit is in the form or the Tc (Collapse Temperature) or the Teut (eutectic melting). Elevating the product temperature above these temperatures may result in product meltback or collapse.

2.2.8 Heat & Mass Transfer – Mathematical Modelling of Primary Drying

Heat Transfer can be defined as the transfer of energy from one body to another by means of convection, conduction or radiation (Pikal et al., 1984). A good understanding of heat transfer during primary drying would allow greater efficiency in process development and would minimize problems encountered during scale up to commercial operations (Pikal et al., 1984).

Heat transfer (thermal) resistance of a barrier may be defined as the ratio of temperature across the barrier and the area normalised heat flow (Nail, 1980). Thermal resistance is nearly all due to the tray – vial interface resistance (when a tray is used) and the shelf - vial interface when the vial is loaded directly onto the shelf (Pikal et al., 1984). Pikal et al. (1984) found that the thickness of the glass vial was not a significant factor in heat transfer resistance. It was also found that thermal resistance is generally less for the glass vial than the product itself (Nail, 1980).

Heat Transfer is a critical aspect of Lyophilisation as the more efficient the heat transfer is and the less heat transfer resistance, the faster the sublimation rate and the shorter the primary drying. Knowledge of the heat transfer coefficient will simplify scale-up of the proposed cycle by

minimising the number of cycles to be run to scale up a developed cycle from small scale to large scale, reducing the cost implications associated with the large-scale cycle development stage.

The vial heat transfer coefficient has contributions from the following parallel mechanisms of heat flow during lyophilisation (Pikal et al., 1984):

1. Direct conduction from the surface to the vial via points of direct contact between the vial bottom and the shelf
2. Radiation heat transfer
3. Conductive heat transfer through gas

The vial heat transfer coefficient (Kv) may be expressed as (Pikal et al., 1984):

$$Kv = Kc + Kr + Kg \quad \text{(Eq. 1)}$$

Where, Kc is the conductive heat transfer, Kr is the radiative heat transfer and Kg is the heat transfer due to conduction from the shelf to the product through the gap at the base of the vial. Heat Transfer can best be described in terms of four barriers (Pikal et al., 1984):

1. The lyophilizer shelf
2. The pan or tray in which the vials are placed (if relevant)
3. The vial itself and surrounding vials (or, in the case of edge vials, chamber walls and doors)
4. The frozen product – between the ice at the bottom of the vial and the ice at the sublimation interface
5. The gap between the vial bottom and the shelf

A simple steady state model (Tchessalov & Warne, 2008) can be utilized in primary drying stage design (equation 2). Calculations may be made for the single vial container similar to the process described in the literature (Pikal, 1985). The model is based on the assumption that all transferred heat is used for the sublimation process. The heat and mass balance at the sublimation

surface for each primary drying segment are described by the following equation (Tchessalov, 2008):

$$(\frac{\partial m}{\partial t})_i = \frac{S_{in} * (P_{Subl} - P_{Chamber})_i}{R(h)_i} = \frac{S_{out} * K_V(P) * (T_{Shelf} - T_{product})_i}{\Delta H_S} \quad \text{(Eq. 2)}$$

Where, $(\frac{\partial m}{\partial t})_i$ represents the sublimation rate at time, i, Sin and Sout are inner and outer surface areas of the vials; ΔH_S is a latent heat of sublimation of water; Psubl and Pchamber are pressure over the sublimation front and chamber pressure respectively; Tshelf and Tprod are the shelf and product temperatures respectively; R(h)i is the cake resistance at dry layer height, h. Tprod is the product temperature at the bottom of the vial.

The following equation is used to estimate the product temperature at the sublimation surface for each given time segment, i (Tchessalov & Warne, 2008):

$$(T_{sublsurf})_i = (T_{product})_i - \frac{dQ}{dt}(t_i)\frac{(h_{frozen} - (h_{dry})_i}{\lambda_{frozen}} \quad \text{(Eq. 3)}$$

Where, h_i illustrates the height of frozen and dry layers and λ_{frozen} is the heat conduction coefficient.

Microsoft ®Excel Solver can be used to calculate the product temperature at each time segment balancing the first mass balance equation. Product cake resistance R(h) can be estimated for the product using the same model along with measured product temperature profiles. These calculations allow the prediction of a product temperature profile as a function of shelf temperature and chamber pressure (Tchessalov & Warne, 2008). The model may be verified by comparing the calculated temperature to the actual measured pressure after executing the lyophilisation cycle in the freeze dryer.

When dealing with metal trays (in which vials are placed), there are two vapour boundaries in action (Nail, 1980):

1. Between the vial bottom and the tray
2. Between the tray and the shelf

It has been demonstrated that for a system of vials in a metal tray placed on a heated shelf, the sublimation rate increased as the chamber pressure decreased (Nail, 1980).

Up to this point, when dealing with the heat transfer coefficient, it was assumed other vials surrounded the vial in question. However, there are instances when there is at least one side of the vial in question not in contact with other vials. This is when the vial is situated as the edge of the shelf. These vials are known as 'edge vials' (Rambhatla & Pikal, 2003).

The vials located along the edge of the shelf receive more heat during primary drying (due to the radiation of heat from the walls and door of the chamber), and their contents sublimate faster (Rambhatla & Pikal, 2003). Pikal found that the average edge vial sublimed 15% faster than an interior vial (Pikal et al., 1984). This heterogeneity in the sublimation rates with respect to the position on the shelf may be an important issue during scale up (Rambhatla & Pikal, 2003).

Mass transfer is defined as the molecular and convective transport of atoms and molecules within physical systems. When discussing mass transfer, we discuss in terms of the resistance offered by a given barrier (Pikal et al., 1984). Mass transfer involves the transfer of water vapour from the product to the condenser coils during both the primary and secondary drying stages (Jennings, 1999). Figure 9 illustrates the mass transfer process during the lyophilisation cycle.

Fig. 9: Mass Transfer during Lyophilisation

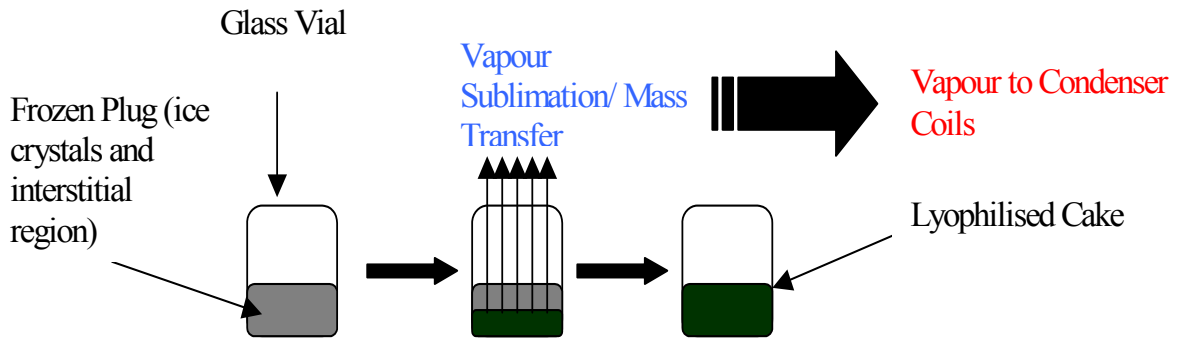

During the Lyophilisation cycle, three (3) barriers or resistances impede moisture (water vapour) (Pikal et al., 1984):

1. The dried product layer above the frozen product (Pikal et al., 1984) – both the ice: vapour interface and the thickness of dried product (Pikal, 1983)
2. Semi-Stoppered vials (Pikal et al., 1984)
3. Resistance in transfer from drying chamber to condenser (Pikal et al., 1984)

During primary drying the frozen product dries in the direction of the top to the bottom of the frozen plug, thereby producing a dried product layer above the ice. This dried layer increases in thickness as the sublimation proceeds. The dried product layer, a porous solid, imposes a resistance to the mass transfer of water vapour, and a corresponding pressure drop across the dried product layer (Pikal, 1985).

The dried product layer above the frozen product is both temperature and vial type dependent (Pikal et al., 1984). The dried layer resistance is particularly important for a relatively thick solution. The dried layer gradually increases during primary drying. The increase in the dried layer resistance results in the increased mass transfer resistance through the dried layer (Kuu et al., 1995).

When the vapour content is larger compared to the dimensions of the pores constituting the path of vapour flow, as in the case of the water vapour flow through the dried product (Pikal et al., 1983), collisions of water molecules with the pore walls are responsible for resistance to vapour

flow, and the flow mechanism is said to be free molecular or Knudsen flow (Dushman & Lafferty, 1962).

Along with the dried product layer, the stopper is a source of mass transfer resistance. The stopper has one or more small openings to allow vapour to pass through. However, the stopper does impede the mass transfer due to it semi blocking the vial opening (Pikal, 1985).

Condenser resistance may be associated with the process of conversion of water vapour to ice on the coils in the condenser chamber, yielding a water partial pressure inside the condenser significantly larger than the vapour pressure of ice on the condenser surface (Pikal, 1985).

2.3 Secondary Drying

Secondary Drying is the removal of bound water molecules remaining by a process known as desorption. Secondary drying occurs after primary drying is completed (Jennings, 1999).

Secondary Drying begins locally when all ice is removed from that region of the product. Once all the ice is removed, what remains are strongly and weakly bound water molecules (Pikal et al., 1990). Proteins, for example, have both strong and weak binding sites to accommodate unfrozen water. Secondary Drying removes weakly bound and some strongly bound water molecules (Wang, 2000). The remaining strongly bound water molecules are known as the residual moisture content of the product (Wang, 2000). Residual moisture content is dependent on the temperature during secondary drying and not the drying time. High temperatures are required to achieve low levels of residual moisture (Pikal et al., 1990).

As a consequence, care must be taken not to overheat the product, because after the removal of ice, the residual product has lost most of its mechanical strength and has become extremely fragile, vulnerable to structural collapse (Franks, 1998). However, with regards to protein products, generally, the lower the moisture content, the more stable the product is (Wang, 2000). Therefore, ideally the temperature should be high but not high enough to affect product potency.

2.3.1 Endpoint of Secondary Drying

The endpoint of secondary drying can be determined in a number of ways. Firstly, during small-scale lyophilisation cycle development, a barometric moisture test during secondary drying is usually used as the first indicator. As in Primary Drying, this method is a barometric end point determination test. The test involves isolating the lyophilizer chamber from the condenser and vacuum system. If there is a pressure rise, this indicates that there is still desorption ongoing and that the step is not completed. A pressure increase is an indication that intensive water desorption is still occurring at this particular product temperature.

Secondly, an electronic hygrometer or a residual gas analyser may be used to determine the residual moisture level during lyophilisation, and therefore, the endpoint of secondary drying (Nail & Johnson, 1992).

Thirdly, the moisture content of final lyophilised product can be determined by the following methods (Wang, 2000):

1. Loss on Drying (loss of moisture)
2. Karl Fischer Titration
3. Thermal Gravimetric Analysis (TGA)
4. Gas Chromatography (GC)
5. Near Infra red Spectroscopy (IR)

The most common method of determining the endpoint of secondary drying is by measuring the moisture content using the Karl Fischer titration method on lyophilized material. Using Karl Fischer and an instrument known as a sample extractor (or sample thief), it is possible to manually stopper selected vials throughout primary and secondary drying steps thereby enabling the measurement of residual moisture as a function of step time. Figure 10 illustrates the output from this approach. Secondary drying time may be determined by assessing the point after which there would be no added benefit to extend the step time. Figure 10 is a plot of percentage (%) moisture versus cycle time. It is clear after a certain point that for the added time in the cycle, there is no significant benefit with respect to decrease in moisture content. As long as the results are within the specification, this can be the endpoint of secondary drying.

Fig. 10: Secondary Drying profiling of residual moisture as a function of cycle time. A sample thief was used to manually stopper vials at different intervals from the end of primary drying (35 hours) to the end of the secondary drying interval (55 hours). The samples were analysed using Karl Fischer moisture analysis to find a point where maximum moisture loss for that time period occurred.

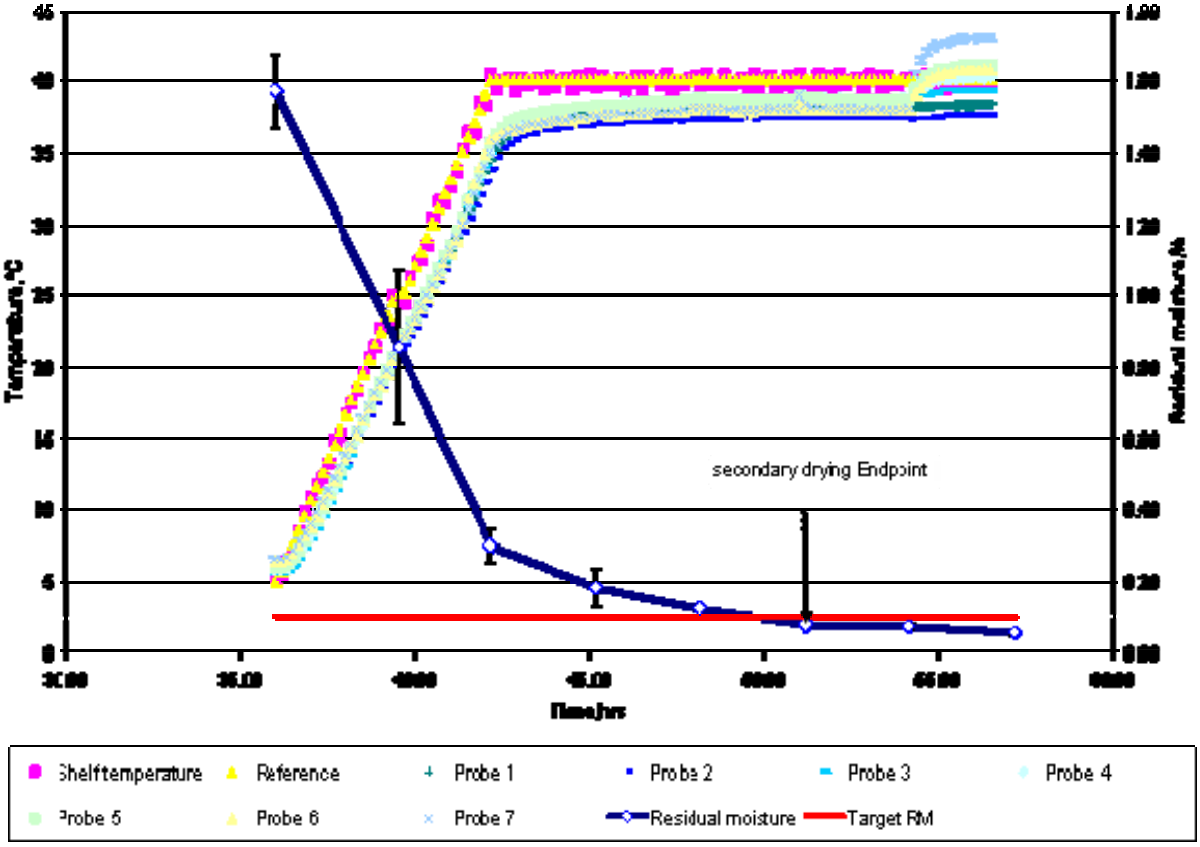

In figure 10, the blue line is the residual moisture of various samples from the same cycle measured using Karl Fischer and trended as a function of cycle time. The red line represents the target residual moisture (in this case 0.1%). Both these lines trend to the secondary y axis. The remainder of the lines are the shelf and product temperatures which trend closely together due to the fact that this trend illustrates secondary drying. This secondary drying step consists of a ramp from 5°C to 40° and a hold at 40°C.

2.3.2 Secondary Drying Cycle Step design

The desired residual moisture level in a lyophilised product dictates the design of the secondary drying step (Wang, 2000). An optimum secondary drying step requires higher temperatures compared to primary drying (Pikal et al., 1990). As the temperature increases, the rate of drying (desorption rate) increases. As a result, the time required to achieve a given level of residual moisture decreases sharply as the product temperature increases. The drying rate also increases with an increase in the specific surface area of the product (Pikal et al., 1990). Smaller ice crystals generally result in faster secondary drying rates along with increased product resistance (Rambhatla et al., 2004). However, with increased product resistance comes slower primary drying rates (longer primary drying time) due to the larger surface area created by the smaller ice crystals (Pikal et al., 1983).

As drying rates may be variable within a given sample, secondary drying may proceed simultaneously with primary drying even within the same sample (Pikal et al., 1990). The chamber pressure has not been found to affect the secondary drying rate to any marked extent (Pikal et al., 1984).

2.4 Lyophilisation above the Collapse Temperature

A significant number of studies (Leuckel et al., 1998; Pikal & Shah, 1990; Wang et al., 2003; Passot et al., 2007; Schersch et. al., 2010) have been conduced over the last number of years investigating the phenomenon of lyophilisation above the collapse temperature, which greatly reduces the primary drying step time. A number of the studies concentrated on the freeze drying of proteins in different buffers and others examined the phenomena with different ratios of amorphous: crystalline components.

Chatterjee et al. (2005) showed that there was no detrimental effect of primary drying above Tg' on the recovery of lactate dehydrogenase (LDH) when LDH was lyophilized in glycine: raffinose and glycine: trehalose formulations. With amorphous to anhydrous sugar ratios of 1.5:1 or greater, it was shown that it was possible to dry the protein product above the collapse

temperature and not have any effect on the initial results. However, it was shown that there was a loss of activity after 6 months of storage at temperatures of 4°C and 25°C. Actual results showed that loss increased from 0% to 25% from drying below collapse to drying above the collapse temperature over a 6 month period. Leuckel et al. (1998) demonstrated that collapse of the lyophilized cake resulted in an increase level of aggregation of Interleukin-6 (IL-6) in a glycine: sucrose formulation.

Passot et al. (2007) investigated the effect of collapse on lyophilized toxins at low protein concentrations of $1 \mu g.mL^{-1}$. It was found that crystalline mannitol provided an effective mechanical resistance during lyophilisation, which enabled performing primary drying at product temperatures that were above Tg' and resulted in acceptable product cake. However, it was documented that the collapse temperature was found to be much higher than that of Tg' for mannitol based formulations. In this paper, freeze drying above the collapse temperature for mannitol based formulations was not examined. For the 4% PVP and 1% sucrose formulation, considerable shrinkage was observed when freeze drying above the Tc, which affected cake appearance. Overall, the antigenic activity was measured after lyophilisation and after 6 months of storage. Losses in antigenicity was found for all formulations examined from 0% for primary drying below Tg', to 25% when performed above Tg'.

Wang et al., (2003) examined different intensities of collapse on low concentration protein based formulations containing Factor VIII and α-amylase. It was shown that for 4°C and 25°C 60% relative humidity storage conditions that there was no positive or negative affect on the activity over time. It was shown that at 40°C conditions, stability was improved over a 6-month period.

3.0 PROTEIN STABILITY

While a lyophilised protein formulation is generally more stable than that of an aqueous formulation, chemical and physical degradation can occur (Hageman, 1992; Pikal et al., 1991; Carpenter et al., 1997). The instability of proteins can be broken into two categories: chemical and physical. Chemical instability involves a covalent modification of a protein or amino acid to produce a new molecule, whereas physical instability refers to a change in the three-dimensional structure, not necessarily involving covalent modifications (Lai & Topp, 1999).

The factors impacting the chemical stability of a protein in lyophilised form is that of residual moisture content and the excipients used in the formulation (Lai & Topp, 1999). Physical processes include denaturation, aggregation, precipitation and adsorption to surfaces (Manning et al., 1989). Chemical instability can be as a result of one of the following chemical reactions: deamidation, proteolysis, oxidation, maillard reaction, and β-elimination (Lai & Topp, 1999).

3.1 Reactions resulting in Chemical Instability

The purpose of the lyophilisation process is to minimise reactions within the product, which, in turn, prolongs shelf life. This is achieved by removing the water, which is necessary for reactions to occur. The following are a number of chemical reactions that may occur in protein solutions:

3.1.1 Deamidation

A side chain amide linkage in a Gln or Asn residue is hydrolysed to form a free carboxylic end (Xie & Schowen, 1999; Manning et al., 1989). While there has been evidence to suggest that deamidation occurs in solution, few reports suggest deamidation in the solid state (Lai & Topp, 1999).

3.1.2 Proteolysis

Peptide bonds of Asp residues are cleaved in dilute acid at a rate of 100 times that of other peptide bonds (Manning et al., 1989). Lyophilised human Relaxin formulated with glucose can

undergo hydrolytic cleavage of the C-terminal Serine (Ser) residue on the β-chain (Trp28-Ser29-COOH) upon storage at 25°C (Li et al., 1996).

3.1.3 Oxidation

The side chains of His, Met, Cys, Trp and Tyr residues in proteins are potential oxidation sites (Manning et al., 1989). It has been reported that with minimal oxygen in the vial headspace (~0.05%), decomposition via oxidation is equal to or greater than decomposition due to deamidation (Pikal et al., 1991). Oxidation will adversely affect the protein product (Pikal et al., 1991). It has been found that both oxygen content and light exposure can affect the oxidation rate (Franson et al., 1996).

3.1.4 Maillard Reaction

The maillard reaction is also known as browning (Jennings, 1999). The maillard reaction occurs when reducing sugars (Li et al., 1996), e.g. lactose, glucose, and maltose, react with free amino or amide groups in proteins, leading to changes in chemical and physical properties (Hageman, 1988).

3.1.5 β-Elimination

High temperature inactivation of proteins often results in the destruction of disulfide bonds as a result of the β-Elimination from the cysteine residue. The resultant thiol groups from the reaction will contribute to other degradation pathways e.g. aggregation, precipitation (Manning, 1989).

3.2 Factors Affecting Chemical Instability

The chemical reactions listed above, are affected by many factors. The following lists some of those factors:

3.2.1 Temperature

Exposure of proteins to extreme temperatures can decrease chemical stability by increasing the chemical degradation rate. An example of this is the deamidation of Asn-hexapeptide increases with increasing temperature (Manning, 1989).

3.2.2 Moisture

Lyophilised protein formulations are more stable at lower moisture contents (Pikal et al., 1991; Hageman, 1992). Lai & Topp (1999) reported that the molecular mobility of a lyophilised protein formulation increases with increasing moisture content. The rate of degradation of Asp-hexapeptide increases as the moisture increases (Lai & Topp, 1999). Deamidation has also been reported to increase with increasing moisture (Oliyai et al., 1994). It has been reported that physical stability of monoclonal antibodies could be even enhanced by increasing residual moisture if stored below the Tg temperature of the lyophilized cake (Breen, 2001).

3.2.3 Excipients

Excipients used in the protein formulation protect the protein from damage during lyophilisation and during long-term storage (Lai & Topp, 1999). However, excipient selection is crucial, as excipients can also influence the stability of a protein in solid state (Jennings, 1999). Reducing sugars are known to react with proteins via the maillard reaction (Hageman, 1992).

3.2.4 Hydrogen Ion Activity

Lia & Topp (1999) have reported a strong correlation between the chemical stability of a protein and the pH of the formulation. Shifts in pH during the freezing step of the lyophilisation cycle are common (Jennings, 1999). In order to minimise pH shifts during freezing, the weight ratio of buffer to other solutes should remain low.

3.2.5 Physical State of the Solid

Upon cooling and crystallization of a bulk formulation, two physical states can exist: Crystalline and Amorphous (Jennings, 1999).

Crystalline - The crystalline drug morphology is generally less prone to chemical degradation than the amorphous form. However formulations, which are at least partially amorphous, appear to be more efficient in protecting the protein against degradation (Pikal et al., 1991). The mechanism behind this is that the crystalline bulking agent (e.g. crystalline mannitol) structurally supports the cake minimizing or removing collapse as an entity even if primary drying has been conducted above the collapse temperature of the formulation.

Amorphous - At low temperatures and low residual moisture content, amorphous solids are said to be brittle, hard and viscous. This state is known as the 'glassy' state. With an increase in the temperature and moisture content (i.e. T>Tg'), the solid converts from the 'glassy' state to what is known as the 'rubbery' state (Lai & Topp, 1999). The reaction rates and mobility associated with the protein product generally increased when deamidation and aggregation was greatly accelerated with temperatures above Tg' (Levine & Slade, 1993; Chang et al., 1993). Thus, an increase in product temperature above Tg' can be detrimental to the protein. The nature of the product must be considered when designing an optimum Lyophilisation cycle.

3.3 Physical Instabilities

Proteins can undergo a variety of structural changes independent of chemical modification, due to their polymeric nature and ability to adopt some form of superstructure (Manning, 1989). The physical instabilities can be one of denaturation, aggregation, precipitation and surface adhesion (Manning, 1989).

3.3.1 Denaturation

This is the alteration of the global fold of a molecule i.e. disruption in structure (Creighton, 1993). Denaturation is often equated with protein instability. It may be reversible or irreversible,

and is caused by a variety of conditions, including temperature variation, extreme pH and the introduction of organic solvents (Manning, 1989).

3.3.2 Aggregation

Aggregation is the development and interaction of partially folded intermediates during the process of denaturation (Manning, 1989).

3.3.3 Precipitation

This is the macroscopic equivalent of aggregation. Like aggregation, precipitation occurs in conjunction with Denaturation (Manning, 1989).

3.3.4 Surface Adsorption

Surface adsorption includes the adhesion of proteins to surfaces such as intravenous bags; or delivery pumps (Manning, 1989).

4.0 PROJECT AIM

Primary Drying is traditionally the longest step in the lyophilisation cycle. During this step, the product is at most risk to degradation and various techniques are utilized to design this step with the end goal where the product is dried aggressively to minimize process time while also minimizing product degradation that might result from temperature and pressure stresses during the cycle. For many years, the primary drying step was conducted in such a way that the product temperature was maintained below the collapse temperature to ensure stable and effective drying (Bellows & King, 1972; Pikal & Shah, 1990). Due to the potential of a long primary drying step (depending on the formulation make up, heat transfer, vial configuration and liquid fill volume), optimization has a significant economic benefit because an overall reduction in the lyophilisation cycle time will reduce processing costs and improve the processing capacity and in turn, the annual batch manufacturing throughput (Pikal – Part 2, 1990).

Varying opinions on the effect of micro collapse during lyophilisation on the long term stability of a protein drug product have appeared in the literature (Pikal & Shah, 1990; Passot et al., 2007; Chatterjee et al., 2005; Wang et al., 2003). It has been extensively reported that micro and gross collapse of partially crystalline/ partially amorphous protein drug products exhibit higher moisture content, slower reconstitution time, uneven product dryness, loss of texture and compromised appearance (Bellows & King, 1972; Pikal & Shah, 1990; Mackenzie, 1976) High residual moisture content may lead to higher levels of protein aggregation. It has been reported that the collapse can cause product degradation and effect product stability (Mackenzie, 1976; Passot et al., 2007; Schersch et. al., 2010). Contrary to this, Chatterjee et al. (2005) and Wang et al. (2003) demonstrated that freeze-drying above microscopic collapse temperature did not have significant impact on protein quality.

The effect of collapse on protein stability (Passot et al., 2007; Wang et al., 2003; Lueckel et al., 1998) and also the effect of various bulking agents on the appearance and structure of the lyophilized cake (Shalaev & Franks, 1996) have been examined. Indeed a number of patents have been filed with respect to performing primary drying above the microcollapse temperatures

for monoclonal antibodies (Colandene et al., 2006) and proteins of various concentrations and excipient combinations (Tchessalov et al., 2010).

There is a divide (Passot et al., 2007; Chatterjee et al., 2005; Wang et al., 2003; Lueckel et al., 1998) on the exact significance of drying above the collapse temperature. Therefore we set out to examine the effect of drying below and above collapse for a 150 kDa fusion Protein and BSA, a common protein, of 66kDa, in a number of formulations that were either mannitol or glycine based. These excipients readily crystallized during the freezing step to maximize cake support upon drying above the critical temperature. For the purposes of the project, protein concentration was set far above those that were reported in a literature related to freeze-drying above microscopic collapse temperature.

5.0 MATERIALS AND METHODS

5.1 Excipient Formulation Selection

Fraction V BSA (Sigma Aldrich) was used for the purposes of this project. Protein X (proprietary protein) in Mannitol – Sucrose – Tris (25mg.mL^{-1} protein concentration) was provided by the Purification Development department at Wyeth Biotech, Grange Castle, Ireland for the purposes of this project. This was the only formulation of Protein X used for further processing. The specific activity of the proprietary protein is 1.7x10^{6} units/mg. All formulations containing BSA were formulated to a target protein concentration of 25mg.mL^{-1}. The following are the suppliers and grades of all excipients used during these experiments:

- Mannitol – Sigma, excipient grade
- Glycine – JT Baker, USP grade
- Sucrose – Sigma, excipient grade
- Sodium Chloride – Merk, USP grade
- Tromethamine – JT Baker, USP grade
- Tris HCl – JT Baker, Bioreagent, made from USP grade Trimethamine

Mannitol and Glycine were chosen to form the basis of each formulation, as these excipients are extremely common bulking agents in the field of formulation design for the purposes of lyophilisation. Mannitol and Glycine both readily crystallize under certain conditions. These conditions may be produced during the freezing step of the lyophilisation cycle. It is known that the crystalline bulking agent provides structural support to the cake, allowing primary drying to be performed at more aggressive conditions (Dixon et al., 2008). Sucrose was chosen as the cyroprotectant. Four formulations in all were designed, two of which contained 100mM NaCl, which was used to reduce the overall glass transition temperature, simplifying the design of a freeze drying cycle (primary drying step) above the Tg'/ Tc. The buffer of choice was Tris buffer at a pH of 7.0. A ratio of bulking agent to sucrose of 4%:1% (w/v) was used during this study. It was reported that this ration is the optimum bulking agent to cyroprotectant ratio that should be used when designing a formulation for freeze drying (Pikal, 1990b). The following is a list of the formulations used for the purposes of this study:

1. 4% w/v Mannitol 1% w/v Sucrose 100mM NaCl 10mM Tris pH 7.0 (Buffer 1)
2. 4% w/v Mannitol 1% w/v Sucrose 10mM Tris pH 7.0 (Buffer 2)
3. 4% w/v Glycine 1% w/v Sucrose 100mM NaCl 10mM Tris pH 7.0 (Buffer 3)
4. 4% w/v Glycine 1% w/v Sucrose 10mM Tris pH 7.0 (Buffer 4)

Each of the protein formulations were processed through a mixing, pH adjustment and a UF/DF (buffer exchange) step prior to filling and lyophilisation. Each of the protein formulations were then transferred to approximately 66 x 5mL glass vials (target 0.5mL or 2mL fill volume per vial), loaded into a lyophilizer and dried using one of two lyophilisation cycles (section 5.4). The output of each cycle was analysed using various analytical tools over a 6 month period at one of three storage conditions. This section details the materials and methods used to generate each of the protein formulations, freeze dry and analytically assess during selected storage conditions over a 6 month period.

5.2 Low temperature modulated Differential Scanning Calorimitery (LT mDSC)

The mDSC was executed based on the ASTM standard method (ASTM Method E 1356-08). DSC measurements were made with a modulated DSC (model Q1000, TA Instruments) equipped with a refrigerated cooling system (RCS). The temperature and cell constant were calibrated with indium (156.6°C) in hermetically sealed aluminum pans heated at 0.5°C/min with a nitrogen cell purge of 50 mL.min-1. Liquid samples of the protein formulations (~10mg) were sealed hermetically in aluminum pans and placed in the mDSC autosampler.

The general procedure is to weigh out ~10mg of a liquid or solid sample in a hermetic aluminium pan and crimp using a specific TA instruments crimper with an aluminium seal. In parallel, a reference is made up in the same way but without a sample. The recipe was loaded into the system through the TA Instruments mDSC software and the cycle is started. The autosampler transferred the reference and sample to the heating block where the heat was applied in order to generate a heat flow. This heat flow is captured on a thermograph, which may be analyzed and further broken down into more signals related to the overall heat flow as per figure 11.

To analyze the sample, the thermograph was adjusted to trend the heat capacity and kinetic signals (also known as the reversing and non reversing heat flow) along with the total heat flow. Equation 4 illustrates components of the total heat flow of a sample i.e. heat capacity and kinetic components. From equation 4, it is evident that the total heat flow is a product of the heat capacity and kinetic components.

$$\frac{dH}{dT} = Cp(\frac{dT}{dt}) + f(T,t) \quad \text{(Eq. 4)}$$

Figure 11 shows the total heat flow along with the reversing and nonreversing heat flow. The green signal illustrates the total heat flow, the blue line illustrates the reversing heat flow and the brown line illustrates the nonreversing heat flow. This figure was generated using the recipe found on table 2.

Fig. 11: Thermograph showing the Total Heat Flow, Reversing and Nonreversing signals of a particular sample prior to analysis. To generate the axes on this thermograph, the signal selector was used which can be found in the universal analysis software. The total heat flow can be broken into the reversing and non reversing heat flow as per equation 4. The green line represents the total heat flow, the blue line, the reversing heat flow and the red line represents the non reversing heat flow. The pink line represents the reversing heat capacity signal.

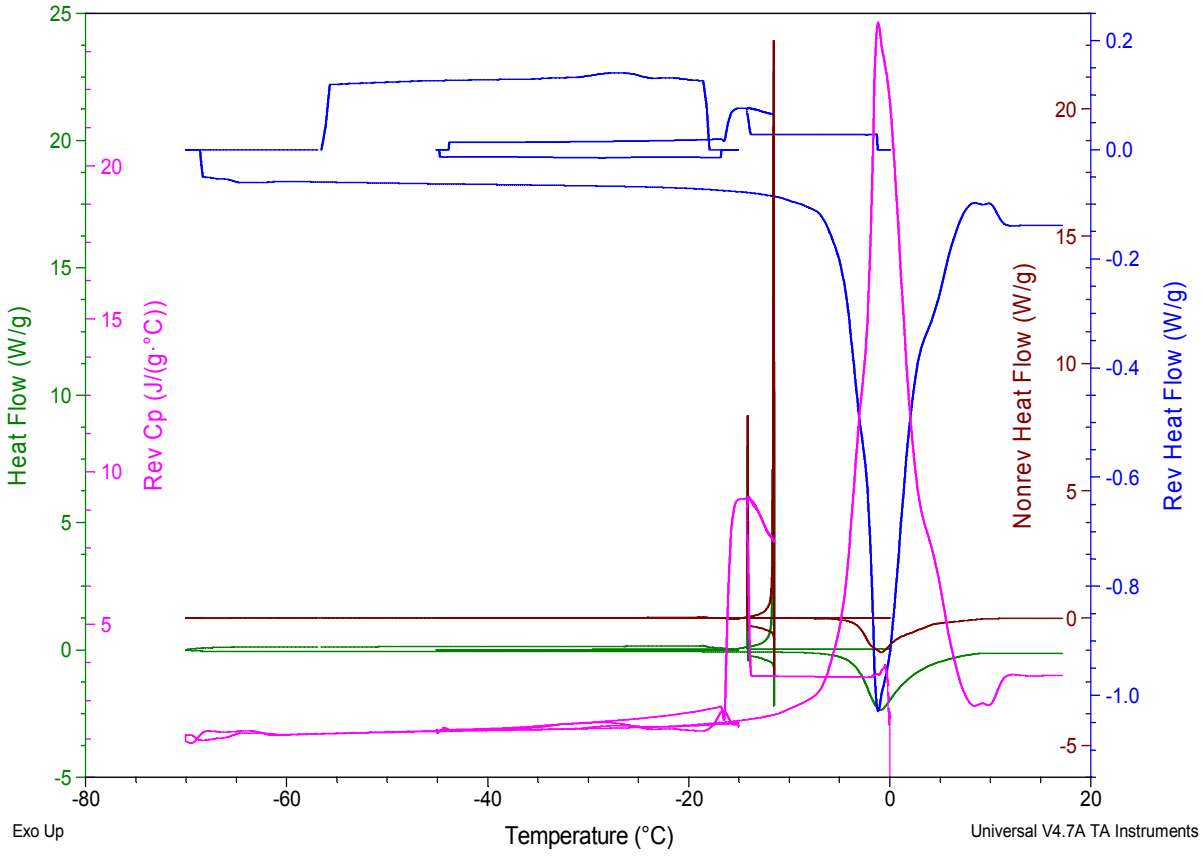

In analyzing the sample using Universal Analysis© software, certain transitions can be identified on certain heat flow signals. They can be broken down as follows:

Total Heat Flow - Total melting; Reversing Heat Flow – glass transition temperature (sub ambient and upper – Tg' and Tg), Melting (some); Nonreversing Heat Flow: Crystallization, Melting (some), Enthalpic Relaxation, Decomposition, Evaporation, Cure; Reversing Heat Capacity – Tg', crystallization of bulking agent, annealing time (Tan).

The total heat flow is the product of the reversing heat flow and the non reversing heat flow (equation 4).The reversing heat capacity is the opposite to the reversing heat flow but is more sensitive to certain transitions. For example, if the Tg' is not detected on the reversing heat flow, it may be evident by examining the reversing Cp signal. From a Lyophilisation cycle design viewpoint, the most important elements are the Tg', Tcrys of bulking agents e.g. Mannitol and Glycine and the Tm.

Modulated DSC was executed for each protein formulation to measure Tg' in the lyophilisation cycle development stage of the project. Once the Tg' was measured for each formulation, it was possible to design the microscopy recipes to measure Tc. It was introduced earlier that Tg' and Tc are the most critical temperatures to consider when designing a lyophilisation cycle for an amorphous or partly amorphous – partly crystalline formulation. In the case of this project, each formulation contained both amorphous and crystalline components.

Table 2 lists the mDSC recipe used for all protein buffer formulations. Once Tg', Tcrys and Tm were measured for each protein buffer formulation, it was possible to design the freeze-drying microscopy (FDM) recipe. An annealing step was used in the recipe in order to crystallize the bulking agent i.e. Mannitol or Glycine. The hold step during annealing was set at 180 minutes in order to ensure that the crystallization transition fully completed.

Table 2: mDSC Recipe for Thermal Analysis of all Protein Formulations. This recipe was entered into the mDSC software and contained annealing as pert of the freezing step. The purpose of annealing in this case was to crystallize the bulking agent (either mannitol or glycine depending on the formulation).

Step	Step Description
1	Equilibrate at 0°C
2	Modulate ±0.5°C every 100 seconds
3	Ramp 0.5°C/min to -45°C
4	Isothermal (hold) for 90 minutes
5	Ramp 5°C/min to -15°C
6	Isothermal for 120 minutes
7	Ramp 5°C/min to -70°C
8	Isothermal for 5 minutes
9	Ramp 2.5°C/min to 25°C
10	End of Method

Analysis of each sample was possible using Universal Analysis software© (TA Instruments), which is compatible with the TA instruments mDSC operating software. Each sample generates a heat flow as a function of temperature.

5.3 Freeze Drying Microscopy (FDM)

The collapse temperature of the protein formulations was measured using a Cryostage suitable for vacuum operations (Model FDCS 196, Linkham Scientific Instruments, Tadworth, Surrey, UK) and viewed with a polarizing microscope (Olympus, Model BX51, Biopharma Accessories and Components, UK). The stage was calibrated with a 5% sodium chloride water solution (Tm = -21.1°C).

A 1µl sample was placed in a quartz crucible and covered with a 9mm cover slip, causing the solution to spread evenly over the area of the smaller cover slip. The sample was secured within the stage and was cooled using liquid nitrogen to the target freezing temperature as per the cycle

recipe. A vacuum was the enabled using a vacuum pump to levels of 100μbar to enable drying and the temperature of the product was increased using a heat exchanger until collapse was evident. The sample was recorded over the drying time period at a magnification of 10x.

Table 3 shows the initial freeze-drying recipe used to determine the collapse temperature for each protein formulation. During the analysis, the temperature at which collapse occurs was determined. However, to precisely verify the collapse temperature, a second experiment was conducted for each formulation, using slower temperature ramp rates (0.5 - 1°C/min) and longer hold times (up to 30 minutes). These new conditions allowed the precise measurement of the Tc and the subsequent comparison to Tg' measured using mDSC. It has been well documented that for amorphous systems (in this case, formulations not containing sodium chloride) the Tg' and Tc are very close and sometimes within 1°C of each other (Pikal et al., 1990).

Table 3: Initial Freeze Drying Microscopy recipe for all Protein Formulations. The vacuum was initiated during the -45°C hold step and the temperature was increased stepwise until collapse was observed.

Step	Rate (°C/min)	Limit (°C)	Time (mins)
1	5	0	0
2	1	-45	30
3	1	-15	180
4	5	-45	15 (start vacuum)
5	2	-40	10
6	2	-30	10
7	2	-20	10
8	2	-10	10
9	2	0	10

5.4 Lyophilisation

Lyophilisation was performed on a Virtis Benchmark 1000 Lyophilizer (Biopharma, Winchester, UK). The Lyophilizer chamber contained 3 shelves which had the capacity of 291 x 5mL Schott

vials (Schott, USA) on each shelf. Five (5) type T thermocouples (Biopharma, Winchester, UK) were connected to the main lyophilizer chamber. All five formulations were lyophilized at the same time for each lyophilisation cycle. Each protein formulation product temperature was monitored during each lyophilisation cycle. As part of the set up, approximately 66 x 5mL vials were filled for each formulation. Each vial was partially stoppered with a 13mm siliconized stopper (West, USA) after filling. This was performed for each formulation and for each lyophilisation cycle. A total of 2 lyophilisation cycles were executed as part of this study. The fill volume varied between lyophilisation cycles. After the lyophilisation cycle, the vials were stoppered using a hydraulic stoppering system and sealed with 13mm overseals. Stoppers were dries at 100°C in a laboratory oven for 12 hours

The samples generated were labelled and transferred to a -40°C freezer after the lyophilisation step. Once all the cycles were sampled, the vials of product were transferred to the stability chambers and sampled at intervals for 6 months. Vials from each formulation were transferred to one of the following stability storage conditions:

1. 4°C
2. 25°C 60% Relative Humidity
3. 40°C 75% Relative Humidity

Samples were tested at times 0, 1 month, 3 months and 6 months using combinations of the following analytical methods: Reconstitution, powder Differential Scanning Calorimetry (pDSC), Karl Fischer (KF), Size Exclusion Chromatography (SEC) and Circular Dichroism (CD).

For lyophilisation cycle 1, a fill volume of 0.5mL was used and for the second lyophilisation cycle (lyophilisation above total collapse), a fill volume of 2mL was used. Prior to the execution of the lyophilisation cycle step, 66 vials are filled with 0.5mL or 2mL of liquid formulation (5 formulations) depending on the cycle and transferred onto the lyophilizer shelves to be processed. After each Lyophilisation cycle, the vials were stoppered under a 500mbar headspace pressure of nitrogen, the chamber was subsequently aerated to atmospheric pressure with process

air and the vials were unloaded. The lyophilizer condenser was left to defrost over night. Prior to the next Lyophilisation cycle, the chamber was cleaned with 70% IPA. Figure 12 shows an empty 5mL vial that is partially stoppered.

Fig. 12: Stopper: Vial Configuration used during each to Lyophilisation Cycle. This image represents a typical glass 5mL vial and 13mm rubber lyophilisation stopper used during this project. For lyophilisation cycle 1, 0.5mL of each protein formulation was transferred using a calibrated pipette into 66 vials. For lyophilisation cycle 2, 2 mL of each protein formulation was transferred using a calibrated pipette into 66 vials.

The high fill volume for the second cycle was used because the cycle time was short due to the target product temperature of 0°C. The first cycle was designed around the lowest Tg', which was measured at approximately -44.59°C.

Each tray of vials was filled, partially stoppered and transferred onto a shelf within the chamber. The tray was removed from under the vials, resulting in the vials being in direct contact with the shelf within a stainless steel ring. This was repeated for each tray of vials. Figure 13 shows the empty vial configuration within a stainless steel ring and on a stainless steel tray. The vials take the shape of a honeycomb structure

Fig. 13: Vial configuration within a given tray. The vials were placed in the form of a honeycomb structure to maximize the number of vials per tray and to maximize heat transfer by ensuring maximum vial to vial contact.

Figure 14 represents a tray of vials, filled with a given protein formulation and partially stoppered ready for loading into the freeze dryer. Product thermocouples were positioned in the

centre of the vial pack. Stoppers were placed in empty vials on the corners to allow stoppering to occur without damaging the shelves.

Fig. 14: Vial, product and thermocouples set up for a given Lyophilisation cycle. The corner vials were empty for the purposes of this experiment. The vials were stoppered in order to ensure that an even weight distribution was placed on the vial pack upon shelf stoppering. The black stoppers represented the vials with the thermocouples.

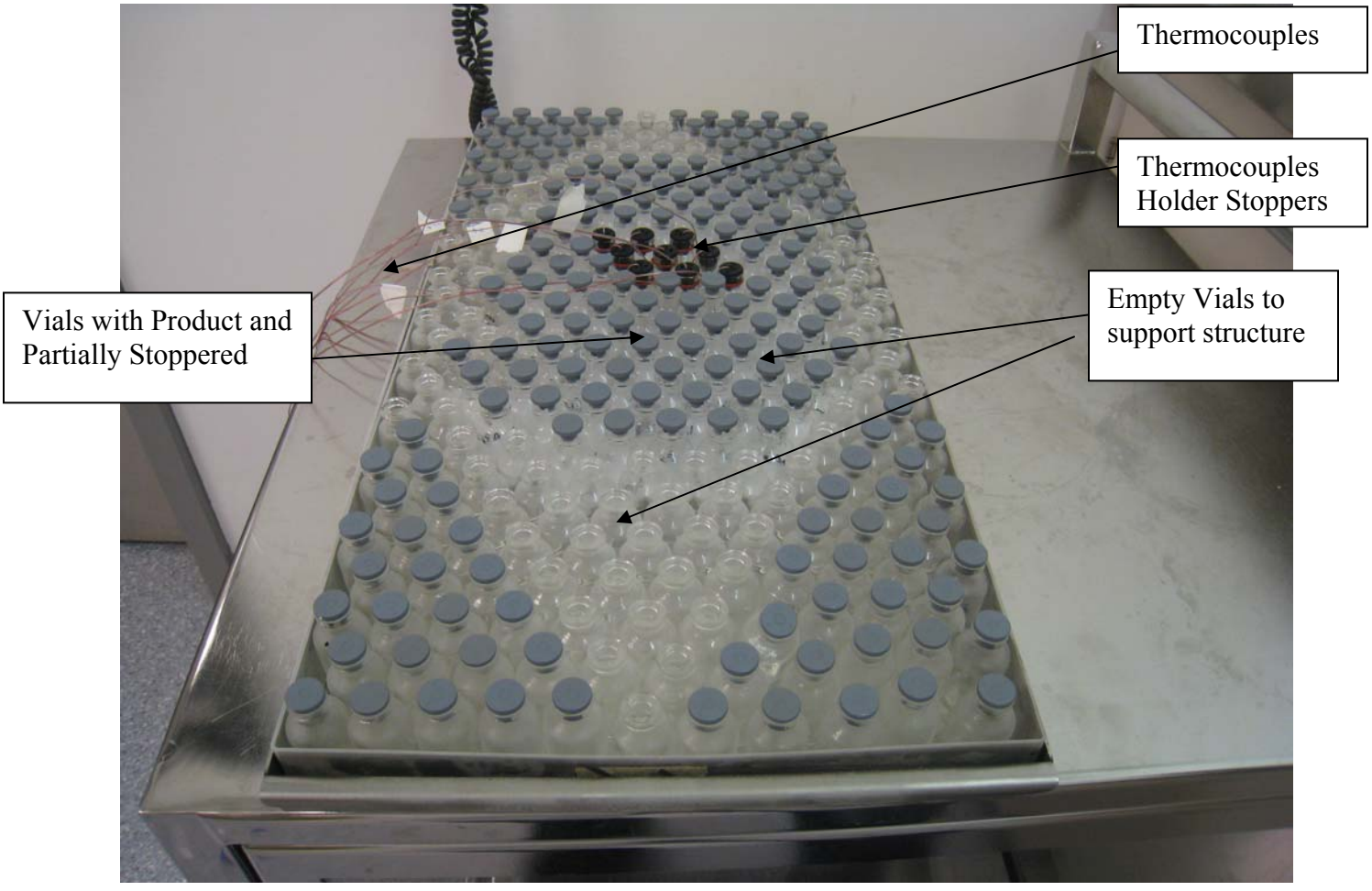

All product vials including thermocouple vials were located within the centre of the vial pack to remove the effects of radiation on the product temperature. Vials located on the edge of the shelf experience radiation, which results in a higher heat transfer coefficient (Kv) and a higher product temperature. The intention of this project was to examine the radiation effects on the edge vials.

Figure 15 shows the complete lyophilizer set up located in the laboratory. Note the SCADA system screen located on the desk behind the machine. This computer application is used to control the lyophilizer.

Fig. 15: Virtis Benchmark 1000 Lyophilizer

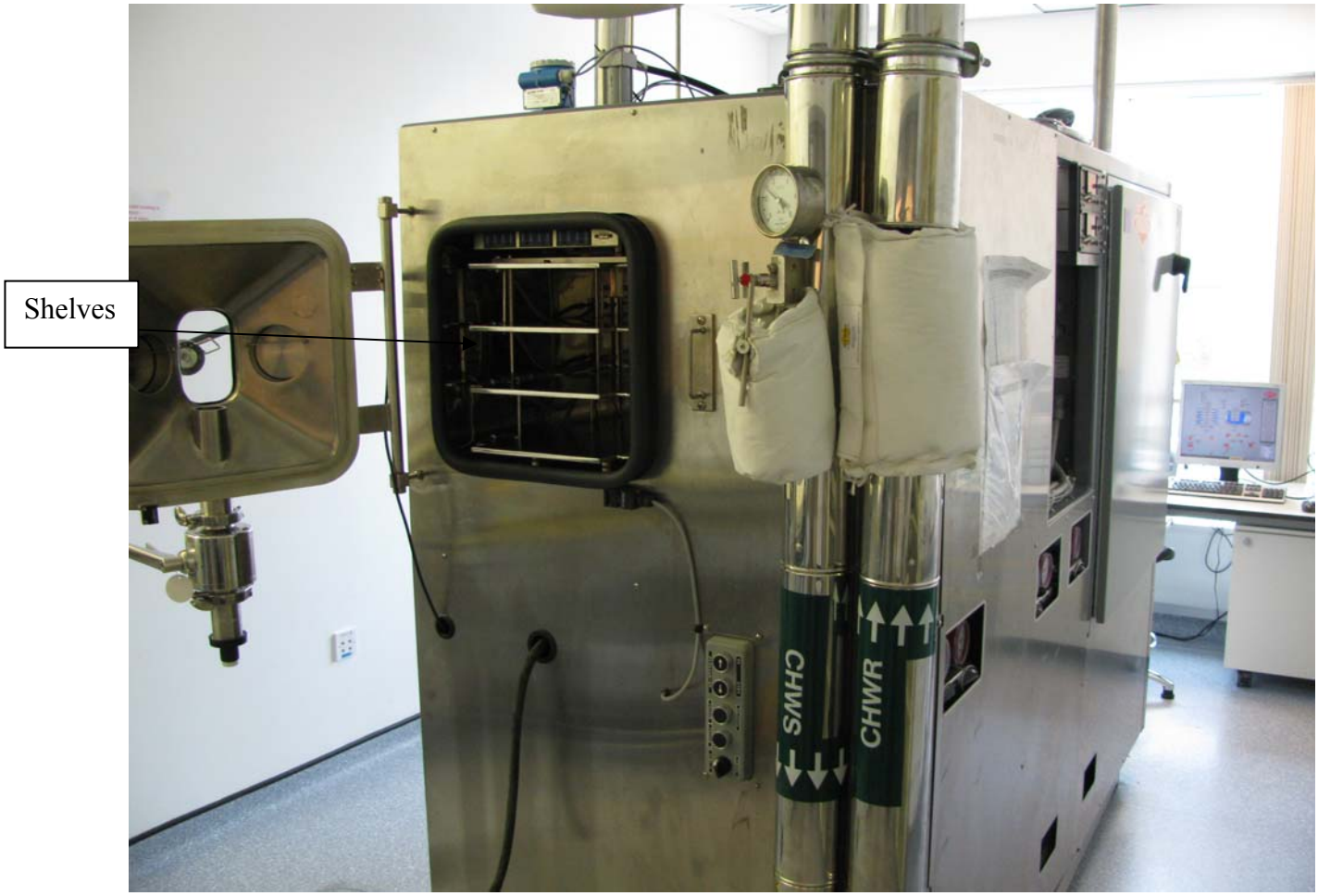

Figure 16 represents an image of the lyophilizer chamber taken from the loading door side of the lyophilizer. The chamber consists of three shelves which can be cooled and heated via silicone oil which is fed through a closed system into the shelves. The silicone oil system consists of a heat exchanger to heat the shelves. The silicone oil was cooled via a refrigeration system located in the bottom of the lyophilisation set up.

The temperature of the shelves was controlled by circulation of heat transfer fluid (HTF) through internal channels within the shelves. The HTF temperature was heated by an electric heating system. The shelf temperature was controlled at a setpoint by the two systems working hand in hand in the form of PID control. The 12 ports at the top of the chamber represent the connection points for 12 type T thermocouples for shelf temperature and product temperature mapping.

Up to eight thermocouples were used for product temperature mapping during each experiment. It is also possible to see the vapour tube at the rear of the chamber. This tube allowed the water vapour to transfer into the condenser during sublimation.

Fig. 16: Image of the Virtis Benchmark 1000 Lyophilizer Chamber taken from the loading door side.

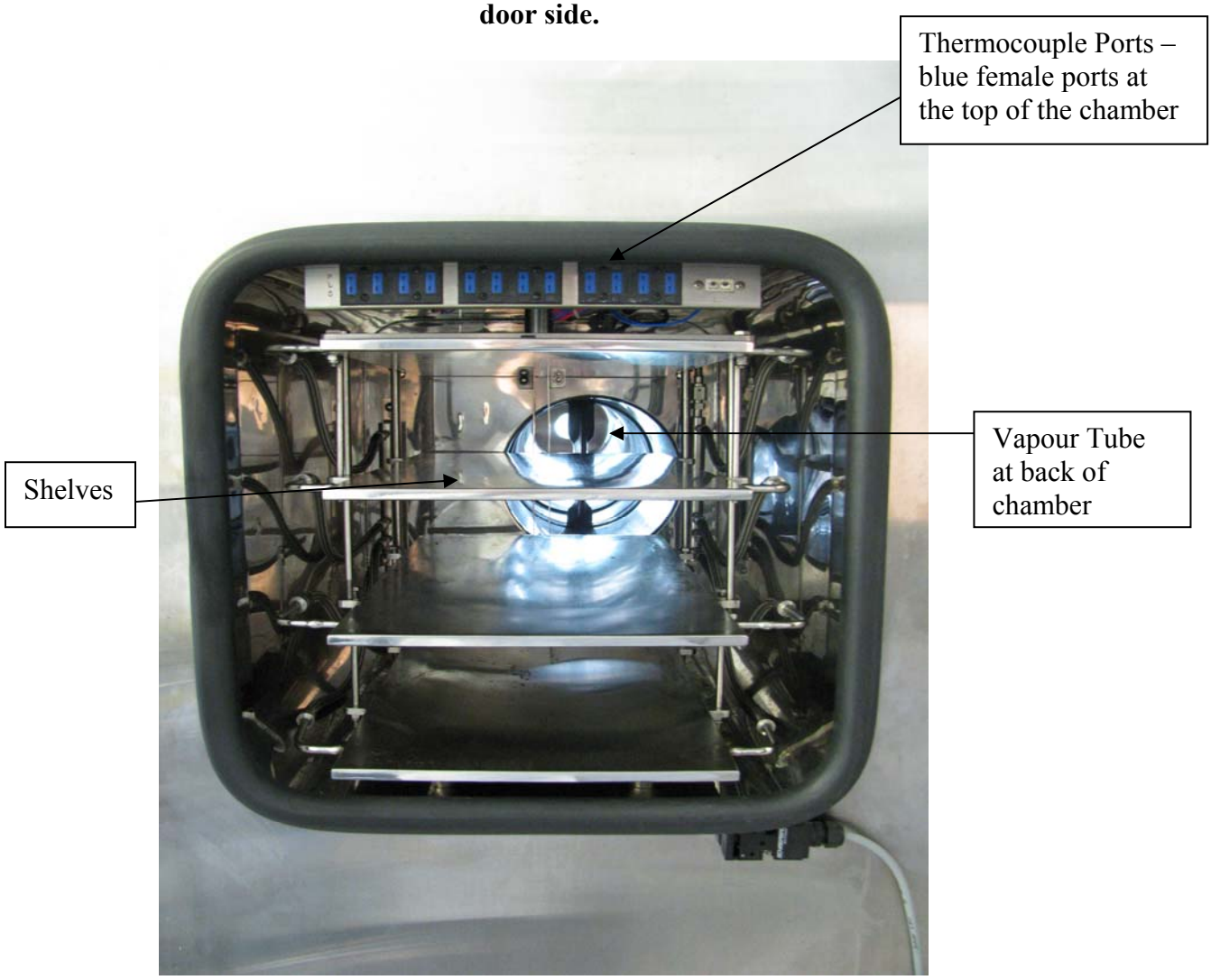

Figure 17 shows the condenser chamber located at the rear of the lyophilizer chamber. The condenser is made up of a number of coils, which are cooled to temperatures below -70°C during the primary drying and secondary drying steps of the lyophilisation cycle. It is the condenser that forms the cold trap, which traps the vapour as ice on the coils.

Fig. 17: Virtis Benchmark 1000 Lyophilizer Condenser. The coils are cooled to temperatures as low as -80°C prior to vacuum initiation at the beginning of primary drying. The purpose of this is to create a vapour trap where the water vapour sublimed from the frozen matrix can solidify as ice. The temperature of the condenser created a slightly lower vacuum pressure in the condenser which results in a pressure differential between the chamber and the condenser, driving the vapour transfer from the product in the chamber to the coils of the condenser.

Figure 18 shows examples of a lyophilized product resulting from a 0.5mL and 2mL fill volume. The 0.5mL and 2mL lyophilized products are an example of a product that has not experienced

gross collapse. As the liquid product is colourless, the resultant lyophilized product is of white appearance.

Fig. 18: Lyophilized Product resulting from a 0.5mL and 2mL (resulting from the below and above collapse lyophilisation cycle) fill volume.

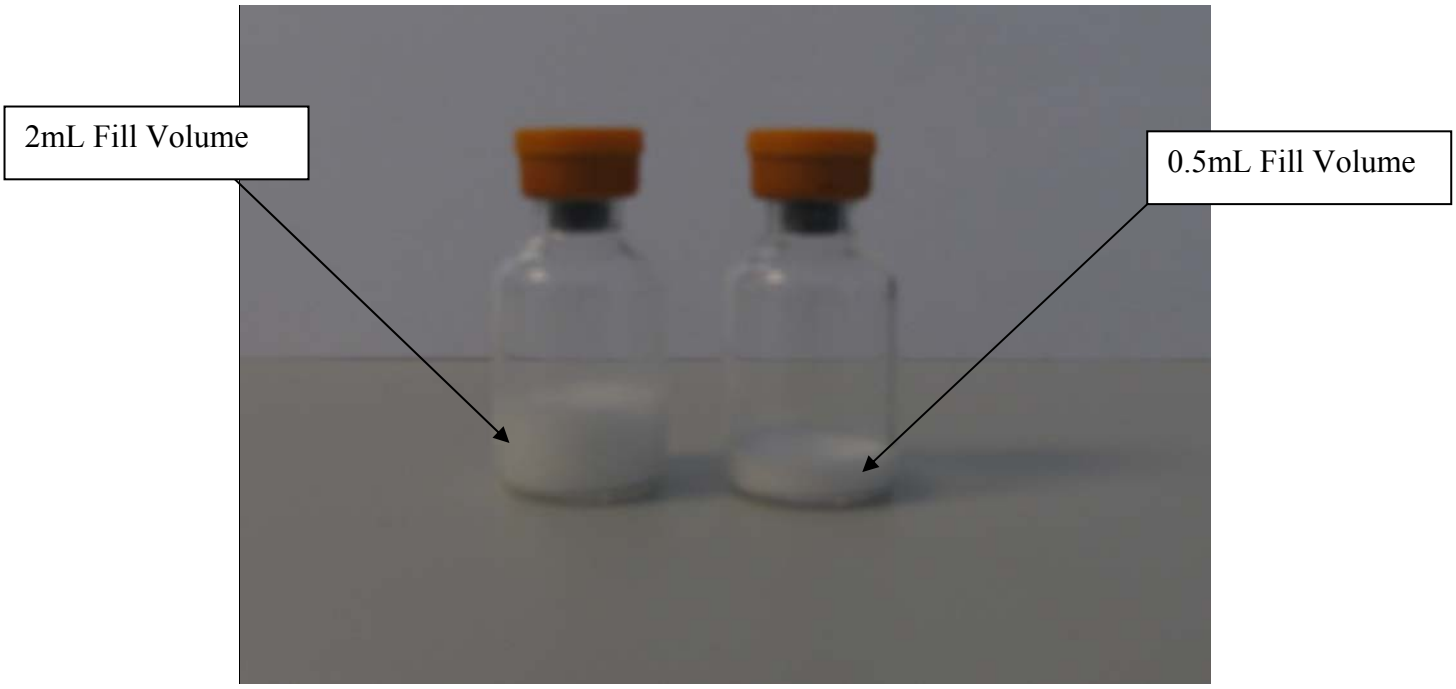

5.5 Visual Inspection

Post the lyophilisation cycles, all product vials were inspected to verify whether collapse was evident. Collapse was represented by a loss of structure and shrinkage of the lyophilized cake. Refer to section 2.2.2 and 2.2.3 for an introduction to collapse, with examples.

5.6 Reconstitution of the Lyophilized Product

Reconstitution was performed on each sample prior to analysis by SEC and CD where each vial was reconstituted with RO water prior to sample analysis. Reconstitution time is important when samples are freeze dried above the collapse temperature as collapse has been reported to yield longer reconstitution times (Pikal, 1990). Even if the reconstitution time is longer for collapsed

product (as detailed in the literature), the stability of the protein in liquid form during prolonged reconstitution may not be an issue.

A 0.5mL syringe was used for reconstitution of freeze dried product resulting from cycle 1 reconstitution and a 5mL plastic syringe was used for cycle 2 product reconstitution. The reconstitution time was measured using a laboratory timer. For lyophilisation cycle 1, the fill volume was 0.5mL, which was made up of approximately 8.0% solids content which equated to a removal of 0.46mL of water during the drying process. Similarly, for the second lyophilisation cycle, the fill volume was 2mL, which for 8.0% solids content required a rehydration volume of 1.85mL of water.

5.7 Karl Fischer Residual Moisture Analysis

Residual moisture content was determined using the Karl Fischer system equipped with a 756 KF Coulometer and 832 KF Thermoprep Oven (Metrohm, USA). The needle associated with the oven was injected directly into the cake. The temperature of the oven was set to approximately 115°C to drive the bound water from the lyophilized cake and in turn enable the measurement of the residual moisture.

The principle behind Karl Fischer moisture analysis involved heating a lyophilized cake using an oven to force the remaining bound residual moisture out of the cake. The vapour evolved from the cake is transported by nitrogen, the carrier gas, into a reaction vessel containing hydranal solvent. Iodine in the reaction cell reacts with the vapour in a 1:1 ratio, allowing the system to indirectly calculate the moisture content by measuring the iodine content.

5.8 Powder DSC – Thermal characterization of the dried (lyophilized) state

The mDSC was executed based on the ASTM standard method (ASTM Method E 1356-08). Powder DSC measurements were made with a modulated DSC (model Q1000, TA Instruments, USA) equipped with a refrigerated cooling system (RCS). The temperature and cell constant were calibrated with indium (156.6°C) in hermetically sealed aluminum pans heated at

0.5°C/min with a nitrogen cell purge of 50 mL.min-1. Powder samples of the protein formulations (~5 – 15 mg) were sealed hermetically in aluminum pans and placed in the mDSC autosampler. Each sample was transferred from a vial to the aluminum pan and lid under an inert environment created by nitrogen purging a glovebox to a humidity level of less than 5%. The pan and lid were crimped in the glovebox and then transported out of the glovebox and placed onto the autosampler along with the reference. This was repeated for each sample.
Modulated DSC (mDSC) was performed to measure the powder Tg for each sample at each storage condition and time point. Table 4 lists the mDSC recipe used for all samples. When analyzing a resultant thermograph, Tg can be observed by a shift in the reversing heat flow/ reversing heat capacity signal and crystallization may be observed as an exothermic peak on the non reversing signal. Melting is represented by an endotherm in the total heat flow signal.

Table 4: mDSC Recipe for Thermal Analysis of all Lyophilized Products

Step	Step Description
1	Equilibrate at -20°C
2	Modulate ±0.50°C every 100 seconds
3	Ramp 2.00°C to 250.00°C

Analysis of each sample was performed using Universal Analysis 2000 software ©, which is compatible with the TA instruments mDSC operating software.

The primary objective of powder DSC analysis was to examine the effect of the storage conditions on Tg, which should trend downwards with the increase in moisture as a function of time during stability. It was expected that the Tg temperature would change as a function of moisture transferred from the stopper into the product over time or due to potential crystallization events of excipients such as sucrose and any remaining amorphous mannitol/ glycine. An increase in moisture would have an expected lowering effect on the Tg as the Tg of amorphous ice is reported at around -135°C (Nail et al., 2002) which would drop the overall Tg' of the product as the water content increases.

Tg is very important in selecting storage conditions of a lyophilized product and setting up stability studies. Storing powder or lyophilized material above the powder Tg may result in an increase in protein aggregation or degradation (Dudde & Dal Monte, 1997). Also, it is important in assessing the impact of collapse on the lyophilized cake. In this case, the Tg is measured for each lyophilized formulation at all time points and storage conditions set in the stability section of this thesis. During storage of lyophilized products, moisture from the stopper transfers into the product over time, the rate of which is dependent on storage conditions. This must be assessed during storage at different time points. One of the ways to examine this is to monitor any changes in Tg over the set time.

Powder DSC may be used to identify and measure the temperature of amorphous excipient crystallization (Dixon et al., 2008). Most of the bulking agent should crystallize during the annealing step of the freeze-drying cycle. However, small amounts of amorphous bulking agent may remain in the dry product along with other excipients that do not readily crystallize during the freezing step, which means that crystallization of the amorphous material may occur over time. This crystallization transition can release bound or entrapped water (Dixon et al., 2008), which potentially affects the stability of the protein. This potentially affects the Tg and residual moisture content in the amorphous phase.

5.9 Size Exclusion Chromatography (SEC)

SEC is an analytical method used to quantitatively determine the relative quantity of high molecular weight (HMW) species, the protein molecule and potentially any buffer peak by separating molecules by their hydrodynamic volume (Harris, 1996). When the analyte is applied to the top of the column bed, molecules that are smaller than the pores of the packing material can diffuse into and out of the pores, whereas those that are larger do not enter the pores. As a result, the larger molecules pass through the column more quickly and the smaller molecules lag behind. Molecules between these extremes elute in order of their molecular size, which is generally proportional to the logarithm of their molecular weights (Harris, 1996). Once the species elute, they are detected by UV absorption at 280nm.

SEC was performed on an Waters Alliance HPLC system (Waters, USA) with a UV detector using a Waters YMC pack Diol-200 300 x 8mm ID column (10kDa to several 100kDa – upper not specified but both 66kDa and 150kDa well within the molecular weight range – refer to http://www.ymc.de/ymceurope/files/catalogue/Normal%20Phase.pdf) and filtered (0.22µm) 100mM sodium phosphate/150mM sodium chloride pH 7.2 as the mobile phase. The carousel temperature was set at 4°C. Each sample was diluted to 2.5mg.mL^{-1} and transferred to a recovery vial. 15µl of each prepared sample was injected onto the column over a 20 minute period and analysed using a UV detector set at a wavelength of 280nm. The flow rate was set as 1.00mL.min^{-1}.

Prior to sample analysis, the column was equilibrated with water and the 100mM Sodium Phosphate/150mM Sodium Chloride pH 7.2 mobile phase using a stepwise flow rate starting at 0.1mL.min^{-1} and reaching 1.0mL per minute over 60 minutes after which the injections began. Table 5 is a sample table as it would be set up using the software prior to run initiation:

Table 5: Sample Set Table for SEC Injection

Sample Name	Vial Number	Replicates	Injection Volume
Water Blank	1	2	15µL
Reference Standard	2	3	15µL
Buffer 1	3	3	15µL
Test Samples	4-30	3	15µL
Reference Standard	2	3	15µL
Water Blank	1	2	15µL

Each buffer was also analyzed to enable buffer peaks to be removed from the overall calculation. Each peak was integrated and reported as a percentage. All high molecular weight (HMW) degradation was analyzed using Arrhenius kinetics, and plotted against the square root of time (Franks, 2008; Wang et al., 2009). All rate constants calculated were reported as part of this project in the final results and discussion section.

5.10 Circular Dichroism (CD)

Circular Dichroism (CD) spectroscopy (near UV wavelength scan of 350nm to 250nm) was used to evaluate the tertiary structure of each of the lyophilized protein formulations at time 0 and at time six months stability. Near CD allowed the protein tertiary structure to be examined by monitoring the packing of disulfide bonds and the aromatic amino acids, Trp, Tyr and Phe (Kelly & Price, 2000). Each scan was plotted as an overlay against the same protein formulation held at different storage conditions and different time points to examine if there was a change in protein tertiary structure as a function of lyophilisation cycle and/or storage conditions.

CD was performed using an Applied Photophysics Chirascan CD Spectrophotometer set to a near UV wavelength range of 350- 250nm, scanning at a rate of $5nm.min^{-1}$ with a bandwidth is 1nm. The time per point was set at 2 seconds. Each lyophilized sample was reconstituted back to a target $25mg.mL^{-1}$ protein concentration and then diluted 1:5 to $5mg.mL^{-1}$ for sample analysis. Refer to section 7.8. In order to achieve this, 200µl of product was transferred to a 1mL eppendorf tube and made up to 1mL with USP water. 400µl of each of these samples were transferred into the 1mm curvette and loaded onto the Chirascan CD Spectrophotometer. Each sample scan time was set at approximately 19 minutes.

The raw data generated by the instrument was in millidegree units. Generally, CD spectra are reported as delta epsilon ($\Delta\varepsilon$, $M^{-1}cm^{-1}$) versus wavelength (nm) or molar ellipticity (deg. $cm^2.dmol^{-1}$) (Kelly & Price, 2000). Each buffer was analysed independently and subtracted from the raw data sample scan after the data were exported to Excel. To generate the final CD spectrum for each protein and buffer combination ($\Delta\varepsilon$), the total sample CD spectrum minus the buffer spectrum, represented by θ, along with the length, l, the molar concentration of the protein formulation, c and a constant, 32980 (dimensionless), were used (Kelly & Price, 2000). These parameters were entered into equation 6 to calculate the final CD spectrum. The spectrum ranges from 350nm to 250nm. The calculated spectrum value at 350nm was equated to 0 to normalize the data and to calculate the constant (or factor). This constant was subtracted from all the data as a function of wavelength, in order to fully convert the data into $\Delta\varepsilon$. This can be represented by the following equations:

$$\text{Molar Concentration (c) (mol/L)} = A_{280}/\varepsilon/Mr \quad \text{(Eq. 5)}$$

Where, A280 is the absorbance at 280nm (in this case the bulk formulation A280 reading was used), ε is the protein extinction coefficient and Mr is the molecular weight (Da).

$$\Delta\varepsilon\ (M^{-1}cm^{-1}) = \theta/\ (l*c*32980) \quad \text{(Eq. 6)}$$

Where, θ is the raw data after the buffer is removed from the spectrum (Kelly & Price, 2000). All data points were plotted together as a function of wavelength and buffer matrix. Therefore, both the samples generated by freeze drying below and above the collapse temperature at each time point in a given buffer matrix were plotted on the same axis against wavelength.

5.11 Stability Design of Experiments

A stability program was set up to allow the assessment of the product arising from each cycle over a 6-month period. The stability storage conditions were set at 4°C, 25°C 60% Relative Humidity (RH) and 40°C 75% RH. The rationale for the sampling and testing was outlined as follows:

Table 6: Stability Program for the samples freeze-dried at a target product temperature of -10°C

Storage Conditions	**T_o**	**Storage time, months**		
		T_1	**T_3**	**T_6**
4°C	3Bch+3RM+1CD+1DSC	-	-	3Bch+3RM+1DSC+1CD
25°C 60% RH		3Bch + 1 DSC	3Bch + 1 DSC	3Bch+3RM+1DSC+1CD
40°C 75% RH		3Bch + 1 DSC	3Bch+ 1 DSC	3Bch+3RM+1DSC+1CD

T_0/ T_1/ T_3/ T_6 Time zero/ 1 month/ 3 month/ 6 month period during stability

3 3 freeze dried product vials

1 1 freeze dried product vial

Bch Biochemical Analysis (SEC)

DSC Differential Scanning Calorimitry

RM Residual Moisture (Karl Fischer)

CD Circular Dichroism

The total number of vials per formulation was 66 vials. The total number of vials per cycle was 330 vials and the total amount of material used per formulation 33mL for cycle 1 (conservative cycle – fill volume of 0.5mL/vial) and 132mL for cycle 2 (aggressive cycle – fill volume of 2mL/vial). 5mL Scott glass vials were used during this project.

6.0 LYOPILIZATION CYCLE DESIGN

6.1 Thermal Characterization

The raw data from each of the mDSC runs was analyzed using universal analysis. The mDSC was used to measure the crystallization of the bulking agent (Tcrys), the sub ambient glass transition temperature (Tg') and the melting temperature (Tm) of the frozen matrix. The freezing step was designed for each lyophilisation cycle based on these measurements.

Figure 20 represents the bulking agent crystallization temperature.

Fig. 20: Thermograph representing Bulking Agent Crystallization. This Thermograph shows the Total Heat Flow, Reversing and Nonreversing signals of the sample prior. The green line represents the total heat flow, the blue line, the reversing heat flow and the brown line represents the non reversing heat flow. The crystallization of the amorphous bulking agent (i.e. mannitol or glycine) is represented by the exotherm on the non reversing heat flow (blue line). This endotherm was integrated and a crystallization temperature was determined.

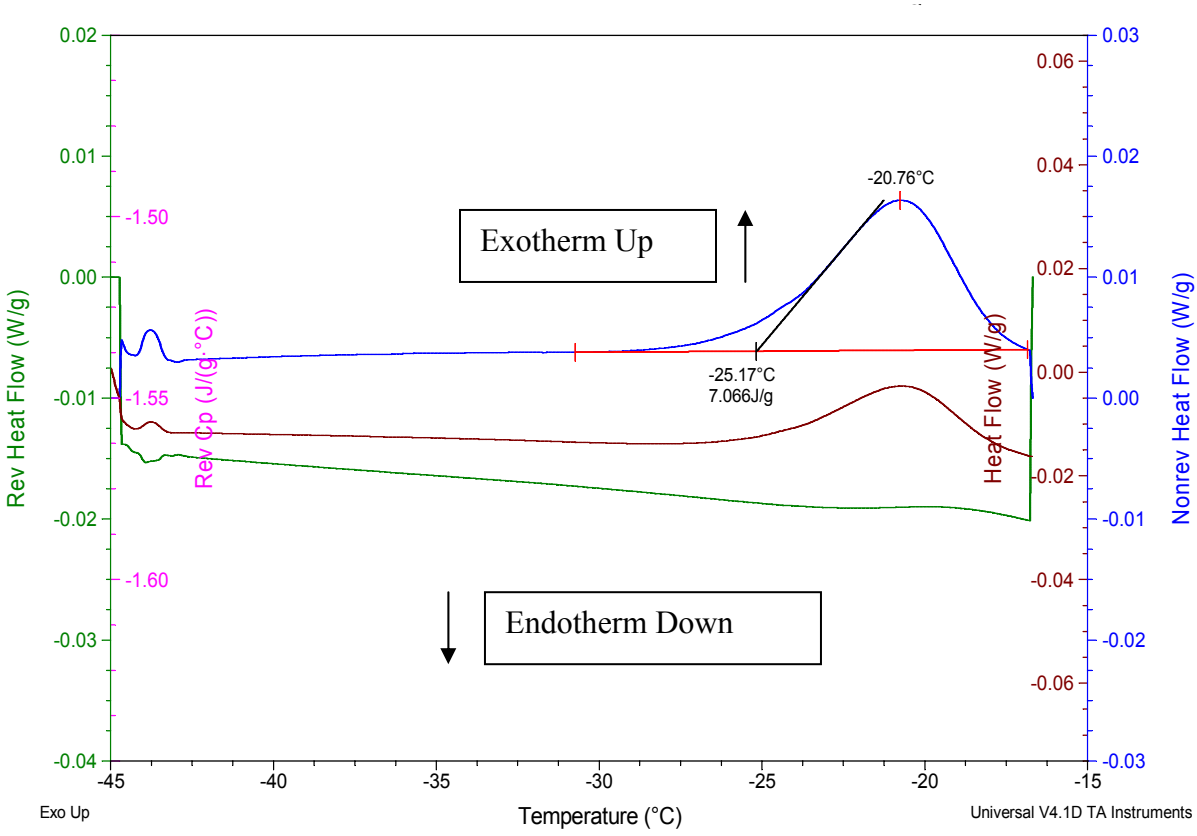

Bulking agent crystallization can be analysed on the non-reversing heat flow signal using Universal Analysis© (TA Instruments) software. Crystallization is represented as an exothermic event. From figure 20, crystallization can be seen by looking at the blue line which coincides with the Y-4 axis (non reversing heat flow). To calculate the Tcrys, the area under the curve is integrated using the Universal Analysis© software, yielding a temperature known as the onset of crystallization. This temperature was reported as part of the data set for each liquid formulation. Depending on the formulation, either the mannitol or glycine (both chosen as crystallizing bulking agents) crystallized during the annealing step as part of the overall freezing stage of the

Lyophilisation cycle. In these formulations, mannitol generally crystallized during the heating ramp into the annealing step and glycine during the annealing thermal hold step.

In order to fully assess the crystallinity of mannitol or glycine, depending on the formulation, the reversing heat capacity signal was examined as a function of time. This was achieved by selecting the reversing heat capacity as part of the thermograph and changing the x-axis to time from the standard temperature values.

Figure 21 represents the analysis of bulking agent crystallization as a function of time in minutes.

Fig. 21: Bulking Agent Crystallization Event. This Thermograph shows the Total Heat Flow, Reversing, Nonreversing and reversing heat capacity signals of the sample. The green line represents the total heat flow, the blue line, the reversing heat flow; the brown line represents the non reversing heat flow and the pink line, the reversing heat capacity. The x axis was converted to minutes and the exothermic crystallization event is evident on the non reversing heat flow (blue line). The change in heat capacity over time determines time taken for the crystallization of the bulking agent at these conditions.

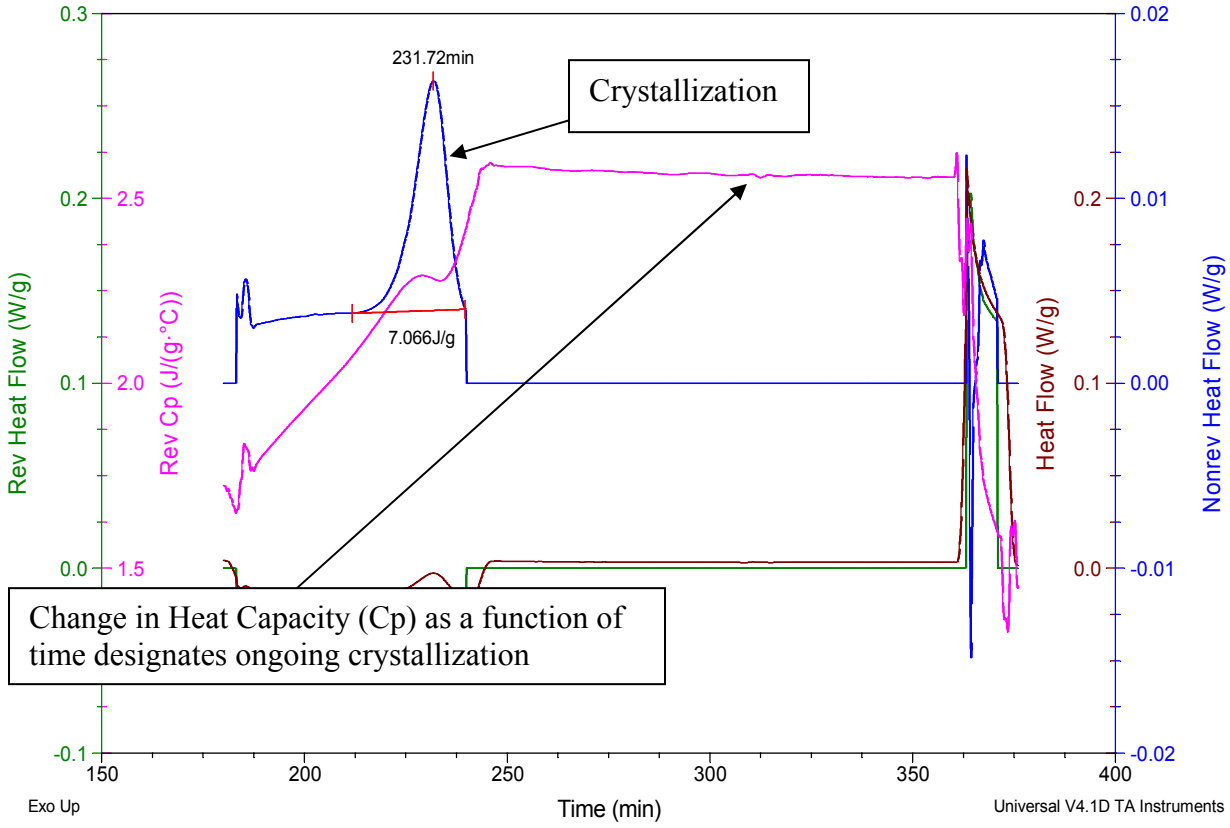

Even after the event represented by the exothermic peak on the non-reversing heat flow (blue line), crystallization could be still be ongoing. The point at which crystallization completes at low conditions was assessed by examining the reversing heat capacity signal as a function of time. The reversing heat capacity signal is represented by the pink line. Crystallization is represented by an endotherm on the non reversing heat flow with a corresponding increase in reversing heat capacity (up to approximately 270 minutes on figure 21). As crystallization

continues, there is a change in the heat capacity signal, usually represented by a drop in the signal over time (represented between 280 and 350 minutes on figure 21). Once the crystallization has completed, this signal will stabilize and there will be no further change as a function of time. When designing lyophilisation cycles for formulations with crystallizing bulking agents, the time taken for the reversing heat capacity to become stable along with the actual crystallization event, would represent the annealing hold time during freezing. The step time of 3 hours was chosen as all formulations completed bulking agent crystallization within this time.

Figure 22 represents the analyzed Tg' for a given frozen liquid. Once the annealing step has been performed and both the crystallization of ice and bulking agent crystallization were observed. After these events the Tg' can be analyzed. This is measured upon heating from the frozen state for the purposes of this process.

Fig. 22: Tg' Temperature Measurement. The Tg' may be measured on the reversing heat flow signal and is supplemented by an endotherm on the non reversing heat flow signal. An endotherm is represented by a depression in the signal (also known as enthalpic relaxation).

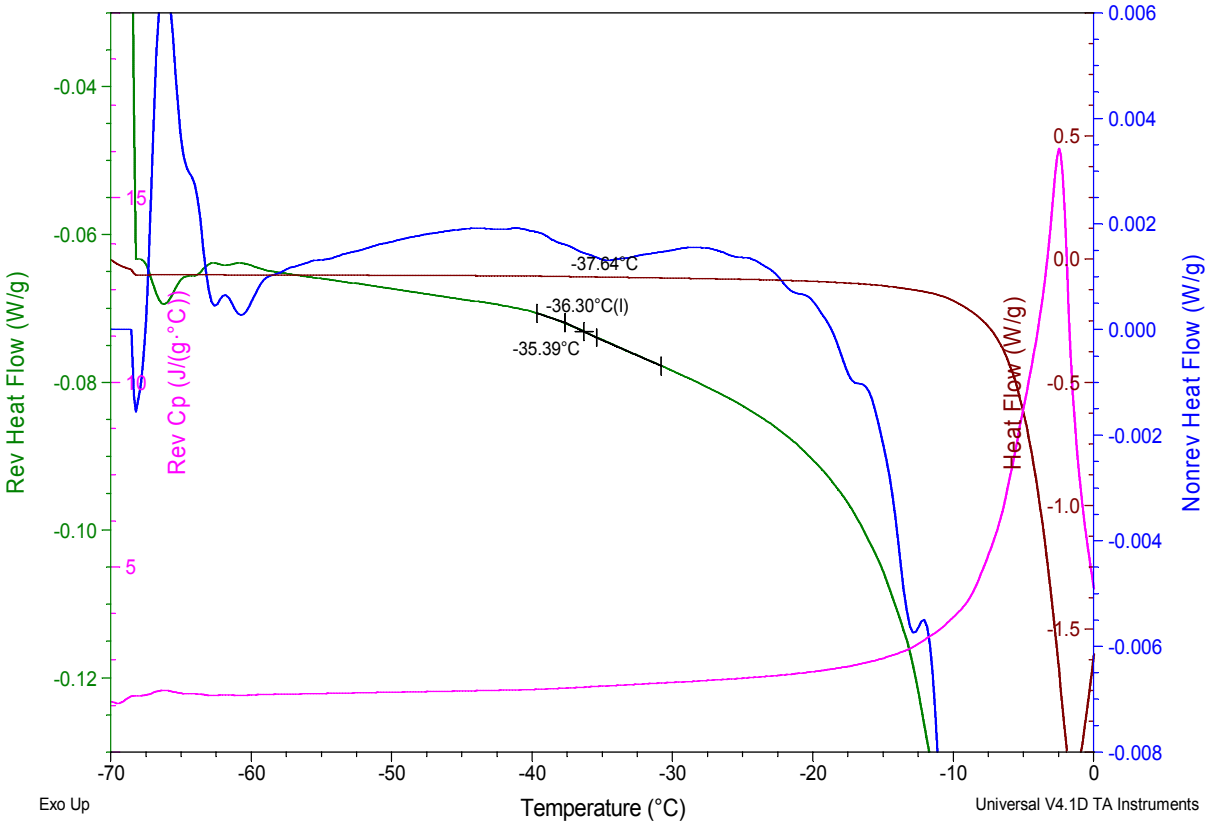

Using mDSC and universal analysis© the Tg' was measured on the reversing heat flow signal (green line on figure 22) during the heating stage of the DSC cycle post freezing. This event is usually complimented by an endothermic event on the non-reversing heat flow indicating that the Tg' even uses heat to drive the transition as opposed to realizing heat like the crystallization event. The FDM recipe was designed based on the measured Tg', as for partially amorphous systems, there is a relationship between the Tg' and the collapse temperature (Pikal et al., 1990).

The Tm is measured on the total heat flow signal and can be identified by an endotherm. The brown line on figure 23 represents the total heat flow and in the case of this figure, the onset of melting occurs around the -4.99°C temperature. Melting occurs on the heat up step of the mDSC cycle recipe after the Tg' event and represents the total collapse temperature of the amorphous material. It is important to design the primary drying step of the lyophilisation cycles in a way

that primary drying would not be conducted at temperatures above this measured Tm, as gross collapse would be observed. This project is designed to examine the effect of drying above the micro collapse temperature which was measured by freeze drying microscopy (section 5.3) and is related to the sub ambient Tg temperature.

Fig. 23: Total Melting/Collapse. Melting temperature is represented by an endothermic even on the total heat flow signal. The area is integrated and a melting temperature is measured.

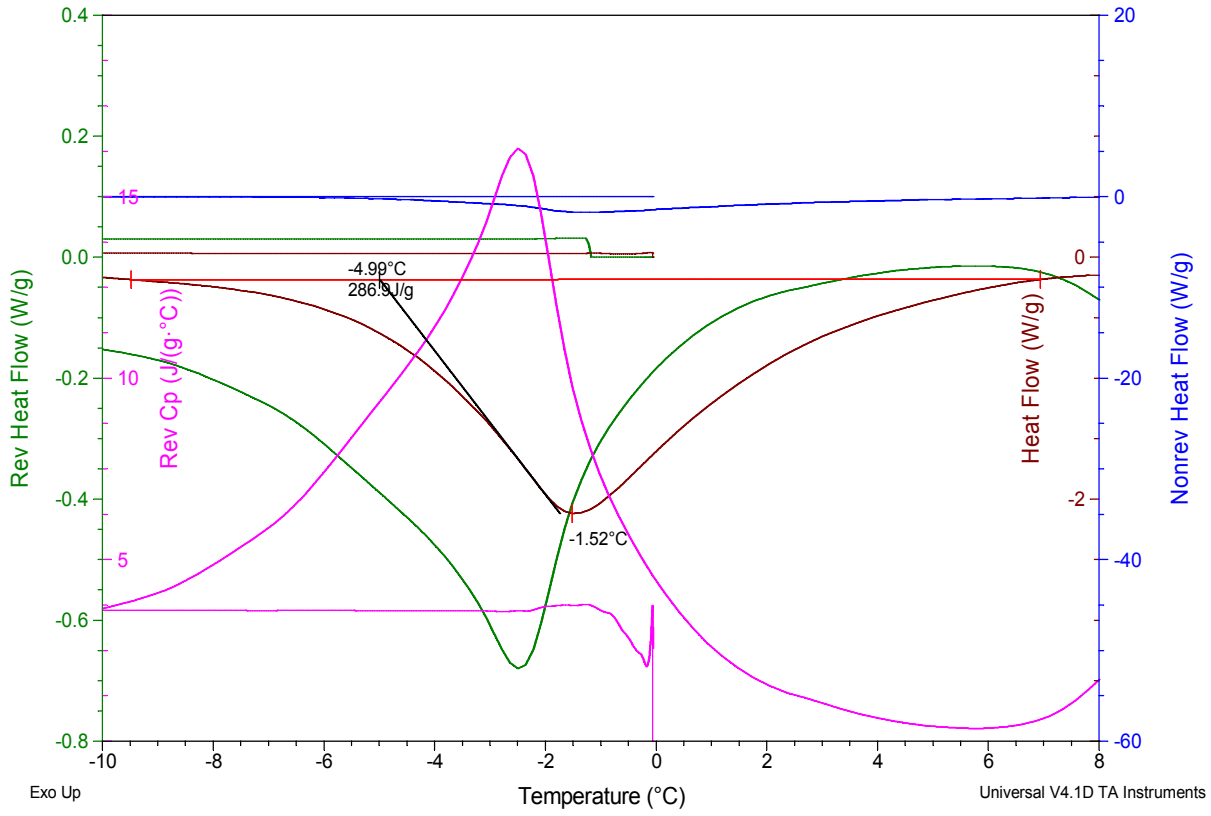

mDSC analysis was carried out on all protein formulations to determine Tg', Tcrys and Tm (thermographs not shown). The full set of results may be seen on table 7.

The next step after mDSC analysis was to design the freeze drying microscopy recipe and execute for each formulation. This allowed the measuring of the collapse temperature (Tc) for each formulation. Refer to section 5.3 for the freeze drying microscopy method that was used to measure the collapse temperature of the amorphous content of each formulation.

Figure 24 shows the region of collapse for Protein X and Buffer 2 (4% Mannitol, 1% Sucrose and 10mM Tris pH 7.0). The image was generated using an Olympus video camera during the freeze-drying microscopy experiment. Each Protein formulation was examined under the freeze-drying microscope and the collapse temperature was measured (images not shown). The results can be seen on table 7. From examining the image, one can see the frozen matrix on the right hand side, the dry region on the left and the drying front represented by the divisionary line between the dry region and the frozen matrix. As drying continues, the front moved from left to right on the image. Once the temperature passed that of the critical temperature, collapse was evident in the sample. This was represented by discrepancies or 'holes' in the dry region, which can be seen on figure 24.

For many of the formulations, especially the glycine based products, collapse was difficult to identify. As the collapse temperature data were only available for certain formulations, it was decided to use Tg' as the critical temperature for the purposes of modelling the primary drying step of each cycle since it can be easily measured by DSC.

Fig. 24: Image of Collapse for Protein X and Buffer 2 (4% Mannitol, 1% Sucrose and 10mMTris Buffer) – generated using Freeze Drying Microscopy. The images were generated over a temperature ramp under vacuum conditions where A represents the frozen matrix, B the initial collapse and C further collapse.

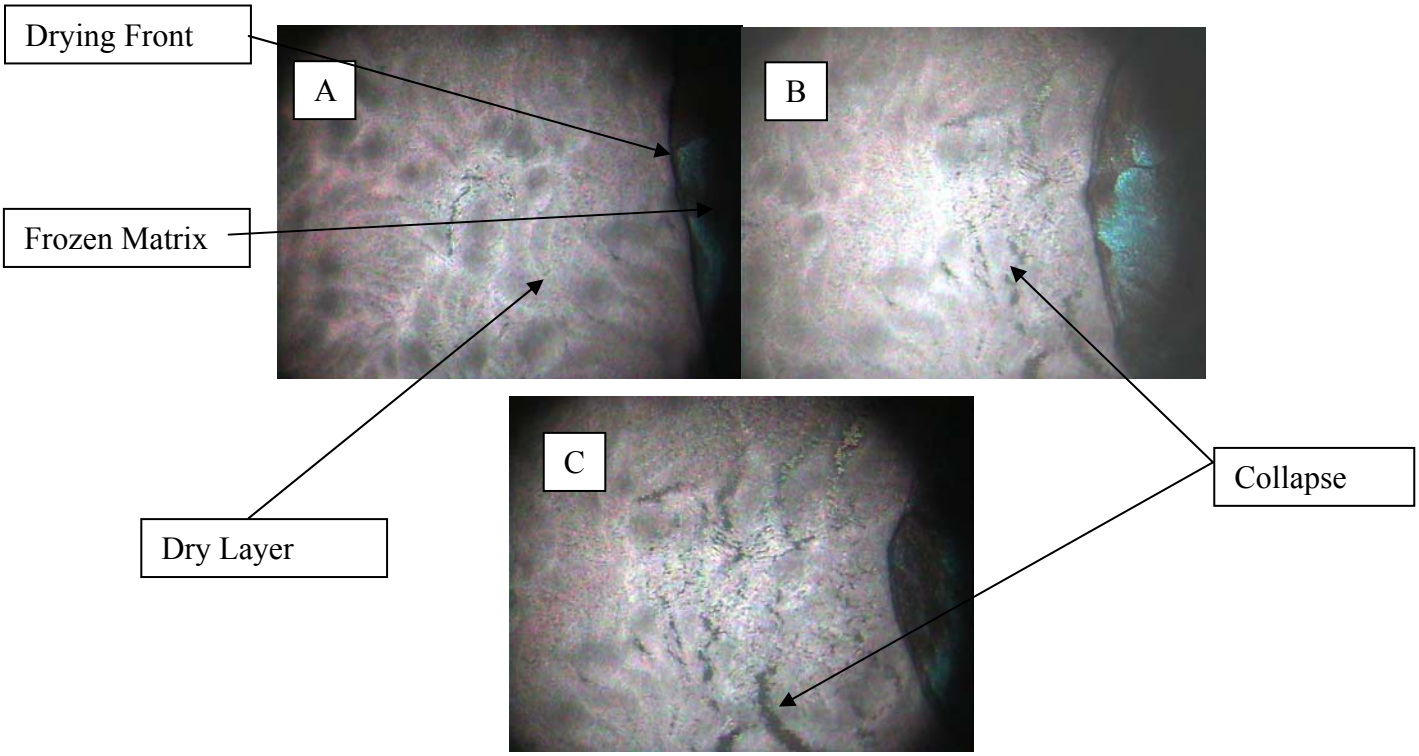

Freeze drying microscopy was performed on all liquid samples post the mDSC analysis to measure the collapse temperature. For all mannitol based formulations, the collapse temperature was easily determined. However, all glycine based formulations yielded microscopic images that were inconclusive. As a result, the Tg' was used as the critical temperature when designing the lyophilisation cycles, which made up the next step of the project. All formulations were treated in the same way using both DSC and freeze drying microscopy (thermographs and images not shown).

Table 7 represents the full compliment of thermal analysis for all formulations. The design of both lyophilisation cycles in section 6.3 of this thesis was based on the results listed. Each freezing step was designed by targeting a Tsh below the lowest Tg' of -44.59°C. The shelf

temperature was set at -45°C. The first lyophilisation cycle primary drying step was designed to target a product temperature below the lowest Tg' and the second lyophilisation cycle above the highest measured collapse temperature of -8.3°C thereby performing primary drying above the collapse temperature.

Table 7: Complete Thermal Analysis Results for all liquid formulations

Sample Name	Tg' (°C)	Tcrys (°C)	$\Delta H_{crystallization}$ J/g	Tm (°C)	ΔH_{fusion} J/g	Tc (°C)
25mg/mL Protein X 4% Mannitol 1% Sucrose 10mM Tris pH 7.0	-19.23	-29.66	5.734	-4.99	286.9	-8.3
25mg/mL BSA 4% Mannitol 1% Sucrose 100mM NaCl 10mM Tris pH 7.0	-42.83	-25.47	5.469	-4.9	291.1	-42
25mg/mL BSA 4% Mannitol 1% Sucrose 10mM Tris pH 7.0	-31.44	-29.1	3.474	-3.19	362.5	-11
25mg/mL BSA 4% Glycine 1% Sucrose 100mM NaCl 10mM Tris pH 7.0	-44.59	-17.89	15.17	-6.31	330.8	*
25mg/mL BSA 4% Glycine 1% Sucrose 10mM Tris pH 7.0	-24.36	-19.35	11.41	-6.86	296.8	*

* Collapse not detected

The differences in the enthalpic heat of crystallization ($\Delta H_{crystallization}$) and heat of fusion ($\Delta H_{fusion}$) was likely due to the crystallization event being a function of the bulking agent only (i.e. Mannitol or Glycine) whereas the melting event (enthalpy of fusion) was a function of the entire formulation including excipients, protein and water. The enthalpy of crystallization was found to be lower than the enthalpy of fusion and the variability in the enthalpy of crystallization was a result of different degrees of crystallization of the bulking agent. The degree of crystallization was found to be dependent on the type of bulking agent (either mannitol or glycine) and the presence of other excipients. Mannitol crystallization seemed to have a lower enthalpy than glycine based formulations (as seen in table 7).

The annealing step within the freezing step was designed based on heating the shelf temperature from the target freezing temperature (-44.59°C) to a temperature above the highest measured

bulking agent crystallization temperature (-17.89°C) but lower than the lowest measured melting temperature of -6.86°C.

6.2 Freezing Step Design

The freezing step was designed based on the mDSC data generated based on the methods in section 5.2. A freezing rate of 0.33°C.min^{-1} was chosen to enable to freeze the product below the measured sub ambient glass transition temperature. As each formulation consisted of bulking agents' mannitol or glycine, an annealing step was incorporated into the freezing step to crystallize these excipients. It is understood that crystallizing the amorphous bulking agents provide structural support to the product during the drying process (Pikal, 1990b).

6.3 Primary drying step design

To reduce the number of lyophilisation cycles that would be required to generate the sample numbers to robustly execute this project, two lyophilisation cycles were to be used for all protein formulations. The first was a conservative cycle to generate good cake for all formulations. This would act as a baseline or control for the experiment. The second cycle was an aggressive cycle, in which the primary drying step was performed at product temperatures much above the measured Tg' or Tc.

As the lowest Tg' of all the protein formulations was measured, using mDSC, as -44.59°C, the target shelf temperature was set at -45°C for the freezing step of each cycle. As the highest Tcrys of the bulking agent was observed to be close to -18°C, annealing was set at a temperature of -15°C. It was understood that an annealing temperature of -15°C for 3 hours would crystallize the amorphous bulking agent (either Mannitol or Glycine depending on the formulation). The ramp rate was kept at a conservative rate of 0.5°C/min to ensure that the product temperature and the shelf temperature remain very close to each other during the freezing step.

The primary drying step was designed for each lyophilisation cycle using a series of mathematical formulae captured in section 2.2.8 (Tchessalov, 2008). For the purpose of the

calculations, a number of assumptions were made. The main assumption was that the vial heat transfer coefficient (Kv) remained constant as a function of pressure. Therefore, at a given vacuum pressure during primary drying, the heat transfer coefficient should not change. This is not necessarily true as vacuum pressure changes as a function of the pressure control mechanism in the lyophilizer chamber, and would require even more complex mathematical modeling to understand the real relationship. However, as this modeling has been proven as valid in his context (Tchessalov, 2008), it was used to design the experiments for the purposes of this project.

The initially chosen cake resistance, R, is represented by the following equation, which was a derived based on the model presented in section 5.2.8:

$$R = 32h^2 + 35h + 0.2 \quad \text{(Eq. 7)}$$

The vial heat transfer coefficient (Kv) was measured (measured based on section 5.2.8) for the 5mL Scott vial and is represented by the following equation:

$$Kv = \frac{97.86P(Torr)}{1 + 11.82P(Torr)} \quad \text{(Eq. 8)}$$

A 5mL Scott vial was chosen for the purposes of this experiment was due to volumetric capacity. This vial is capable of holding fill volumes of both the target 0.5mL and 2mL fill volumes (under half the capacity of the vial), which would allow generating material from the cycle where primary drying was performed above the collapse temperature. The goal was to use the initial resistance and heat transfer coefficient equations to design a cycle to freeze dry all the formulations below the lowest Tg'/ Tc, which was determined by mDSC and FDM. After executing the first cycle, the data were analyzed and the cake resistance recalculated to allow the second cycle (above the collapse temperature) to be designed.

The following parameters were known and consistent for this project and were critical in calculating cycle conditions:

- Fill volume:
  - Cycle 1 – Vfill = 0.5mL
  - Cycle 2 - Vfill = 2mL
- Vial dimensions:
  - Dout = 2.075cm
  - Din = 1.855cm
- ΔH_S =676 cal/g- specific heat of sublimation

For the purposes of this project, from this point forward, the statement 'freeze drying below or above Tg' or Tc' relates directly to performing the primary drying step below or above Tg' or Tc.

6.3.1 Design of Primary Drying Conditions for Lyophilisation Cycle 1 - Freeze Drying below Tg'

The target product temperature during the first lyophilisation cycle primary drying step was set not to exceed the lowest Tg' measured using mDSC. This was to ensure that all formulations were dried below the collapse temperature, which was the purpose of this cycle. To reduce the number of freeze drying cycles, all the formulations were freeze dried together, with a target product temperature of -44.59°C (lowest Tg' - BSA based formulation in Glycine-Sucrose-NaCl-Tris buffer). The product temperature target for each formulation was set at-45°C based on the measurement of Tg' and Tc for each formulation. However, it was not expected that all the formulations would dry at the same product temperature due to the differences in formulation components, which in turn affects resistance to vapor flow during primary drying. The goal was to dry at a product temperature lower than the relevant Tg' or Tc of a given formulation.

Figure 25 shows the theoretical primary drying calculated performance. It is evident that theoretically, the calculated product temperature (blue line) is below the critical temperature (brown line) when 100% of the free water is removed (green line) at a shelf temperature or -43°C and a vacuum setpoint of 30mT (40µbar), known as lyophilisation cycle 1. From these

calculations, it is evident that the cycle conditions allow the drying below the critical temperature during primary drying.

Fig. 25: Calculated product profile during primary drying: freeze-drying below the critical temperature. The shelf temperature was set at -43°C and the vacuum pressure was set at 30mT allowing the temperature to target close to -45°C (which was below the target temperature of -44.59°C)

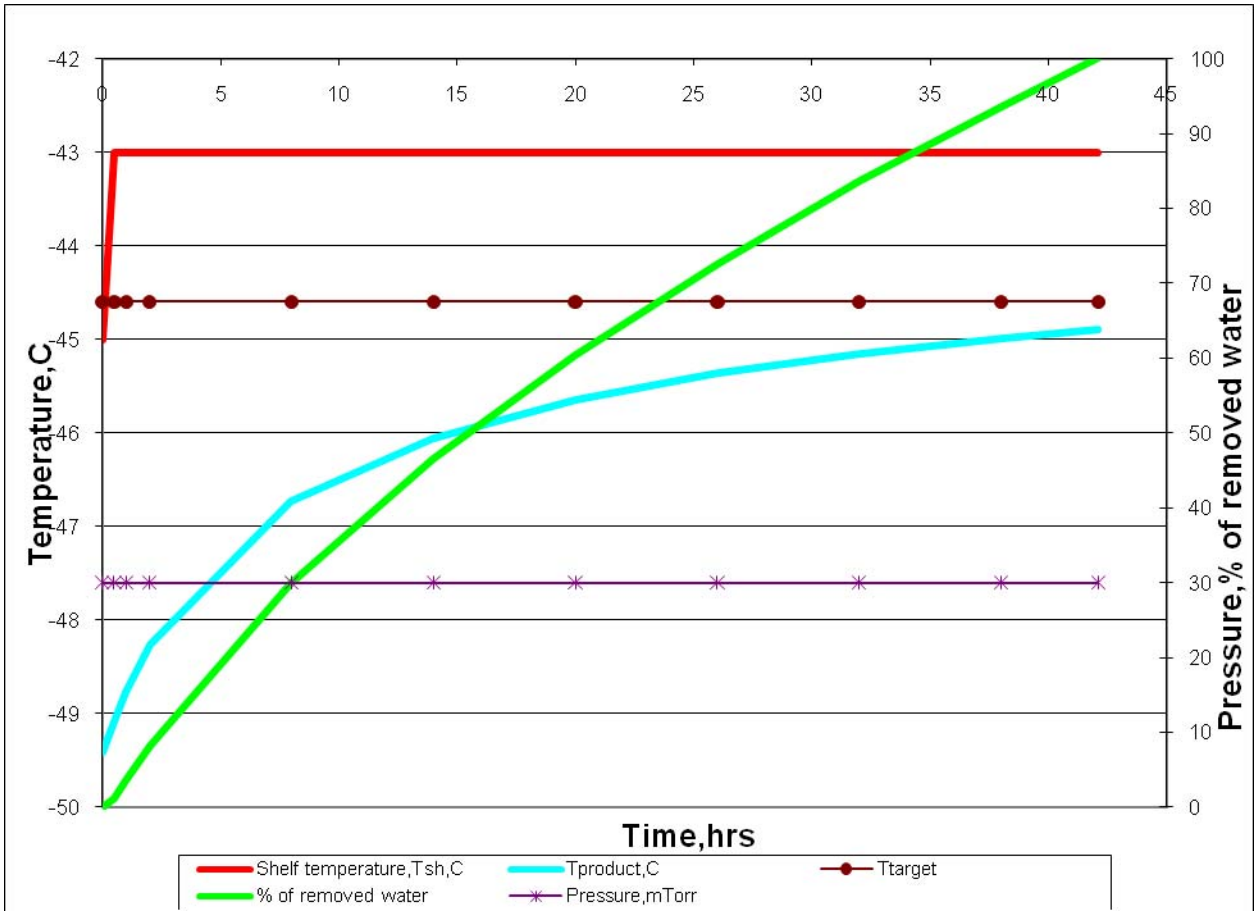

The red line represents the shelf temperature, the purple line represented the vacuum pressure, the brown line, the target product temperature and the blue line represented the predicted product temperature. The green line showed the % removed water due to the primary drying step which indicated the predicted end point. However, when loading the recipe onto the freeze drying system, due to the fact that the primary drying conditions were set very low setpoint at a shelf

temperature of -43°C and a chamber pressure of 30mT, an additional 50% of time was added to the step to ensure complete primary drying (Tchessalov, 2008). The modeling of primary drying is difficult at low conditions.

Table 8 lists the cycle parameters that were run as part of this section of the experimental work. Primary Drying was calculated theoretically to complete after 42 hours.

Table 8: Cycle parameters for freeze-drying below Tg' – Lyophilisation Cycle 1

Step #	Shelf temperature	Chamber pressure, mT	Cumulative time, hrs
1	Ramp 1°C/min to 5°C, hold for 45 min	-	1.0
2	Ramp 0.5°C/min to -45°C, hold for 90 min	-	4.17
3	Ramp 0.5°C/min to -15°C, hold for 180 min	-	8.17
4	Ramp 0.5°C/min to -45°C, hold for 30 min	-	9.67
5	Pull vacuum	30	10.17
6	Ramp 0.5°C/min to -43°C, hold for 3300min	30	65.23
7	Ramp 0.2°C/min to 45°C, hold for 240 min	30	76.57

*50% was added to the calculated primary drying time of 42 hours

6.3.2 Design of Primary Drying Conditions for Lyophilisation Cycle 2 - Freeze drying at target product temperature of 0ºC

For this lyophilisation cycle, the primary drying setpoints of Tsh and Pch were set at much more aggressive setpoints to achieve a target product temperature of 0°C. Due to the difference in formulations, cake resistance would be different. This would mean that each product temperature would be different during primary drying. However, by mathematically estimating 0°C to be the target product temperature, the probability of each of the formulations reaching product temperatures much higher than the relevant Tc for each formulation would be very high. Due to

the differences in formulation make up, it was expected that the product temperature for each would differ under the same processing conditions.

After analyzing the initial cycle, the resistance was recalculated using the mathematical modeling in primary drying modeling section 2.2.8. The following cake resistance was used along with the 5mL vial Kv to calculate cycle 2 primary drying conditions:

$$R = 16.38h \quad \text{(Eq. 9)}$$

Even though the cake resistance was calculated, however, it is very difficult to model a freeze drying cycle above the collapse temperature as the resistance to vapour flow changes. To simplify the designing of the primary drying step, equation 8 and 9 were used in this case. The target temperature for all formulations was 0°C, which was well above Tg' or Tc for all formulations. However, it was not expected to achieve this as the resistance in reality was different for each formulation as resistance is a function of not only stopper and freeze dryer itself, but also solids content and ice crystal structure (Searles et al., 2001a).

Figure 26 shows the primary drying calculated performance for lyophilisation cycle 2. It is evident that theoretically, the calculated product temperature (light blue line) is as the target temperature of when 100% of the free water is removed (green line) at a shelf temperature of 50°C and a vacuum setpoint of 450mT (600µbar). Freezing was kept constant as per cycle 1 and secondary drying was continued at 50°C for a further 4 hours.

Fig. 26: Calculated product profile: freeze-drying at a target product temperature of 0°C

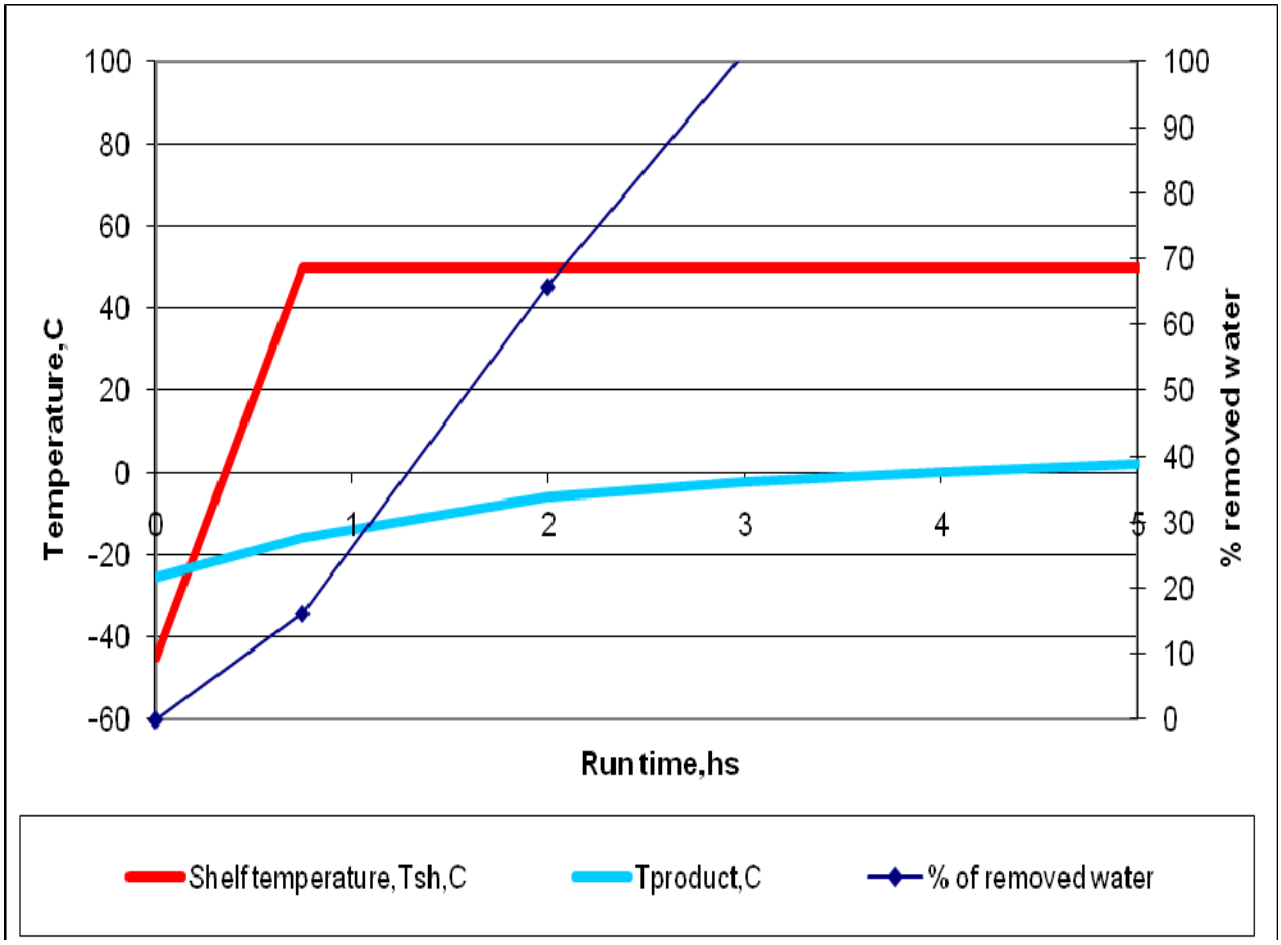

Figure 26 represents the calculated primary drying conditions targeting a product temperature of 0°C, which is well above the highest collapse temperature of -8.3°C (Protein X and B2). The red line represented the shelf temperature of 30°C. The vacuum pressure was set at 450mT (not displayed on plot). The light blue line represents the product temperature, which was predicted to reach 0°C at the end of primary drying.

Table 9 lists the lyophilisation cycle recipe used to achieve a target product temperature of 0°C. The goal was to purposely collapse the product of each formulation for further studies. Primary Drying was calculated theoretically to complete after 3 hours. However, due to potential calculation error, 30% extra time was purposely added onto the primary drying time to ensure completion of the drying step. It is important to note that even though the intent was to collapse

the product at this point, the objective was to avoid melting. This would be achieved if the primary drying time was set at a time that was too short to ensure all ice was removed.

Table 9: Cycle parameters for freeze-drying at a target temperature of 0°C – Lyophilisation Cycle 2

Step #	Shelf temperature	Chamber pressure, mT	Cumulative time, hrs
1	Ramp 1°C/min to 5°C, hold for 45 min	-	1.0
2	Ramp 0.5°C/min to -45°C, hold for 90 min	-	4.17
3	Ramp 0.5°C/min to -15°C, hold for 180 min	-	8.17
4	Ramp 0.5°C/min to -45°C, hold for 30 min	-	9.67
5	Pull vacuum	450	10.17
6	Ramp 0.5°C/min to 50°C, hold for 210 min	450	16.83
7	Hold for 240 min	450	20.75

*30% was added to the calculated primary drying time of 3 hours

7.0 RESULTS AND DISCUSSION

7.1 Bulk Formulation

Note that Tris was chosen as the buffer at pH 7.0 as this was the buffer of choice for the proprietary protein X. This was applied to all BSA formulation to simplify formulation procedures. It is understood that the buffering capacity of Tris at pH 7.0 is limited especially as the pKa of Tris is 8.3. In future studies, the buffer will be carefully selected based on buffering ability at the target pH.

10mM Tris pH 7.0

A 40L solution of 10mM Tris buffer was made up by weighing out 63.04g of Tris HCl (formula weight of 157.59g) and adding the said quantity to 36L of Reverse Osmosis (RO) water. The solution was left to mix for approximately 1 hour after which it was made up to the 40L mark. This 40L total volume of 10mM Tris HCL was divided into four 10L volumes.

10L of 10mM Tris base (Tromethamine) was made up by weighing out 12.11g of Tris base (formula weight 121.1g) and adding it to 9L Reverse Osmosis water. This solution was mixed for approximately 1 hour after which it was made up to a target of 10L. Each 10L solution of 10mM Tris HCl was pH adjusted to 7.0 using the 10mM Tris base solution. The pH of each 10mM Tris buffer was as follows:

1. 10mM Tris solution 1 6.99
2. 10mM Tris solution 2 7.01
3. 10mM Tris solution 3 7.00
4. 10mM Tris solution 4 6.99

Using each of the 10mM Tris solutions, four buffer formulations were made up. Each formulation contained multiple excipients. The formulations made up were as follows:

1. 4% Mannitol 1% Sucrose 100mM NaCl 10mM Tris pH 7.0

400g Mannitol, 100g Sucrose and 56.5g NaCl were mixed in 8L of pH 7.0 10mM Tris buffer. After agitation of approximately 1 hour, the solution was made up to the 10L mark using the same buffer resulting in a 10L solution of 4% Mannitol 1% Sucrose 100mM NaCl 10mM Tris pH 7.0.

2. 4% Mannitol 1% Sucrose 10mM Tris pH 7.0

400g Mannitol and 100g Sucrose were mixed in 8L of pH 7.0 10mM Tris buffer. After agitation of approximately 1 hour, the solution was made up to the 10L mark using the same buffer resulting in a 10L solution of 4% Mannitol 1% Sucrose 10mM Tris pH 7.0.

3. 4% Glycine 1% Sucrose 100mM NaCl 10mM Tris pH 7.0

400g Glycine, 100g Sucrose and 56.5g NaCl were mixed in 8L of pH 7.0 10mM Tris buffer. After agitation of approximately 1 hour, the solution was made up to the 10L mark using the same buffer in a 10L solution of 4% Glycine 1% Sucrose 100mM NaCl 10mM Tris pH 7.0.

4. 4% Glycine 1% Sucrose 10mM Tris pH 7.0

400g Glycine and 100g Sucrose were mixed in 8L of pH 7.0 10mM Tris buffer. After agitation of approximately 1 hour, the solution was made up to the 10L mark using the same buffer resulting in a 10L solution of 4% Glycine 1% Sucrose 10mM Tris pH 7.0.

Each solution was split into two 5L volumes to be used during the diafiltration step. This was to accommodate the two proteins that were used in association with each buffer formulation. This resulted in a total of five (5) protein formulations being used as part of this study. The 5L volumes were stored at 4ºC until used.

7.2 Protein Formulation

Fraction V BSA (Sigma Aldrich) was used for the purposes of this project. Protein X in Mannitol – Sucrose – Tris (25mg.mL^{-1} protein concentration) was provided by the Purification Development department at Wyeth Biotech, Grange Castle for the purposes of this project. This

was the only formulation of Protein X used for further processing. All formulations containing BSA were formulated to a target protein concentration of 25mg.mL^{-1}. The following steps detail the formulation for the BSA based formulations:

1. 25mg/mL BSA in RO Water
   25g of BSA was weighed out and added to 850mL of RO water. This protein solution was mixed for approximately 1 hour and then made up to the 1L mark. This procedure was repeated three times to result in four 1L 25mg/mL BSA solutions (in RO water).

2. Diafiltration of Buffer into protein solution
   For the BSA Diafiltration step, a 10kDa 0.1m^2 PES Pellicon II mini filter screen type C (Millipore) was used.

The concentration of each of the final protein solutions were measured using a UV-vis spectrophotometer, where 20µl of protein solution was gravimetrically diluted 1:50 with the relevant buffer, agitated on a vortex, and transferred to a curvette and read at an absorbance of 280nm. Prior to reading the absorbance spectra of the samples, the spectrophotometer was blanked using the relevant buffer. The procedure was repeated three times. Table 10 lists the protein concentration for each formulation. The target protein concentration was 25mg.mL^{-1}. The extinction coefficient for protein X was 1.14 L.mol^{-1}.cm^{-1} (sources for a proprietary reference) and for BSA was 0.667 L.mol^{-1}.cm^{-1} (Sigma Aldrich BSA fraction V product data) for the purposes of calculating concentration based on the A280 UV absorption analysis. Internal references were used as part of the analysis.

In the preparation of samples for protein concentration analysis, dilutions were gravimetrically calculated as prepared using an analytical balance and a Gilson pipette. The purpose of this step was to verify that the protein recovery after UF-DF step was sufficient to continue through the project.

Table 10: Protein Concentration of each Formulation measured using A_{280}

Sample Name	Conc. 1 (mg/mL)	Conc. 2 (mg/mL)	Conc. 3 (mg/mL)	Average (mg/mL)
Protein X 4% Mannitol 1% Sucrose 10mM Tris pH 7.0 (Buffer 2)	20.32	20.03	20.46	20.27
BSA 4% Mannitol 1% Sucrose 100mM NaCl 10mM Tris pH 7.0 (Buffer 1)	23.79	25.12	27.6	25.5
BSA 4% Mannitol 1% Sucrose 10mM Tris pH 7.0 (Buffer 2)	23.9	23.2	23.2	23.43
BSA 4% Glycine 1% Sucrose 100mM NaCl 10mM Tris pH 7.0 (Buffer 3)	29.95	28.48	22.63	27.02
BSA 4% Glycine 1% Sucrose 10mM Tris pH 7.0 (Buffer 4)	24.7	28.18	23.81	25.56

Variations in the average protein concentration calculations may have been due to equipment variability or most likely, variations on recovery of the protein during the diafiltration step. However, as the concentrations are close to the target 25mg.mL^{-1} concentration, this was deemed acceptable. This project focuses on the degradation and structural profiles of the protein formulations when performing freeze drying below and above the collapse temperature and also storing at various storage conditions over a six month period at the protein concentrations listed on table 10. Most work performed to date consisted of low protein concentrations (Wang, 2003; Passot et al., 2007). Therefore, the selected protein formulations formed the basis of the rest of the project.

7.3 Lyophilisation

7.3.1 Lyophilisation Cycle 1 - Freeze drying below Tg'

Refer to section 5.4 for the methods associated with the design of lyophilisation cycle 1. Freezing was set at a shelf temperature of -45°C with an annealing step at -15°C. The annealing step was used to crystallize the bulking agent (Mannitol or Glycine depending on the formulation). The annealing time was set at 180 minutes. This time (crystallization time) was determined using DSC by examining the heat capacity signal immediately after the crystallization event. For primary drying, the shelf temperature was set at -43°C and the pressure at 30mT. Secondary drying parameters were set at Tsh of 45°C and Pch 30mT. This step was used to drive off bound moisture. Figure 27 shows the lyophilisation cycle trend from cycle 1.

Fig. 27: Lyophilisation Cycle 1 Trending – Performing Primary drying below the collapse temperature. The yellow line represents the shelf temperature and the blue line represents the capacitance manometer. The purple line represents the pirani and the collection of lines trending near the shelf temperature represents the product temperature profiles. Due to the low conditions, primary drying Tsh = -43°C and the vacuum pressure of 30mT, it is difficult to examine the primary drying performance.

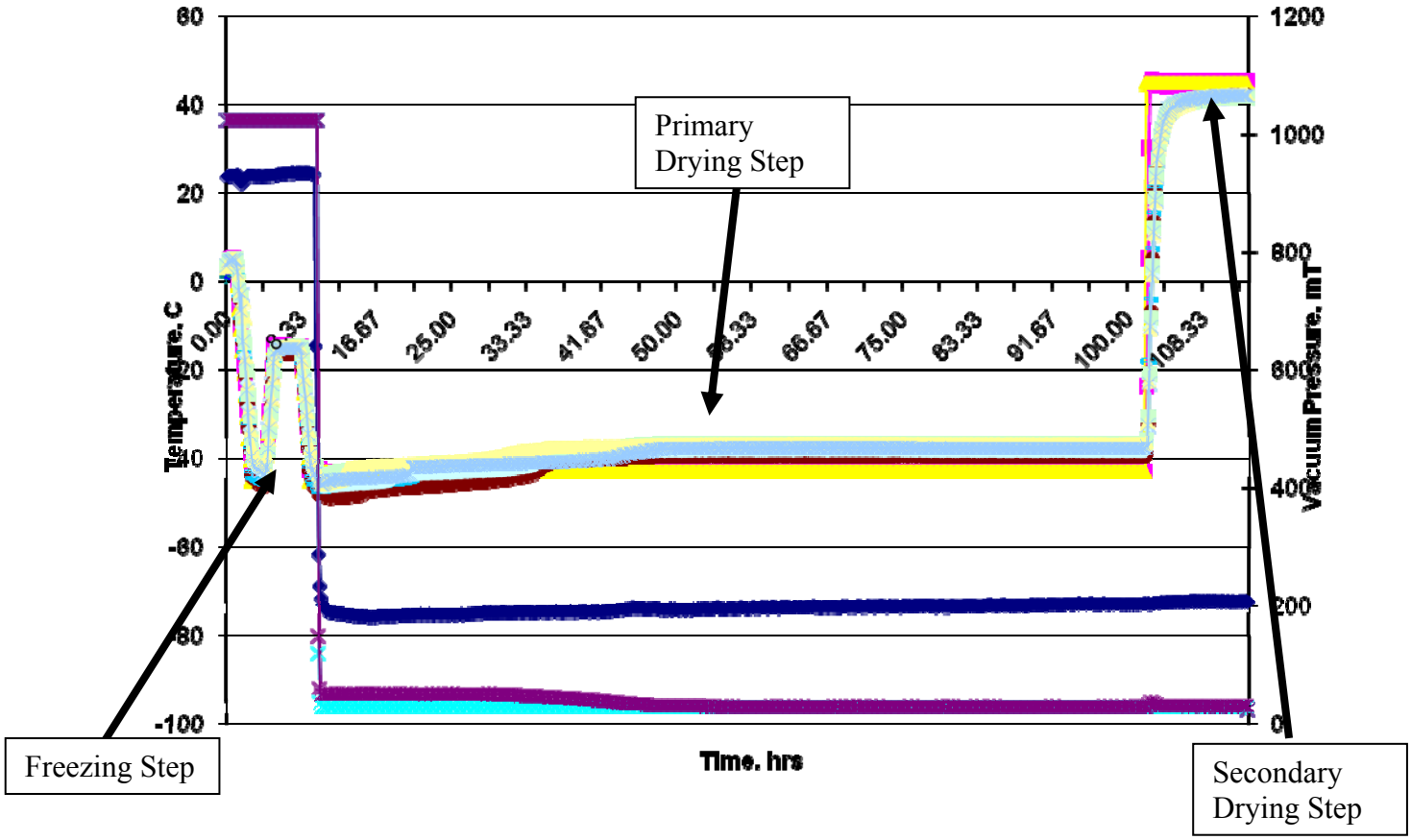

Due to the difficulty in reading the primary drying step in figure 27, the primary drying section was focused on in figure 28. This was achieved by zooming in on the Y1 axis (temperature) and the X axis (time). Figure 27 tells us that the freezing step and the secondary drying step completes without any issues. The initial freezing target temperature of -45°C and the annealing setpoint of -15°C were achieved and the secondary drying target temperature of 40°C was also achieved.

Figure 28 represents the primary drying step from figure 27 with a focus on the product temperature, showing that the temperature of each product during drying remained below the relevant Tg' or Tc. Refer to table 11 for the start and end temperatures compared to the relevant Tg' or Tc.

Fig. 28: Lyophilisation Cycle 1 Trending – Zoom in on the product temperature trending due to the difficulty in reading the full lyophilisation cycle trend. The yellow line represents the shelf temperature, the blue the capacitance manometer vacuum pressure and the purple line, the pirani gauge. This trend is a focus trend on the primary drying step that was introduced on figure 27. The collection of lines grouped together represents the product temperature. It is clear by the sudden change in product temperature represents the collapse event.

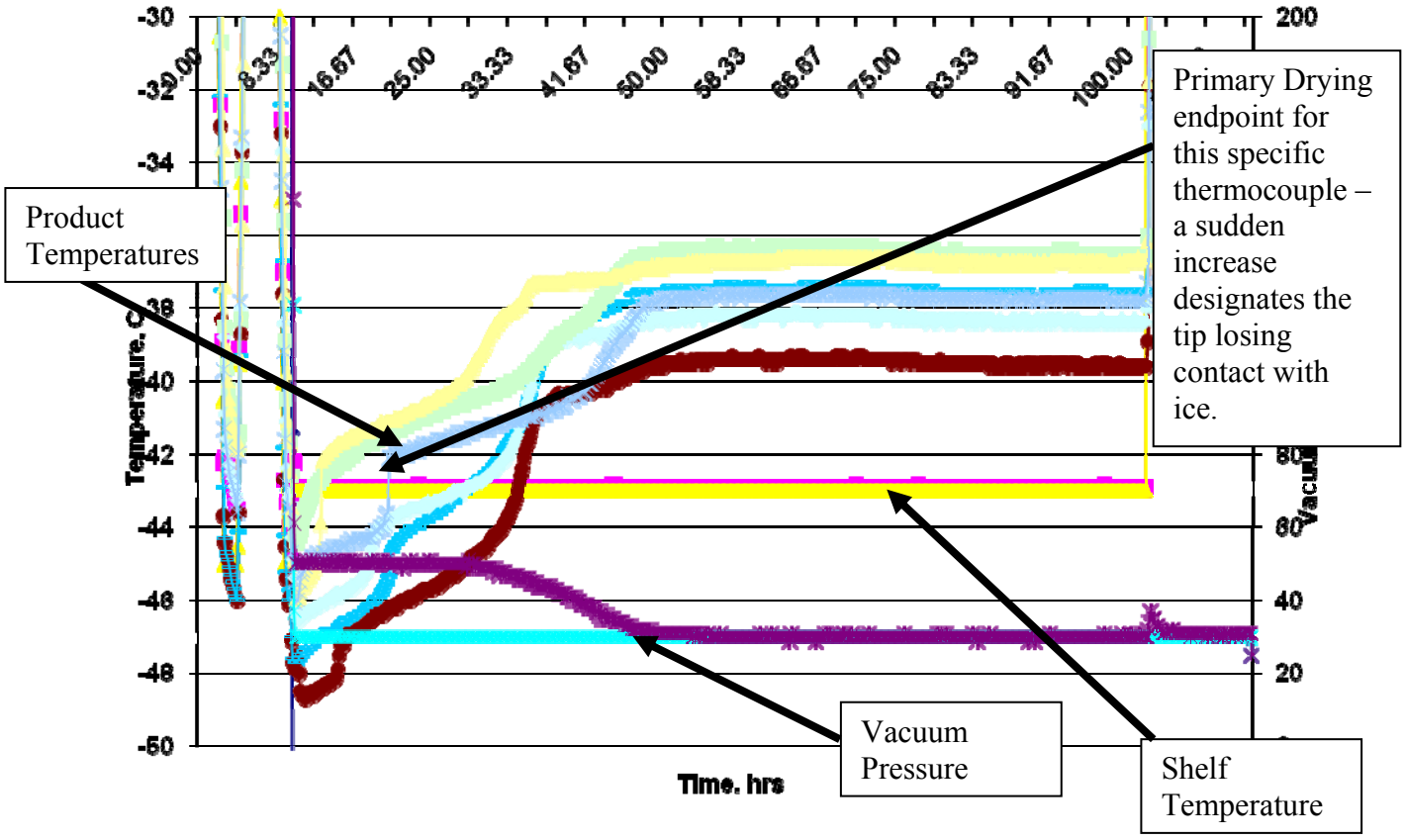

Refer to section 2.2 for an in-depth introduction into primary drying including primary drying trending. From observing the thermocouple behaviour, it was evident that they equilibrated or trended slightly above the shelf temperature during primary drying. This would be the first indication of the endpoint of primary drying. The product temperatures are observed to be

reading above slightly above the shelf temperature, which is common at such low primary drying conditions, especially under vacuum. However, the fact that the thermocouple begins to equilibrate with the shelf temperature once the tip loses contact with ice, means that another verification method must be used. The thermocouple may indicate the primary drying endpoint but as the tip of the thermocouple is not at the extreme bottom, there is a high probability that sublimation is still ongoing. Secondly, the thermocouple is not fully representative of what was actually happening during the step, as it acts as a nucleation site during freezing. It is generally accepted that the nucleation rate and ice crystal structure affects the rate of primary drying (Searles et al., 2001a).

The second method of primary drying endpoint determination consists of the Pirani gauge (purple line) equilibrating with the capacitance manometer (blue line). As the Pirani gauge measures vapour pressure as long as there is vapour in the chamber, the pressure reading will be higher than that of the capacitance manometer (absolute pressure reading) (Patel et al., 2010). Once sublimation (removal of free water) has completed, the Pirani reads the same pressure as the manometer. This, along with thermocouple monitoring, is a good method of determining the endpoint of the primary drying step. Therefore, it can be seen that primary drying completed as planned by examining the purple line (pirani gauge) against the capacitance manometer (light blue). Once the sublimation completes fully, the vapour pressure drops to that of the absolute pressure as measured by the manometer (Patel et al., 2010).

The product temperature raw data were analysed using heat transfer and mass transfer equations (section 2.2.8), to allow better understanding of the primary drying performance. Cake resistance (resistance of dried solids to vapour flow during sublimation of ice) was measured and used to design lyophilisation cycle 2 (freeze drying above the collapse temperature). Each product temperature was analysed for starting temperatures (at the beginning of drying) and end temperatures (at the point the thermocouple lost contact with ice). The target was that the product temperature observed was below the Tg' for that product in question. Refer to table 11 for the complete set of data.

Figure 29 represents the lyophilized cake generated a result of lyophilisation cycle 1. The cake height was small due to the low fill volume of 0.5mL. The cake appearance was acceptable in that the cake was white in colour and uniform in structure with no evidence of meltback or collapse.

Fig. 29: Lyophilized product resulting from Lyophilisation Cycle 1 (consistent for all protein formulations)

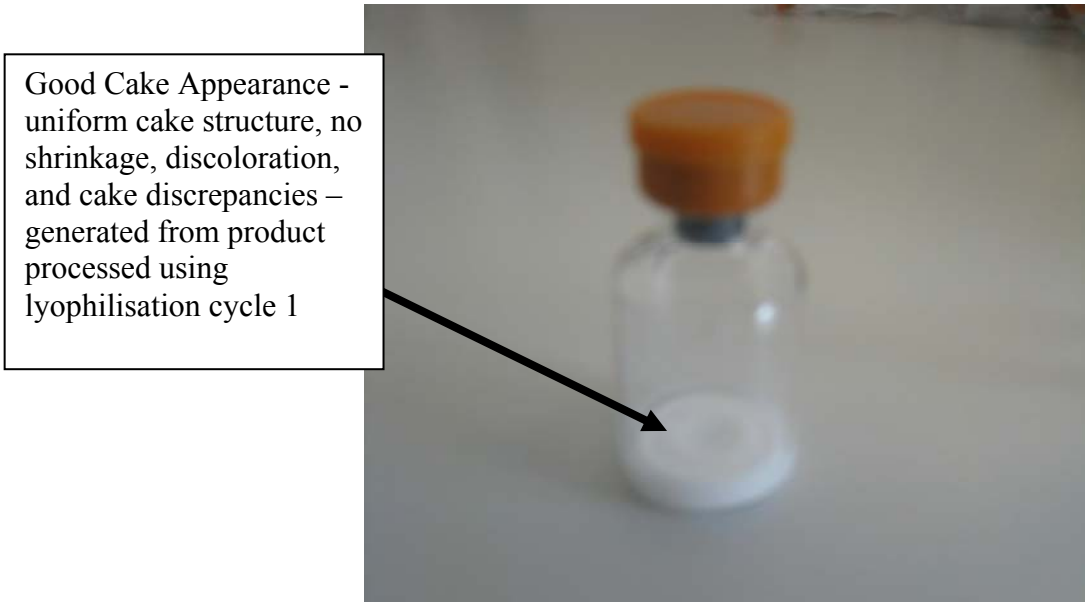

In order to quantitatively show that the primary drying conditions were achieved for all formulations, table 11 lists the primary drying product temperature at both the start and the end of primary drying step for lyophilisation cycle 1 (performed below the collapse temperature). The endpoint was determined by the product temperature losing contact with ice. The goal with this cycle was to create the primary drying conditions where primary drying was performed well below the measured Tg's and/or Tc for all protein formulations. At a high level, by examining the temperatures on table 11, primary drying was found to be performed below the Tc and/ or Tg' of each formulation except BSA and buffer 3, where cycle 1 was conducted slightly above collapse. From this point forward, the goal was to assess each formulation processed using lyophilisation cycle 1 for cake and product characteristics at time 0 through to time 6 months of stability, stored at conditions of 4°C, 25°C 60% relative humidity and 40°C 75% relative

humidity with an view to compare and contrast freeze drying both below (cycle 1) and above collapse (cycle 2) for two model proteins in the presence of various excipients.

Table 11: Table of Parameters associated with the Primary Drying Step of Lyophilisation Cycle 1

Formulation	Tsh (°C)	Pch (mT)	Tp start (°C)	Tp end (°C)	Tc/ Tg' (°C)
Protein X & B2	-43.00	30.00	-48.60	-44.40	-8.30
BSA & B1	-43.00	30.00	-46.40	-45.20	-42.00
BSA & B2	-43.00	30.00	-42.30	-40.00	-11.00
BSA & B3	-43.00	30.00	-42.00	-40.20	-44.59
BSA & B4	-43.00	30.00	-44.80	-44.00	-24.36

The product temperature during primary drying was below the Tg' for that each formulation apart from BSA and B3, which had the lowest measured Tg'. Therefore, for this formulation, primary drying was actually performed above the collapse temperature. To achieve a product temperature lower than the Tg of -44.59°C, primary dying conditions would have had to be set at much lower shelf temperature and vacuum pressure setpoints. The Tg' for BSA & B3 was used as the target temperature for the design of primary drying conditions for cycle 1, where the cake resistance (eq. 7) was assumed and the 5ml vial heat transfer coefficient (eq. 8) was used for the purposes of this study to predict primary drying conditions for all formulations below the collapse temperature. The cake appearance as shown in figure 29 represents the typical appearance for all formulations freeze dried using this lyophilisation cycle. This appearance showed that the cake displayed a uniform solid structure, indicating that there was no evidence of collapse and therefore, the product temperature performance for this formulation was deemed as acceptable to continue on using as part of this project.

The remainder of the formulations all freeze dried well below the collapse temperature. For example, for Protein X & B2, the product temperature at the end of primary drying was measured as -44.40°C, which was well below the measured collapse temperature of -8.30°C.

This assumption may have led actual product temperature conditions to trend that bit higher during primary drying.

7.3.2 Lyophilisation Cycle 2 - Freeze drying above Tg'

Refer to section 5.4 for the methods associated with the design of lyophilisation cycle 2. Figure 30 shows the lyophilisation cycle trend from cycle 2. The freezing temperature was set at -45°C initially but consists of an annealing step at -15°C to crystallize the bulking agent (mannitol or glycine) after which the vacuum pressure (yellow line) is pulled to 450mT and the shelf temperature (red line) was increased to 50°C. The purpose of these conditions was to attempt to force collapse by drying aggressively. The product temperatures and pirani gauge (vapour pressure) shows clearly that primary drying completed fully. The experimental set up was the same for the first cycle with the exception of a fill volume of 2mL being used. It is clear when examining figure 30 that primary drying completed effectively.

Fig. 30: Lyophilisation Cycle 2 Trending – Performing Primary drying above the Collapse Temperature. This cycle was executed in a Virtis Benchmark 1000 freeze dryer with a fill volume within each vial of 2mL. The freezing step initially targeted -45°C and then an annealing step at -15°C after which vacuum pressure of 450mT and a shelf temperaure of +50°C was initiated as the primary drying step.

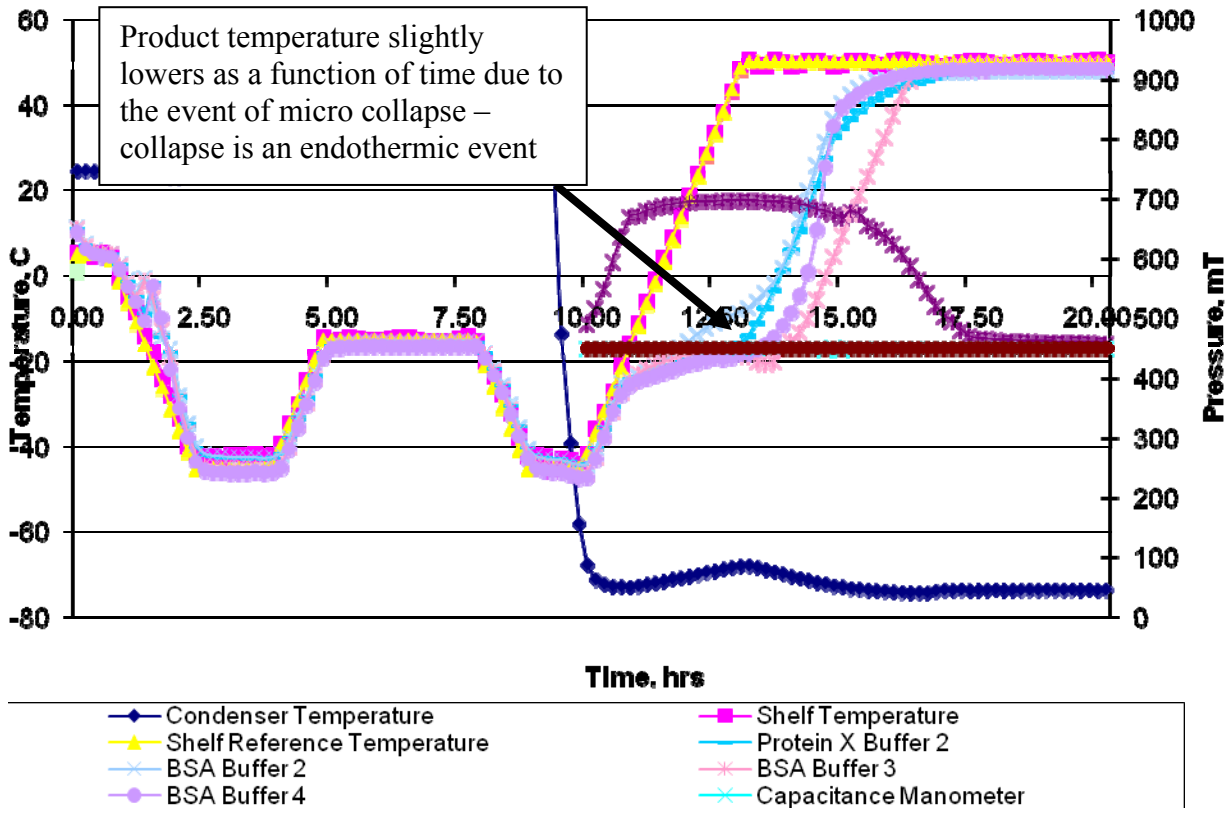

Each product temperature was analysed for start temperatures (at the beginning of drying) and end temperatures (at the point the thermocouple lost contact with ice). The target was that the product temperature prior to losing contact with ice was above the Tg' for each individual formulation.

Table 12 shows the primary drying product temperature at both the start and the end of primary drying for lyophilisation cycle 2 (aggressive – above the collapse temperature). The purpose of this table was to show that the intention to dry above the collapse temperature was achieved for the formulations in question. When examining the table, it becomes clear that primary drying

was conducted below collapse for Protein X and B2 which was not the aim. However, it was achieved for all other formulations. Therefore, there was more relevance in the BSA formulations for the purpose of this study.

Table 12: Table of Parameters associated with the Primary Drying Step of Lyophilisation Cycle 2

Formulation	Tsh (°C)	Pch (mT)	Tp start (°C)	Tp end (°C)	Tc/ Tg' (°C)
Protein X & B2	50	450	-46	-11	-8.30
BSA & B1	50	450	-45.6	-18.5	-42.00
BSA & B2	50	450	-45.4	-8.9	-11.00
BSA & B3	50	450	-46.3	-18	-44.59
BSA & B4	50	450	-47.3	-18.5	-24.36

Figure 31 shows the product cake appearance resulting from the aggressive lyophilisation cycle (cycle #2). From examining the lyophilized cake images resulting from cycle 2, it is clear the resultant cake from the mannitol based formulations (a, b and e) are of acceptable quality. Acceptable cake appearance means that the cake appearance does not show evidence of meltback, collapse, cake discolouration or shrinkage. However, the glycine based formulations (c & d) exhibit various degrees of collapse. It appears that crystalline mannitol was more effective in maintaining cake structure when drying aggressively than crystalline glycine. It is understood that crystalline bulking agents provide macroscopic support to the lyophilized cake during drying (Dixon et al., 2008).

Fig. 31: Lyophilized product resulting from Lyophilisation Cycle 2 for all proteins – (a) BSA & Buffer 1, (b) BSA & Buffer 2, (c) BSA & Buffer 3, (d) BSA & Buffer 4 & (e) Protein X & Buffer 2

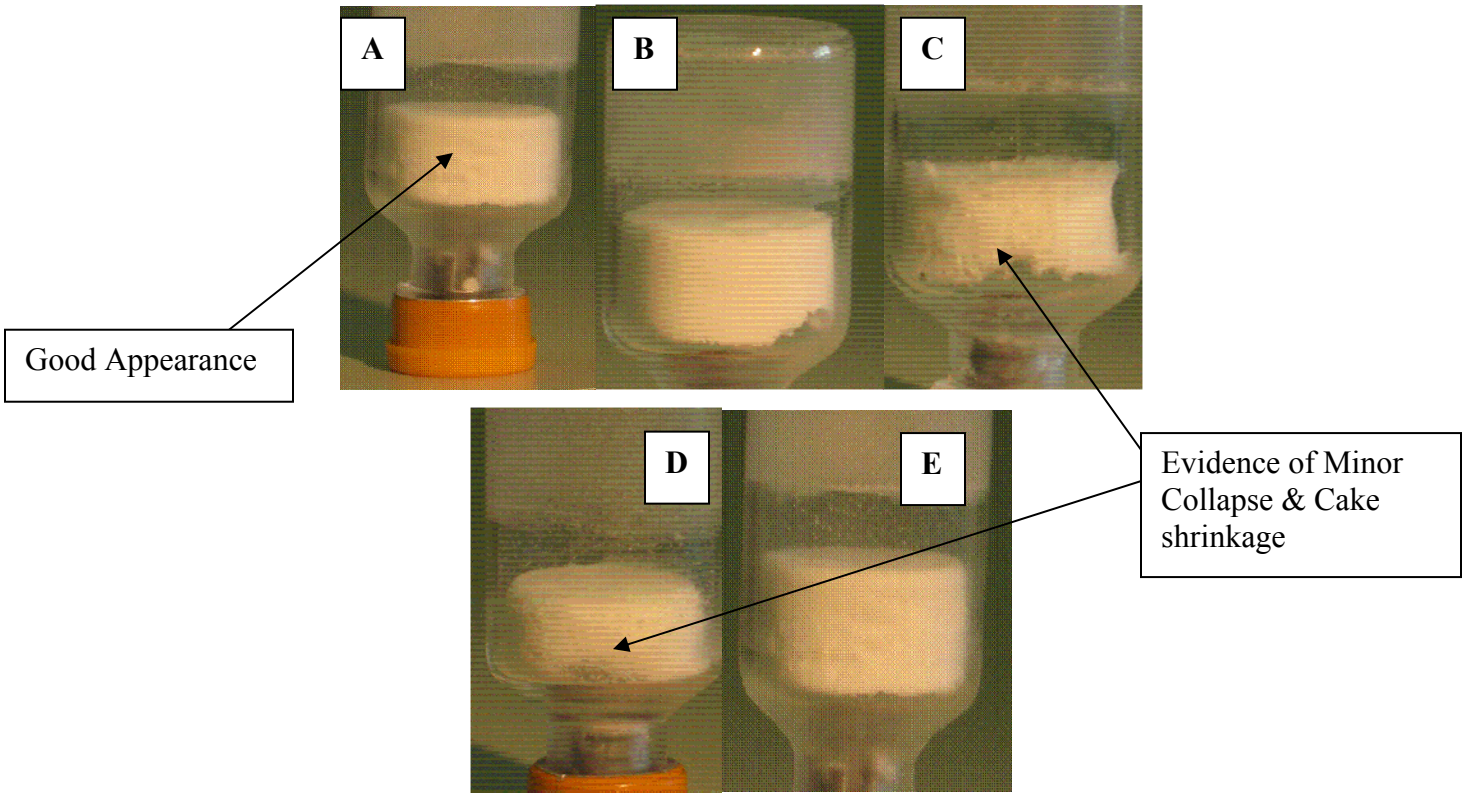

Overall, lyophilisation cycle 1 performed as expected (primary drying product temperatures below the collapse temperature for all but one formulation - BSA and buffer 3) and produced product of uniform cake appearance with no evidence of collapse both from an appearance perspective and from a product temperature perspective (thermocouples show a decrease in temperature upon collapse during primary drying). However, it is clear that from examining the product trending from the second cycle (figure 30), the majority of products experienced microscopic collapse due to the majority of the product temperatures decreased in temperature for a time during primary drying (which is clear when examining the product temperature performance) However, only the glycine based products showed evidence of collapse when examining cake appearance.

7.4 Reconstitution of the Lyophilized Product

Refer to section 5.6 for the reconstitution methods used as part of this project. For the lyophilisation cycle performed at a product temperature below that of the collapse temperature, reconstitution was found to be instantaneous for all samples generated. It was not possible to quantitatively measure the reconstitution time for the majority of vials for cycle 1. For the lyophilisation cycle performed at a product temperature above that of the collapse temperature, reconstitution was found to be up to 1 minute (but not more than 1 minute) for samples generated for all formulations using this lyophilisation cycle. Therefore, drying above collapse affected the reconstitution time of the lyophilized product.

Foaming was consistent in the majority of samples generated from cycle 2. The lyophilized solid content of the material generated from cycle 1 was less than that of cycle 2. The reason for this was that it would take a very long time to freeze dry 2mL fill volume using cycle 1 by using the primary drying conditions associated with lyophilisation cycle 1. The foaming (common for protein formulations at this concentration) may also be a result of this. Overall, drying above the collapse temperature is known to increase reconstitution time (Pikal & Shah, 1990).

Other analytical tools were used to assess the impact of drying above the collapse temperature on the final product post the lyophilisation step. Refer to the Karl Fischer, SEC and CD sections for the analytical analysis (sections 5.7, 5.9 and 5.10). The next step was to analyze the residual moisture content of a select number of samples (n=3) for each formulation.

7.5 Karl Fischer Moisture Analysis of Lyophilized Drug Product post Lyophilisation for each formulation

Refer to section 5.7 for the methods associated with Karl Fischer moisture analysis of lyophilized products. Examining the moisture content of lyophilized cake also allows documenting the differences in the moisture content between the two cycles and to highlight and understand the reasons for this difference over a 6 month time period at different storage conditions.

As expected, storage conditions and time play a significant role in the residual moisture content of the lyophilized cake. Figure 32 shows the % residual moisture increase for BSA in a 4% mannitol 1% sucrose 10mM tris buffer (Buffer 2) lyophilized below the collapse temperature. The lyophilized samples were stored at 2-8°C, 25°C 60% relative humidity and 40°C 75% relative humidity. It is clear that the % moisture increases as a function of storage time for all storage conditions. The blue line illustrates the storage temperature of 2-8°C; the purple line illustrates the temperature 25°C 60% humidity and the light red line, 40°C 75% humidity. An increase in moisture may be due to the moisture released by the rubber stopper over time and also due to potential crystallization of the excipients due to the conditions. The release of moisture from the stopper is expected over time as the stopper has its own residual moisture content as it is an elastomer and that elevated temperatures may cause this moisture to be driven out of the stopper into the product (Pikal, 1992). As the lyophilized drug product is hygroscopic, the moisture will be absorbed by the product over time thereby increasing the residual moisture content of the lyophilized cake. The crystallization of excipients like sucrose, mannitol and glycine, which results in the release of bound water molecules may result in the lyophilized cake absorbing moisture as the crystallization process continues during storage at certain conditions (Dixon et al., 2008).

When examining figure 32, it is demonstrated that the residual moisture content reaches levels of 1.75% when stored for 6 months at a temperature of 40°C and a relative humidity of 75%. The starting time 0 residual moisture was recorded as 0.04%.

Fig. 32: Bar Graph of % Residual Moisture as a Function of Storage Timepoint and Conditions for 25mg/mL BSA 4%Glycine 1% Sucrose 10mM Tris pH 7.0 (Buffer 4) Lyophilized below the collapse temperature (Tc) – Lyophilisation Cycle 1 (Lyophilisation below the collapse temperature). Residual moisture was measured using Karl Fischer equipped with an oven which removes any sample handling in the process of analysis.

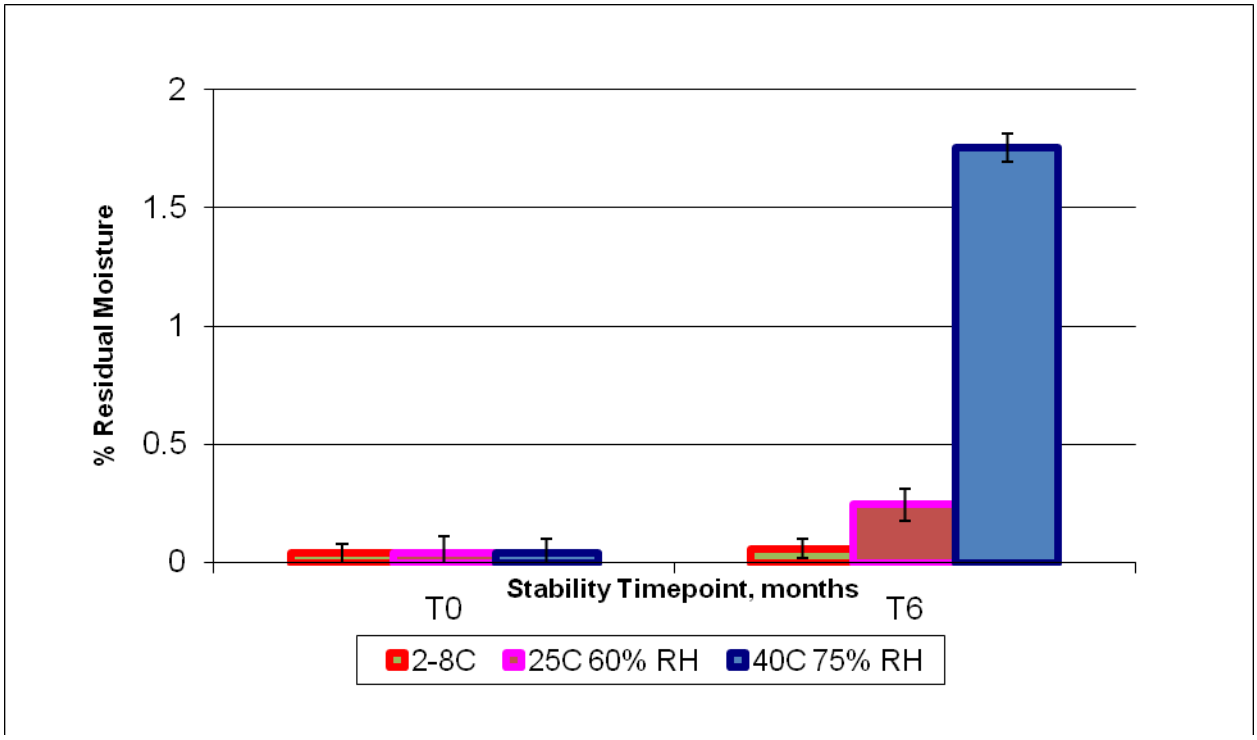

The blue bar represents the moisture resulting from storage at 40°C and 75% relative humidity, the pink and purple bar represents moisture data resulting from storage at 25°C and 60% relative humidity and the red and green bar represents moisture data from storage at 2-8°C. As expected, residual moisture content increases as a function of time to varying degrees depending on storage conditions. The increase in moisture is generally due to the transfer of water molecules from the rubber stopper into the lyophilized cake over time (Pikal & Shah, 1992) along with amorphous excipient crystallization events (Dixon et al, 2008). The moisture from the stopper is driven out at different rates over time depending on the storage conditions.

Figure 33 illustrates the residual moisture measured using Karl Fischer as a function of stability time point and storage conditions.

Fig. 33: Bar Graph of % Residual Moisture as a Function of Storage Timepoint and Conditions for 25mg/mL BSA 4% Glycine 1% Sucrose 10mM Tris pH 7.0 (Buffer 4) Lyophilized above the collapse temperature (Tc) – Lyophilisation Cycle 2 (Lyophilisation above the collapse temperature)

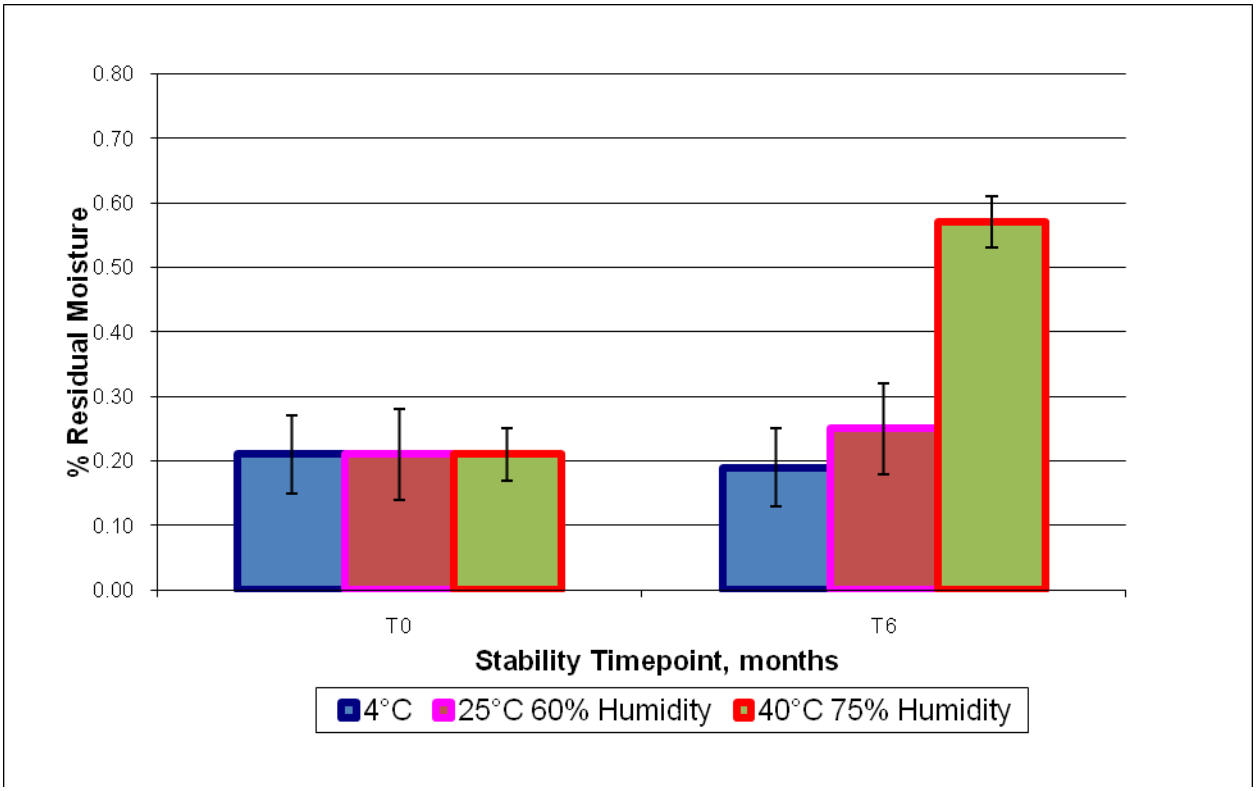

The red and green bar represents the moisture resulting from storage at 40°C and 75% relative humidity, the pink and purple represents the moisture resulting from storage at 25°C and 60% relative humidity and the blue bar represents the moisture resulting from storage at 2-8°C. For this formulation, the time 0 residual moisture content was higher for the material lyophilized above the collapse temperature. It was clear from comparing the results from both below and above collapse lyophilisation cycles that the residual moisture increase was lower for the material lyophilized above the collapse temperature. The moisture content for time 6 month lyophilized material when lyophilized above collapse as found to be lower than that of the material lyophilized below the collapse temperature. It is important to note and consider, however, that the fill volume for the cycle 2 was four times larger than cycle 1. Also, the same vials and stoppers were used for each lyophilisation cycle. It was also understood that the effect

of moisture leaching into the product would be different and dependent on fill volume and in turn cake weight.

It is evident that the time 0 results were higher for the material generated from cycle 2. This is due mainly to the fact that freeze drying (or specifically primary drying) was performed above the collapse temperature during cycle 2, which results in a subsequent increase in residual moisture content (Pikal & Shah, 1990). Table 13 lists all the residual moisture results for all protein formulations lyophilized both below and above the collapse temperature. It was found that the time zero moisture results were higher for the products from lyophilisation cycle 2 (above collapse). However, at the end of the storage conditions, it was evident that the result for the product from cycle 2 was found to be much lower than the material from cycle 1. Clearly, drying above collapse has a negative effect on moisture content at time zero (Pikal et al., 2000).

Table 13 captures the complete residual moisture result data set for all formulations as a function of storage conditions and time.

Table 13: Residual Moisture Full Table of Results for all cycles executed

Protein Formulation	Stability Time point, months	Storage Conditions	% Residual Moisture	
			Cycle 1 % (Standard Deviation)	Cycle 2 % (Standard Deviation)
Protein X Buffer 2	0		0.03 (0.002)	0.09 (0.009)
	6	4°C	0.05 (0.01)	0.09 (0.02)
	6	25°C 60% Humidity	0.22 (0.03)	0.10 (0.05)
	6	40°C 75% Humidity	1.62 (0.11)	0.48(0.05)
BSA Buffer 1	0		0.04 (0.03)	0.21(0.04)
	6	4°C	0.06 (0.01)	0.19 (0.06)
	6	25°C 60% Humidity	0.24 (0.03)	0.25 (0.07)
	6	40°C 75% Humidity	1.75 (0.18)	0.57 (0.04)
BSA Buffer 2	0		0.02 (0.003)	0.06 (0.002)
	6	4°C	0.05 (0.01)	0.06 (0.01)
	6	25°C 60% Humidity	0.22 (0.03)	0.08 (0.01)
	6	40°C 75% Humidity	1.80 (0.10)	0.44 (0.11)
BSA Buffer 3	0		0.03 (0.003)	0.46 (0.01)
	6	4°C	0.10 (0.05)	0.45 (0.01)
	6	25°C 60% Humidity	0.29 (0.09)	0.46 (0.02)
	6	40°C 75% Humidity	1.91 (0.05)	0.80 (0.05)
BSA Buffer 4	0		0.21 (0.02)	0.27 (0.02)
	6	4°C	0.27 (0.08)	0.26 (0.005)
	6	25°C 60% Humidity	0.40 (0/14)	0.24 (0.01)
	6	40°C 75% Humidity	1.89 (0.06)	0.63 (0.05)

During crystallization of amorphous material such as mannitol or sucrose, some water remains in the amorphous phase. The total amount of water in the product is the same (assuming that no water transfers from the stopper to the product); the water is just distributed differently

throughout the material. The total amount of amorphous phase decreases as excipients such as mannitol and sucrose are crystallized upon storage of the lyophilized drug product at different conditions; therefore the moisture content of amorphous part of cake is increasing due to the crystallization reaction releasing bound water. Crystallization of excipients in the dried powder phase along with Tg and melting of the dried phase was examined by powder mDSC.

7.6 Powder DSC

Powder DSC was used to measure the Tg, crystallization (Tcrys) and melting (Tm) events in the solid state (lyophilized). Refer to section 5.8 for the procedure used. The purpose of this analysis was to examine the change in Tg, crystallization of the amorphous excipients and melting of the solids as a function of stability storage conditions and time. Time 0, 1, 3 and time 6 months were selected as storage points of interest for moisture analysis at storage conditions of 2-8°C, 25°C 60% relative humidity and 40°C 75% relative humidity as per section 5.11 (stability study design section).

The importance of changes in Tg, Tcrys and Tm of the solid state as a function of time supports the moisture content increase due to moisture transferring from the stopper to the cake, causing the Tg to lower in temperature as the Tg' of ice is reported to be -135°C (Nail et al., 2002), along with the fact that water is released by the crystallization of amorphous excipients such as mannitol, glycine or sucrose, which also causes the moisture content to increase and subsequently the Tg to drop.

Fig. 34: Powder mDSC of a given protein formulation – this thermograph was generated using a TA instruments mDSC system where the sample was placed in an aluminium hermetic pan for analysis. The blank was represented by an empty pan and the heat flow was the difference in heat capacity between the two samples as a function of time and conditions

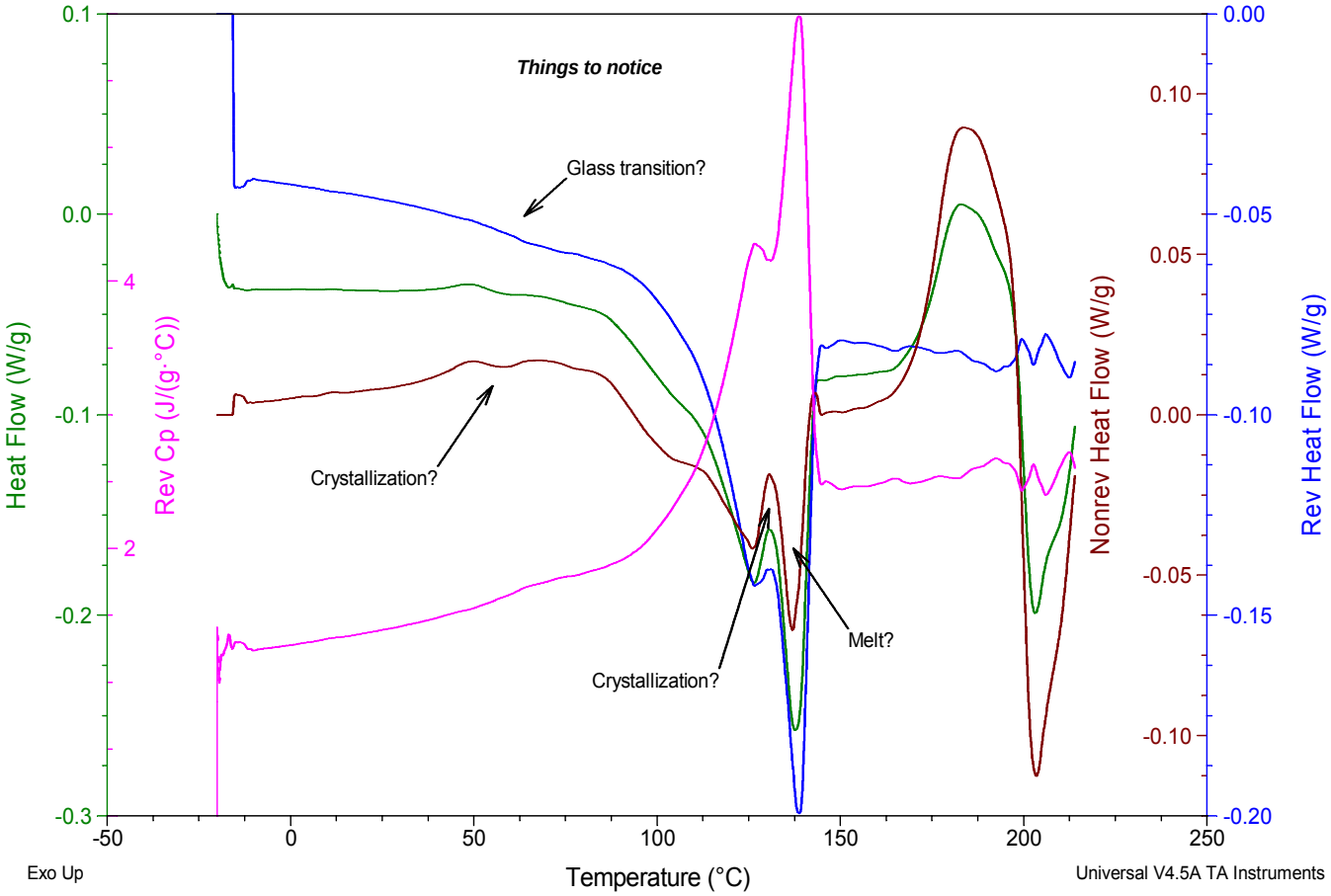

The total heat flow is represented by the green line and the Y1 axis. As described, the heat flow is the resultant difference in energy (heat flow) between the sample pan and the reference pan. The signal was broken down into three extra signals using the universal analysis software®. The first is the reversing heat flow (blue line – Y2 axis) and the second is the non reversing heat flow (brown line, Y4 axis). Importantly, the total heat flow is a product of the reversing and non reversing signals (equation 4). The final signal was the reversing heat capacity (pink line – Y3 axis) which is opposite to the reversing heat flow. The reversing heat capacity signal is very sensitive and is good to use to identify subtle Tgs. (TA Instruments presentation/ website www.tainstruments.com).

Tg was found on the reversing heat flow or the reversing heat capacity signals, crystallization was evident on the non reversing signal and melting on the total heat flow signal. From examining figure 34, it is clear that a number of potential crystallization peaks of the amorphous bulking agent (non crystalline mannitol/ glycine) and excipients (sucrose) along with the Tg and the Tm are evident in this thermograph. Glass transition temperature (Tg) results may be examined in tables 14 to 23 of this section of the thesis. Crystallization and melting temperatures were not examined further in this document. As there was no availability of test methods to examine the crystallinity of the powder (for example, XRD), the important point is that the increase in moisture content as a function of time may also be as a result of the crystallization or amorphous nature. The endotherm found on the powder mDSC thermographs could not be identified due to XRD not being available to use at the time of product analysis and stability time point. The Tg results over time were used to compliment the residual moisture data measured by Karl Fischer (section 5.7).

Tables 14 to 23 are the complete powder Tg temperature results for all lyophilized cakes from all formulations and storage conditions. Potential variation in mDSC analysis may be as a result of sample handling, sample size and analyst interpretation of where to drop the limits when analysing using the universal analysis software. In order to minimize sample handling, samples were prepared in a glovebox at 5% relative humidity with a nitrogen overlay. Some of the formulations exhibit multiple Tg temperatures which may have been due to micro collapse in the sample (drying above collapse). When examining tables 14 to 23 all samples freeze dried below

the collapse temperature did not display multiple Tgs, whereas the majority of the freeze dried formulations above the collapse temperature seemed to display this event. As the protein X formulation did not experience processing conditions above the collapse temperature of the formulation and that there was still evidence of multiple Tgs, this may point to the fact that phase changes may result when dried below but close to the collapse temperature. Alternatively, there may have been error in the measurement of the collapse temperature for this formulation.

Figure 35 represents the powder Tg trend as a function of storage time for BSA buffer 3 (4% Glycine 1% Sucrose 100nN NaCl 10mM Tris buffer) freeze dried below the collapse temperature using lyophilisation cycle 1.

Fig. 35: Trend showing the relationship of Tg plotted as a function a function of time for BSA and buffer 3 (4% Glycine 1% Sucrose 100mM NaCl 10mM Tris buffer) freeze dried using lyophilisation cycle 1.

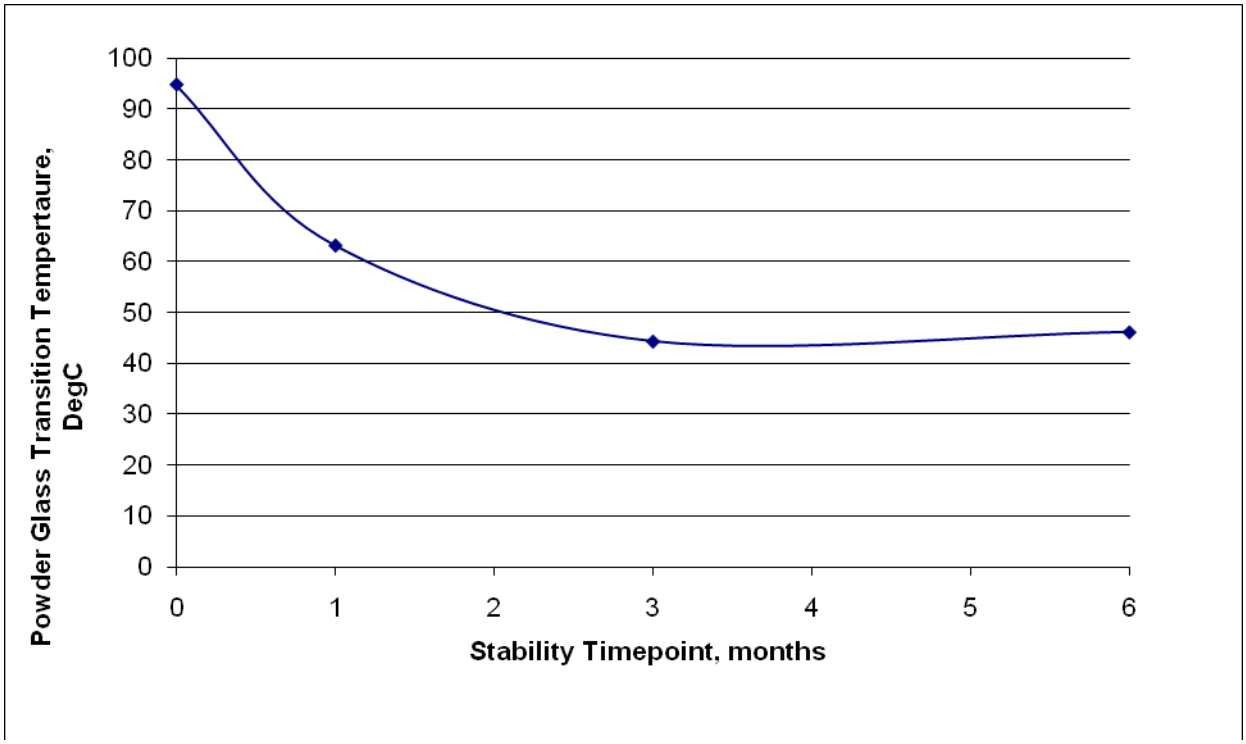

This figure shows the decrease of the powder Tg for this formulation as a function of storage time. The Tg' of ice is -135°C (Nail et al., 2002), which has an impact on the overall powder/ lyophilized product Tg. Generally, as the moisture content increases, the Tg of the powder decreases (Dixon et al, 2008). Unlike the glycine based formulations, the mannitol based formulations did not experience a change in Tg as a function of moisture over time for the material processed using cycle 1. This may be due to the presence of a lower amorphous content in the lyophilized cake during storage for mannitol based formulations compared to glycine based formulations as there may have been a high degree of mannitol crystallization during the freezing step of the freeze drying cycle. The amorphous content remaining in the cake is likely to attract the moisture from the stopper over the stability storage time.

Amorphous excipients crystallize over time, which would cause an increase in residual moisture content. Also, as the fill volume was less for the cycle 1 product than cycle 2 product, moisture

content was found to be lower at T0 but higher as a function of time for the cycle 1 product, which could result in a lower powder Tg. As the same stopper was used for both lyophilisation cycles and that the rate of moisture transfer over the storage conditions and time was likely the same for both, the same stopper moisture transfer would have a different effect on the overall % residual moisture result due to differences in overall fill volume and in turn dry product.

Analysis of the powder Tg also enables us to determine if collapse is likely to be present in the sample. Collapse results in variable moisture levels from vial to vial and within a given lyophilized product. Variability in moisture locally within a given cake, as a result of various degrees of collapse across the freeze dried cake, would potentially result in local glass transition temperatures and would show up in mDSC thermographs as multiple glass transition temperatures. As there are multiple glass transition temperatures in the majority of samples processed by using cycle 2 and based on the presence of multiple glass transition temperatures, micro collapse may be present in the sample. Coupled with moisture data, appearance and product thermocouple data trending, this technique proves to be a verification technique in the assessment of lyophilized product.

Table 14 represents the Tg measurements of protein X and buffer 2, freeze dried below the collapse temperature of the formulation.

Table 14:Powder DSC - Tg Temperatures of lyophilized Protein X 4%Mannitol 1%Sucrose 10mM Tris pH 7.0 (Buffer 2) Lyo Cycle 1 – below collapse

Stability Time point (months)	Storage Conditions	Tg (°C)
0	n/a	129.28
1	25°C 60% Relative Humidity	127.56
1	40°C 75% Relative Humidity	127.20
3	25°C 60% Relative Humidity	125.82
3	40°C 75% Relative Humidity	118.73
6	4°C	128.14
6	25°C 60% Relative Humidity	128.44
6	40°C 75% Relative Humidity	128.89

Even though the moisture content was found to increase at the 40°C storage conditions at time 6 months, the Tg showed a reduction up to time 3 months but an unexpected increase at the 6 month time point. This may have been due to error in analysis and should be assessed in a further project. The moisture content was found to increase for 2-8°C or 25°C storage conditions.

Table 15 represents the Tg measurements of protein X and buffer 2, freeze dried slightly below (or approaching) the collapse temperature of the formulation. The target when designing the lyophilisation cycle was to attempt to freeze dry above the collapse temperature but due to the resistance and the assumptions made this was not achieved. Instead, freeze drying was performed below the collapse temperature but closer than that of cycle 1 conditions.

Table 15: Powder DSC - Tg Temperatures of lyophilized Protein X 4%Mannitol 1%Sucrose 10mM Tris pH 7.0 (Buffer 2) Lyo Cycle 2 – approaching collapse

Stability Time point (months)	Storage Conditions	Tg 1 (°C)	Tg 2 (°C)
0	n/a	-	131.87
1	25°C 60% Relative Humidity	-	131.79
1	40°C 75% Relative Humidity	39.49	135.82
3	25°C 60% Relative Humidity	36.16	135.46
3	40°C 75% Relative Humidity	39.50	136.38
6	4°C	50.62	134.96
6	25°C 60% Relative Humidity	-	129.86
6	40°C 75% Relative Humidity	-	134.60

From the data set, it becomes evident that there are multiple glass transition temperatures which may be due to drying close to the collapse temperature. As already stated, it is understood that collapse results in high moisture content, which in turn results in potential changes to the glass transition temperature. Collapse may happen at varying degrees across the dry layer, which may result in localized variable moisture levels and thereby multiple glass transition temperatures. It is accepted at this point that during this cycle for this formulation, primary drying was conducted at a product temperature below that of the collapse temperature, which can be verified by examining table 12. The original intention was to attempt to dry above the collapse temperature. As discussed, the reason why this was not achieved was due to the Tc being very high and the fact that the cake resistance did not allow the design of a lyophilisation cycle to target a product temperature above this value. However, due to the nature of the microscopy method used to measure the collapse temperature, in that it is based on interpretation and extremely slow

ramping to specify collapse, it is possible that there may be error in the measurement of the collapse temperature for this particular formulation.

Table 16 represents the Tg measurements of BSA and buffer 1, freeze dried slightly below (or approaching) the collapse temperature of the formulation.

Table 16: Powder DSC - Tg Temperatures of lyophilized BSA 4%Mannitol 1%Sucrose 100mM NaCl 10mM Tris pH 7.0 (Buffer 1) Lyo Cycle 1 – below collapse

Stability Time point (months)	Storage Conditions	Tg (°C)
0	n/a	133.78
1	25°C 60% Relative Humidity	131.17
1	40°C 75% Relative Humidity	133.20
3	25°C 60% Relative Humidity	132.23
3	40°C 75% Relative Humidity	133.36
6	4°C	132.72
6	25°C 60% Relative Humidity	129.14
6	40°C 75% Relative Humidity	124.13

Again, similar to table 14, drying below the measured collapse temperature results in a single Tg. The trend in Tg as a function of storage temperature and time shows a slight increase, which is likely due to an increase in moisture content, which is evident when examining table 13. Specifically, table 16 shows that there was no significant change in Tg until time 6 months. It is difficult to align these findings up with the moisture analysis as the analysis of residual moisture were only performed on time zero and 6 month stability time points. However, the increase in moisture at time 6 months is supported by the drop in Tg at both the 25°C and 40°C storage temperatures.

Table 17 represents the Tg measurements of BSA and buffer 1, freeze dried above the collapse temperature of the formulation.

Table 17: Powder DSC - Tg Temperatures of lyophilized BSA 4%Mannitol 1%Sucrose 100mM NaCl 10mM Tris pH 7.0 (Buffer 1) Lyo Cycle 2 – above collapse

Stability Time point (months)	Storage Conditions	Tg 1 (°C)	Tg 2 (°C)
0	n/a	85.07	152.01
1	25°C 60% Relative Humidity	77.21	153.13
1	40°C 75% Relative Humidity	37.38	153.13
3	25°C 60% Relative Humidity	72.94	145.60
3	40°C 75% Relative Humidity	39.19	152.28
6	4°C	40.76	152.51
6	25°C 60% Relative Humidity	42.22	152.46
6	40°C 75% Relative Humidity	38.22	150.64

For the Protein X and buffer 2, drying above the collapse temperature was not achieved mainly due to the thermal characteristics of the formulation and the fact that the conditions were not aggressive enough. However for table 17 (BSA and buffer 1), drying above collapse was achieved and the first observation was that there were two Tg's reported (Tg 1 and Tg 2). As the collapse phenomenon leads to heterogeneous structure across the cake, this results in different local residual moisture contents and subsequent change in Tg as a function of time. This also seems to result in this case in multiple glass transition temperatures. The difference in the Tg values (Tg 1 and Tg 2) reported in table 17 along with the different profile of each of the Tg's as a function of time may have been due to the heterogeneity in collapse and in turn, moisture content. The high Tg values were likely from non collapsed portion of the cake while the lower Tg values are likely from collapse areas of the cake, where the residual moisture content if higher. The degree of collapse in certain locations of the cake may increase over time due to an increase in moisture content resulting in lower Tg values, hence the significant downward trend in Tg as a function of time. Similar to the previous formulations and lyophilisation cycles, the Tg changes as a function of time and storage conditions and again is supported by the residual

moisture results (table 13). However, the significant change is not noticed until time 6 months at both 25°C and 40°C for both Tg measurements.

Table 18 represents the Tg measurements of BSA and buffer 2, freeze dried below the collapse temperature of the formulation.

Table 18: Powder DSC - Tg Temperatures of lyophilized BSA 4%Mannitol 1%Sucrose 10mM Tris pH 7.0 (Buffer 2) Lyo Cycle 1 – below collapse

Stability Time point (months)	Storage Conditions	Tg (°C)
0	n/a	127.88
1	25°C 60% Relative Humidity	137.51
1	40°C 75% Relative Humidity	134.31
3	25°C 60% Relative Humidity	127.48
3	40°C 75% Relative Humidity	129.69
6	4°C	125.18
6	25°C 60% Relative Humidity	123.84
6	40°C 75% Relative Humidity	136.68

There is slight variability in the Tg results in the data set but there is no evidence of a significant trend to associate with the change in residual moisture over time. The variability in the measurements may be more a function of the application software (TA Universal analysis) as the analysis is very much related to where the analyst drops the limits of integration. Only one Tg was detected for each formulation over time and storage conditions, which is consistent with the previous batches manufactured below the collapse temperature of the specific formulation.

Table 19 represents the Tg measurements of BSA and buffer 2, freeze dried above the collapse temperature of the formulation.

Table 19: Powder DSC - Tg Temperatures of lyophilized BSA 4%Mannitol 1%Sucrose 10mM Tris pH 7.0 (Buffer 2) Lyo Cycle 2 – above collapse

Stability Time point (months)	Storage Conditions	Tg (°C)
0	n/a	130.06
1	25°C 60% Relative Humidity	131.21
1	40°C 75% Relative Humidity	127.90
3	25°C 60% Relative Humidity	130.59
3	40°C 75% Relative Humidity	131.52
6	4°C	129.61
6	25°C 60% Relative Humidity	132.75
6	40°C 75% Relative Humidity	129.77

Even though this formulation was dried above the collapse temperature, no trend was observed in relation to Tg over time and stability storage conditions. Also, only one glass transition temperaure was observed, which is contrary to the findings for the majority of the previous batches freeze dried above the collapse temperature. This formulation did not contain NaCl as an excipient which may be a reason for this. To understand this further, a wide variety of formulations with and without NaCl should be formulated, lyophilized and examined using powder DSC both above and below collapse.

Table 20 represents the Tg measurements of BSA and buffer 3, freeze dried below the collapse temperature of the formulation.

Table 20: Powder DSC - Tg Temperatures of lyophilized BSA 4%Glycine 1%Sucrose 100mM NaCl 10mM Tris pH 7.0 (Buffer 3) Lyo Cycle 1 – below collapse

Stability Time point (months)	Storage Conditions	Tg (°C)
0	n/a	94.75
1	25°C 60% Relative Humidity	86.99
1	40°C 75% Relative Humidity	63.22
3	25°C 60% Relative Humidity	63.31
3	40°C 75% Relative Humidity	44.41
6	4°C	64.47
6	25°C 60% Relative Humidity	39.58
6	40°C 75% Relative Humidity	46.22

Based on the data presented in table 20, there was a significant decrease in the Tg measurements, which complemented the moisture increase. There is evidence of one glass transition temperature, which agrees with all lyophilized products generated by lyophilisation cycle 1. However, this was the formulation which was dried above the glass transition temperature of -44.59°C as it was very difficult to design a lyophilisation cycle to dry below the glass transition temperature in this case. The collapse temperature was not detected for this formulation, so it was not known whether or not drying below collapse in this case was achieved. As there was only one glass transition temperature determined in the powder state, there is a high probability that this product was dried below the collapse temperature when using other formulations as a frame of reference.

Table 21 represents the Tg measurements of BSA and buffer 3, freeze dried above the collapse temperature of the formulation.

Table 21: Powder DSC - Tg Temperatures of lyophilized BSA 4%Glycine 1%Sucrose 100mM NaCl 10mM Tris pH 7.0 (Buffer 3) Lyo Cycle 2 – above collapse

Stability Time point (months)	Storage Conditions	Tg 1 C)	Tg 2 (°C)
0	n/a	66.21	144.76
1	25°C 60% Relative Humidity	72.53	160.21
1	40°C 75% Relative Humidity	64.58	158.05
3	25°C 60% Relative Humidity	32.86	160.66
3	40°C 75% Relative Humidity	26.86	157.45
6	4°C	*	*
6	25°C 60% Relative Humidity	*	*
6	40°C 75% Relative Humidity	*	*

* Data not available - material not available at time of analysis

Drying above collapse was achieved and the first observation (consistent with other formulations) was that there were two Tg's reported (Tg 1 and Tg 2), as the collapse phenomenon is heterogeneous across the cake, resulting in different local residual moisture contents and subsequent variability in the measurement of Tg. This seems to result in this case in multiple glass transition temperatures. Similar to the previous formulations and lyophilisation cycles, Tg changes as a function of time and storage conditions and again this is supported by the residual moisture results (table 13). However, the significant change is not noticed until time 6 months at both 25°C and 40°C for both Tg measurements. All T6 month samples were not analysed due to loss of samples during storage. T0 analysis resulted in slightly out of trend measurements and when examining all the other results, there is a significant decrease in both Tg's as a function of time and if T6 month samples were analyzed, it would be expected for the trend to continue. This agrees and falls in line with the increase in moisture over time mainly due to crystallization events and moisture transfer from the stopper to the freeze dried cake.

Table 22 represents the Tg measurements of BSA and buffer 4, freeze dried below the collapse temperature of the formulation.

Table 22: Powder DSC - Tg Temperatures of lyophilized BSA 4%Glycine 1%Sucrose 10mM Tris pH 7.0 (Buffer 4) Lyo Cycle 1 – below collapse

Stability Time point (months)	Storage Conditions	Tg (°C)
0	n/a	83.48
1	25°C 60% Relative Humidity	78.92
1	40°C 75% Relative Humidity	59.31
3	25°C 60% Relative Humidity	39.58
3	40°C 75% Relative Humidity	44.59
6	4°C	41.86
6	25°C 60% Relative Humidity	34.77
6	40°C 75% Relative Humidity	45.30

Consistent with all other formulations, there was only one glass transition temperature evident when analyzing the mDSC profile. Also, when examining the results, it is clear that there was a decrease in the measured Tg as a function of time for both storage conditions. This is in line with the increase in moisture as can be seen when examining table 13.

Table 23 represents the Tg measurements of BSA and buffer 4, freeze dried above the collapse temperature of the formulation.

Table 23: Powder DSC - Tg Temperatures of lyophilized BSA 4%Glycine 1%Sucrose 10mM Tris pH 7.0 (Buffer 4) Lyo cycle 2 – above collapse

Stability Time point (months)	Storage Conditions	Tg 1 (°C)	Tg 2 (°C)
0	n/a	34.60	131.66
1	25°C 60% Relative Humidity	40.12	132.88
1	40°C 75% Relative Humidity	*	*
3	25°C 60% Relative Humidity	*	*
3	40°C 75% Relative Humidity	20.21	131.58
6	4°C	25.79	131.76
6	25°C 60% Relative Humidity	20.63	132.75
6	40°C 75% Relative Humidity	*	*

* Data not available - material not available at time of analysis

Multiple glass transition temperatures were measured for BSA and buffer 4 when freeze dried above the collapse temperature. From the results available, there is no evidence of a trend in Tg as a function of time for both storage conditions. However, for three of the timepoints, there was no sample available for analysis, thereby no data available to discuss and trend. This was due to vial breakage during storage.

In order to investigate if drying above collapse and the increase in moisture over time had any effect on the degradation rate of the proteins in question, size exclusion chromatography (SEC) was used.

7.7 SEC

SEC method may be review in section 5.9. SEC Data analysis was performed using Empower© software, where the peak was integrated to calculated percentage relative high molecular weight (HMW) and percentage protein monomer (main peak). For this particular project, a marked

increase in the rate of aggregation (degradation – note that the word degradation will be used throughout this document from this point forward) is represented by an increase in the HMW peak. Samples were placed on stability at different storage conditions over a 6 month period (refer to section 5.11), selected and analysed using SEC for an increase in the HMW peak. Refer to section 5.9 for the materials and methods for this SEC method.

Figures 36 and 37 represent the typical chromatograph of protein X (figure 36) and BSA (figure 37). Internal standards (minimum n=3) for both proteins were run prior to each sample analysis. For Protein X, high molecular weight degradation yields a peak after approximately 7.2 minutes denoted as peak β and the protein monomer at 8 minutes. For BSA based formulations, two high molecular weight degradants are evident (denoted as peak β and γ peak) along with the protein monomer at 10 minutes retention time. Each of the peaks were integrated, recorded as a percentage and analysed for rate constant degradation using Arrhenius kinetics (Wang et al., 2003; Franks, 2008).

The HMW peaks that elute during the SEC run were identified by associating the Greek letters β and γ to them, but are not identified chemically. The protein molecule was represented by the Greek letter α and the focus of this assessment was based on the HMW degradation (β and γ peaks). BSA is known to have two HMW degradants - β and γ degradants (Hunter & Carta, 2001). All high molecular weigh fractions elute before the protein peak (earlier in the retention time) as high molecular weight molecules are larger than the target molecule and SE HPLC separates out molecules in size, with the largest eluting first.

The following figures 36 and 37 represent examples of the HPLC chromatograms that resulted from the analysis in support of this project.

Fig. 36: SEC sample Chromatogram for Protein X. The lyophilized sample was reconstituted back to the original protein concentration and injected into the SEC column. This chromatogram does not necessarily represent a specific timepoint.

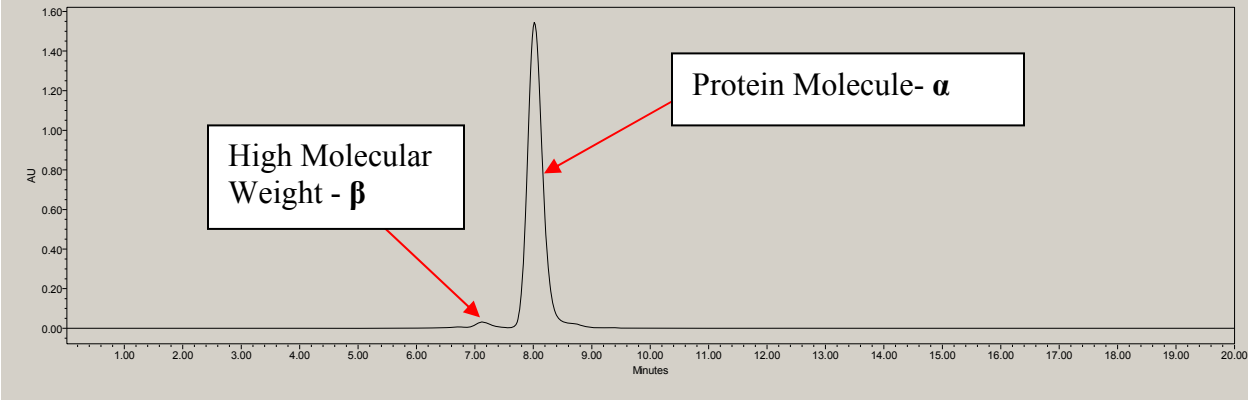

Fig. 37: SEC sample Chromatogram for BSA. The lyophilized sample was reconstituted back to the original protein concentration and injected into the SEC column. This chromatogram does not necessarily represent a specific timepoint.

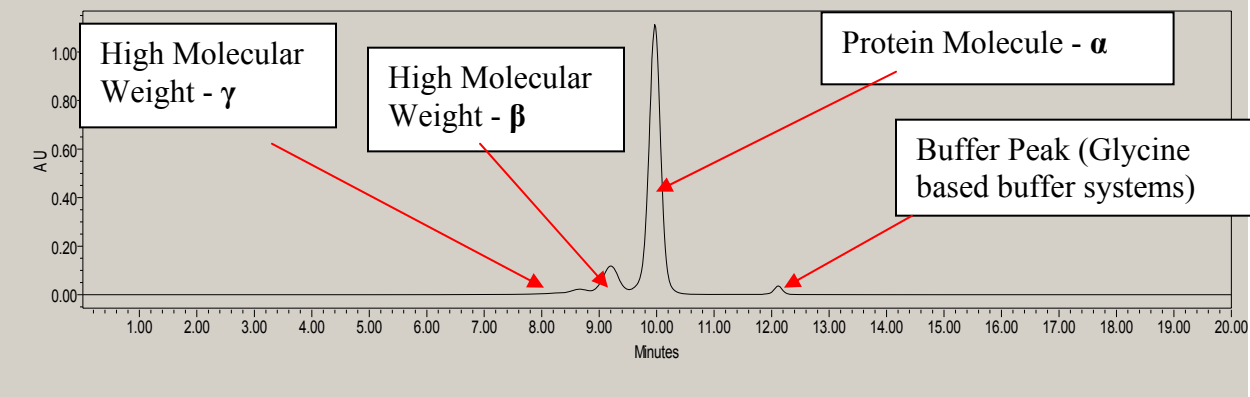

Data analysis consisted of integrating the peaks of a chromatogram like the one above to calculate the %HMW. The following formula was used:

$$\%HMW = \frac{AreaHMW}{TotalArea} x100 \quad \text{(Eq. 10)}$$

The results were reported in % area of each peak. The % HMW were plotted against stability time point for samples of each protein formulation from both cycles 1 (primary drying conducted at a product temperature below collapse) and 2 (primary drying conducted at a product temperature above collapse).

The HMW fractions were assessed and reported as the degradation rates of the proteins in question. When plotting the degradation as a function of time, a non linear relationship was observed. However, when plotting against the square root of time, a linear relationship was observed. This is known as square root of time degradation kinetics (Wang et al., 2009). Rate constant kinetics as a function of the square root of time is a common method when assessing protein degradation (Pikal et. al., 1991; Chang et. al., 2005; Wang et al., 2009) and predicting the degradation rate to times further out than the planned stability storage profile. For this section of the project, the objective was to examine the rate constant kinetics of lyophilized product processed both below and above the collapse temperature.

Figure 38 illustrates actual data for one of the BSA based formulations. This is provided to illustrate what the actual data trending looked like for all protein formulations. However, as part of this thesis, the raw data will not be presented from this point forward.

Fig. 38: % Degradation of β degradant for 25mg/mL BSA 4% Glycine, 1% Sucrose 10mM Tris pH 7.0 (Buffer 4) for both lyophilisation cycles over a 6 month stability period at 4°C, 25°C @ 60% Relative Humidity & 40°C @ 75% Relative Humidity. The samples were reconstituted, diluted to 1mg/mL and injected onto the HPLC (SEC) column as per section 5.9 of this project. The results were reported as % HMW degradation and plotted as a function of stability time point.

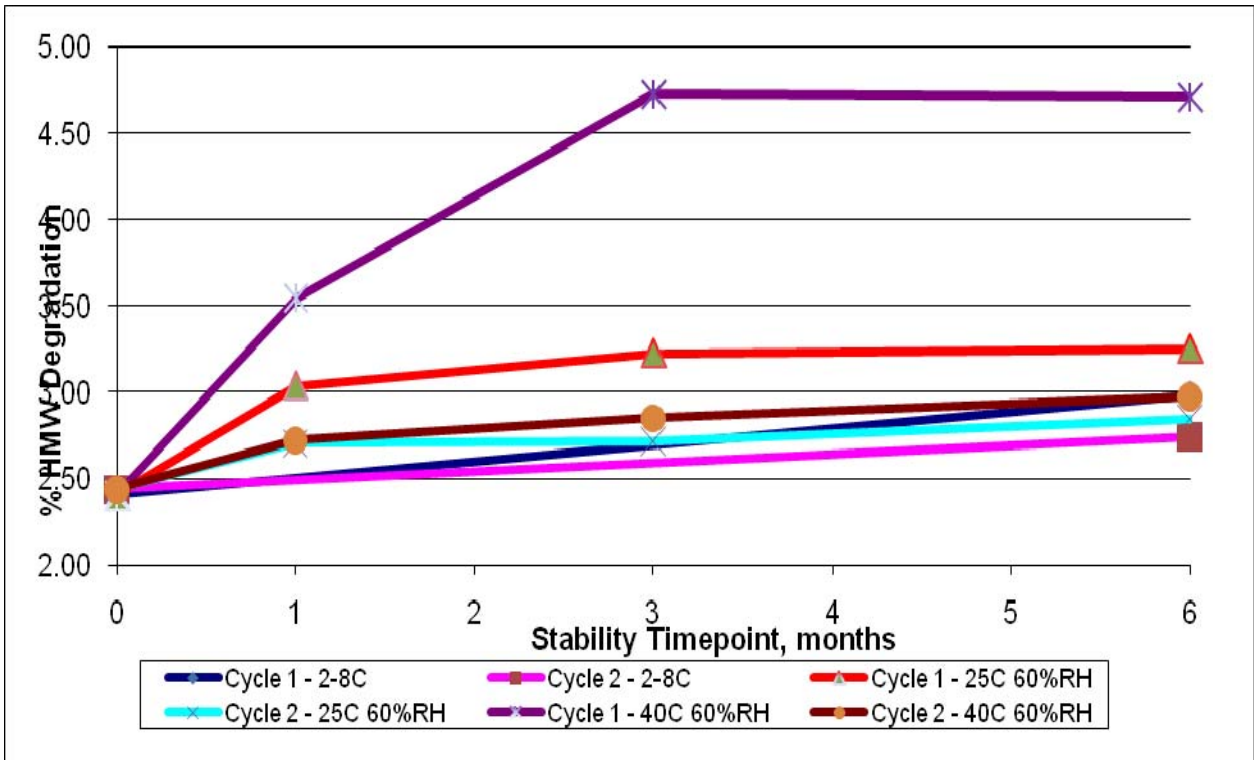

Examining Figure 38 illustrates when plotting the level of HMW degradation versus the time, a non linear relationship is observed, which has been reported (Wang et al., 2009). Note that the stability studies associated with this project was designed over a four sample point plan. Ideally, this could be increased to a minimum of 5 data points to maximize the fit when applying Arrhenius kinetics, but due to the timeframe of the study, 4 points (6 months timeframe) per formulation and storage conditions was applied.

When plotting the % level of high molecular weight (HMW) degradation versus the square root of time (known as square root of time kinetics or stretched time kinetics), it was then possible to

analyze the data in a linear fashion (Pikal et. al., 1991; Chang et. al., 2005; Franks, 2008). The degradation rate constants obtained as the slope of the straight line filling the data to equation 14:

$$HMW(t) = HMW(t_0) + k(T_i)\sqrt{t} \qquad \text{(Eq. 11)}$$

In order to calculate the % HMW as a function of time, the degradation rate constant must be calculated using the Arrhenius equation (Atkins, 2009):

$$k(T_i) = \exp(LnA - \frac{\Delta E}{RT_i}) \qquad \text{(Eq. 12)}$$

Finally, to complete the mathematical requirements, ΔE and A can be calculated by the following equations:

$$\Delta E = R(\frac{\sum_{i=1}^{n} Lnk(T_i) - nLnk(T_1)}{\frac{n}{T_1} - \sum_{i=1}^{n}\frac{1}{T_i}} \qquad \text{(Eq. 13)}$$

$$A = \exp(\frac{1}{n}(\sum_{i=1}^{n} Lnk(T_i) + \sum_{i=1}^{n}\frac{1}{T_i}(\frac{\sum_{i=1}^{n} Lnk(T_i) - nLnk(T_1)}{\frac{n}{T_1} - \sum_{i=1}^{n}\frac{1}{T_i}}))) \qquad \text{(Eq. 14)}$$

Where,

$k(T_i)$	Rate constant for the reaction (in this case protein degradation)
HMT(t)	High molecular Weight as a function of temperature
HMW (t_0)	High molecular Weight as a function of temperature at time zero
$\sqrt{t}$	Square root of time
A	Pre-exponential Factor (prefactor)
ΔE	Activation Energy
R	Gas Constant

T_i Storage Temperature at time i

Using equations 11 through the 14, the rate constant was calculated for each degradant identified for each protein formulation. Refer to tables 24 and 25 for the full set of calculated results for all protein formulations freeze dried using both cycles. Overall, protein X formulations generated one single degradant peak, represented by β, and for BSA based formulations, two degradation peaks were evident, represented by β and γ. The calculated data were normalized to allow time zero equal 0% degradation. Therefore both sets of data start at 0 on all graphs (figures 38 through 41). All subsequent data points were normalized by subtracting the actual time zero result.

Figure 39 illustrates the high molecular weight degradation (γ Degradant) for 25mg/mL BSA in buffer 4 held at storage conditions of 25°C 60%RH plotted as a function of the square root of time (Pikal et. al., 1991; Chang et. al., 2005; Franks, 2008). The normalized rate constant data seems non linear when examining figure 39 closely, however applying square root of time kinetics to the analysis of the data takes a linear analysis approach.

Fig. 39: Normalized % Degradation (γ Degradant) plot of 25mg/mL BSA 4% Glycine, 1% Sucrose 10mM Tris pH 7.0 (Buffer 4) held at Storage Conditions of 25°C 60% Relative Humidity over a 6 month period: rate constant plotted as a function of the square root of time.

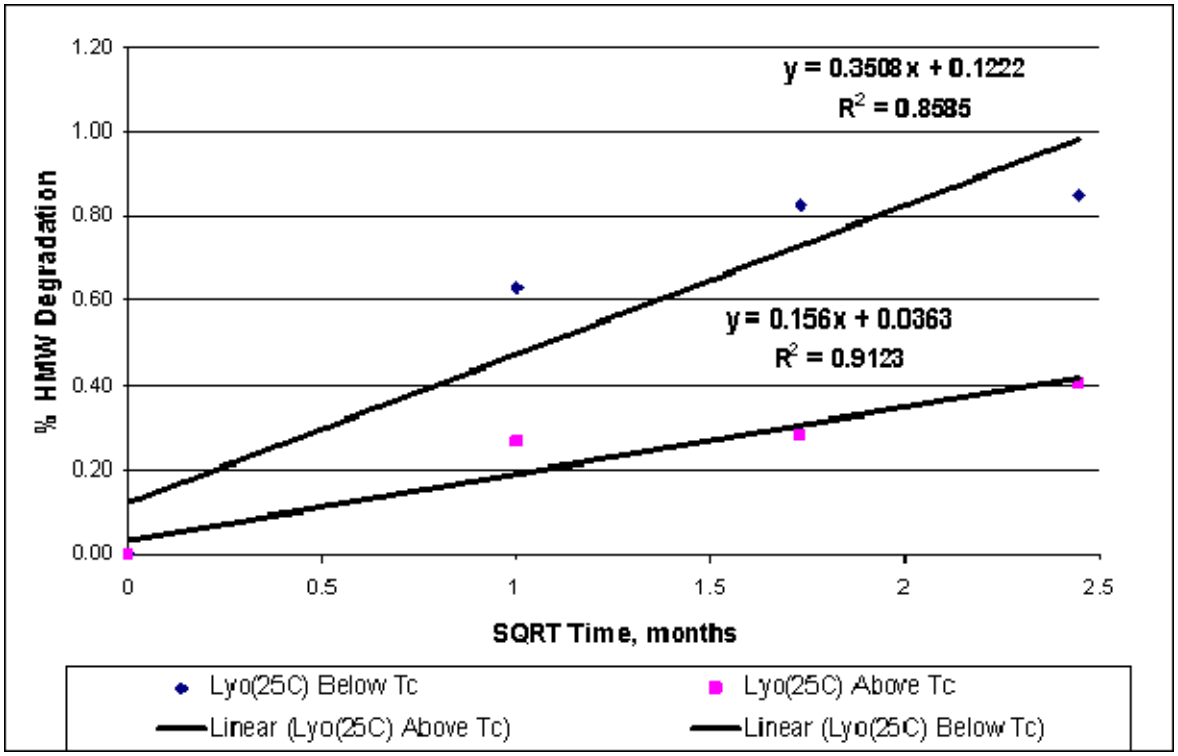

The blue points represent the rate constants calculated for the product freeze dried conservatively (below the collapse temperature) and the pink dots represent the rate constants calculated from the HMW degradation of product lyophilized above the collapse temperature. The black lines represent the linear best straight line calculated using excel, resulting in R^2 values of 0.8585 and 0.9123 respectively. The data analysis fit, especially for the data form the cycle below collapse (R^2 = 0.8585), was poor. This poses the model fit to the analysis. A poor fit may be also due to laboratory analysis error. However, from comparing the data form both cycles in figure 39, it is clear that the degradation rate of the γ degradant for the lyophilized material generated above the collapse temperature is lower for the material generated below collapse, which supports published work (Chatterjee et al., 2005; Wang et al., 2003).

Figure 40 illustrates the high molecular weight degradation (γ Degradant) as a function of the square root of time (Pikal et. al., 1991; Chang et. al., 2005) for 25mg/mL BSA in buffer 4 at held storage conditions of 40°C 75%RH over a 6 month period. Buffer 4 consisted of 4% Glycine 1% Sucrose and 10mM Tris at a pH of 7.0.

Fig. 40: Normalized % Degradation (γ Degradant) plot of 25mg/mL BSA 4% Glycine, 1% Sucrose 10mM Tris pH 7.0 (Buffer 4) held at Storage Conditions of 40°C 75% Relative Humidity over a 6 month period: Square root kinetics

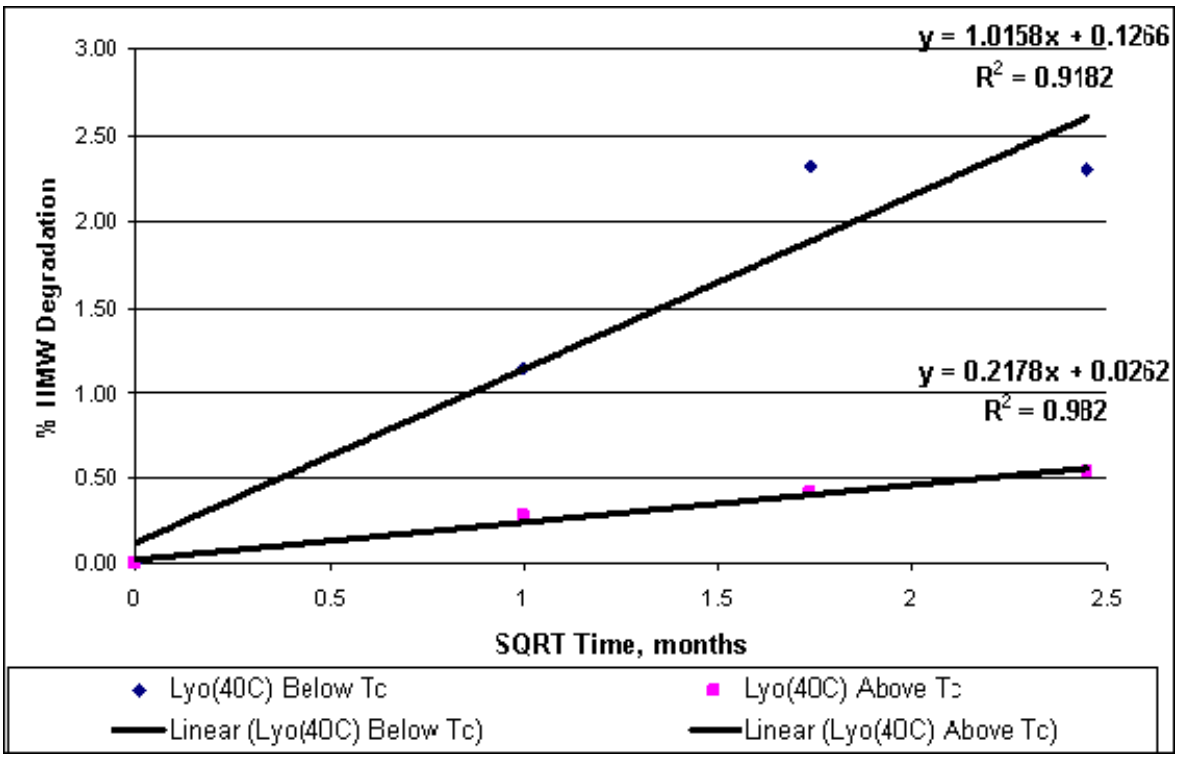

The blue points represent the rate constants calculated for the product freeze dried conservatively (below the collapse temperature) and the pink dots represent the rate constants calculated from HMW degradation of product lyophilized above the collapse temperature. The black lines represent the linear best straight line calculated using excel, resulting in R^2 values of 0.9182 and 0.982 respectively. Again, the fit for the data generated form freeze drying below collapse resulted in a poor fit. However, the data clearly shows the difference in degradation rates of the protein product generated using each of the cycles. Note also that the rate of degradation for the

β degradant (or aggregate) is much higher than the γ degradant. Examining figures 36 and 37 shows that the γ degradant rate increases at a higher rate as a function of storage conditions, in that the more aggressive the conditions, the higher the rate. This is also a factor for the β degradant (as seen on figures 41 and 42). This finding was consistent for all formulations and with both proteins excluding BSA and Buffer 3 (as can be seen on table 24).

It is evident that the rate of degradation is lower for the product resulting from processing above the collapse temperature, which is also consistent with the storage conditions of 25°C 60% relative humidity. These observations are interesting in that the suggestion may be that for this particular product and excipient formulation, drying above the collapse temperature may not be an issue from a degradative perspective. In fact, it seems that there was an improvement in protein HMW degradation.

Figure 41 illustrates the high molecular weight degradation (β Degradant) as a function of the square root of time (Pikal et. al., 1991; Chang et. al., 2005) for 25mg/mL BSA in buffer 4 at held storage conditions of 25°C 60%RH over a 6 month period. Buffer 4 consisted of 4% Glycine 1% Sucrose and 10mM Tris at a pH of 7.0.

Fig. 41: Normalized % Degradation (β Degradant) plot of 25mg/mL BSA 4% Glycine, 1% Sucrose 10mM Tris pH 7.0 (Buffer 4) held at Storage Conditions of 25°C 60% Relative Humidity over a 6 month period: Square root kinetics

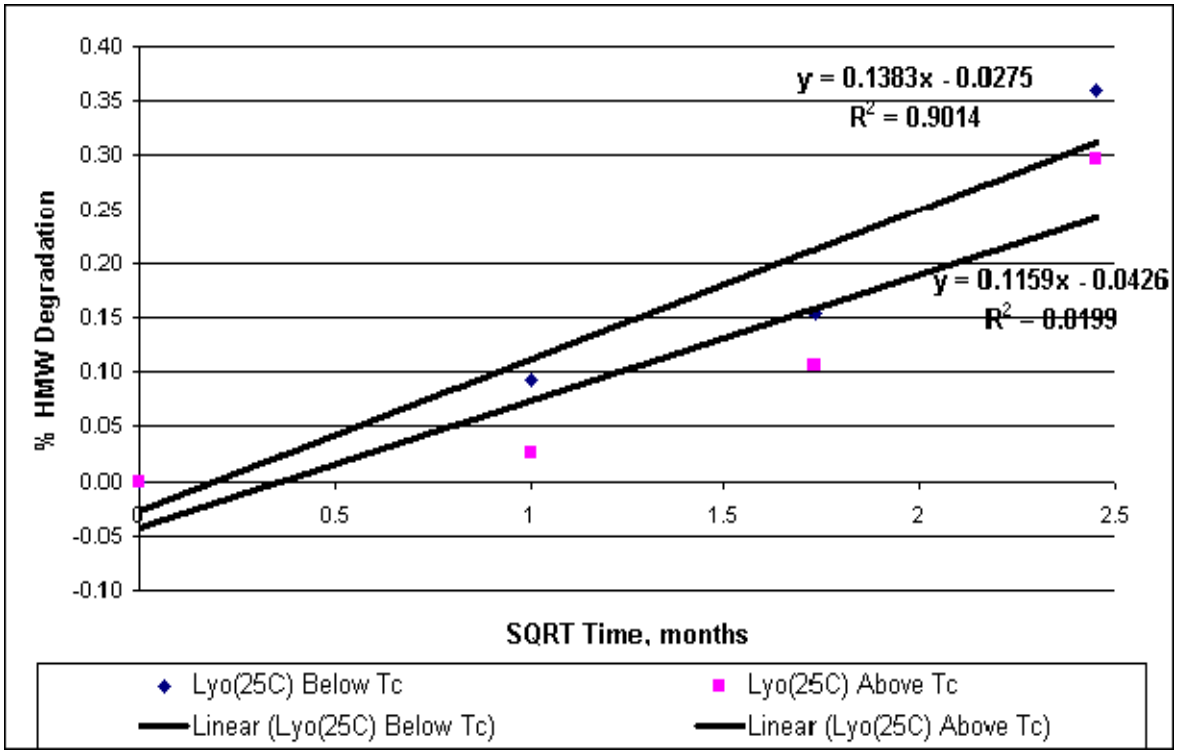

The blue points represent the rate constants calculated for the product freeze dried conservatively (below the collapse temperature) and the pink dots represent the rate constants calculated from the HMW degradation of product lyophilized above the collapse temperature. The black lines represent the linear best straight line calculated using excel, resulting in R^2 values of 0.9014 and 0.8199 respectively.

Again, it is evident that the rate of degradation is lower for the product resulting from processing above the collapse temperature. These observations are interesting in that the suggestion may be that for this particular product and excipient formulation, drying above the collapse temperature may not be an issue from a degradative perspective.

Figure 42 illustrates the high molecular weight degradation (β Degradant) as a function of the square root of time (Pikal et. al., 1991; Chang et. al., 2005) for 25mg/mL BSA in buffer 4 at held storage conditions of 40°C 75%RH over a 6 month period. Buffer 4 consisted of 4% Glycine 1% Sucrose and 10mM Tris at a pH of 7.0.

Fig. 42: Normalized % Degradation (β Degradant) plot of 25mg/mL BSA 4% Glycine, 1% Sucrose 10mM Tris pH 7.0 (Buffer 4) held at Storage Conditions of 40°C 75% Relative Humidity over a 6 month period: Square root kinetics

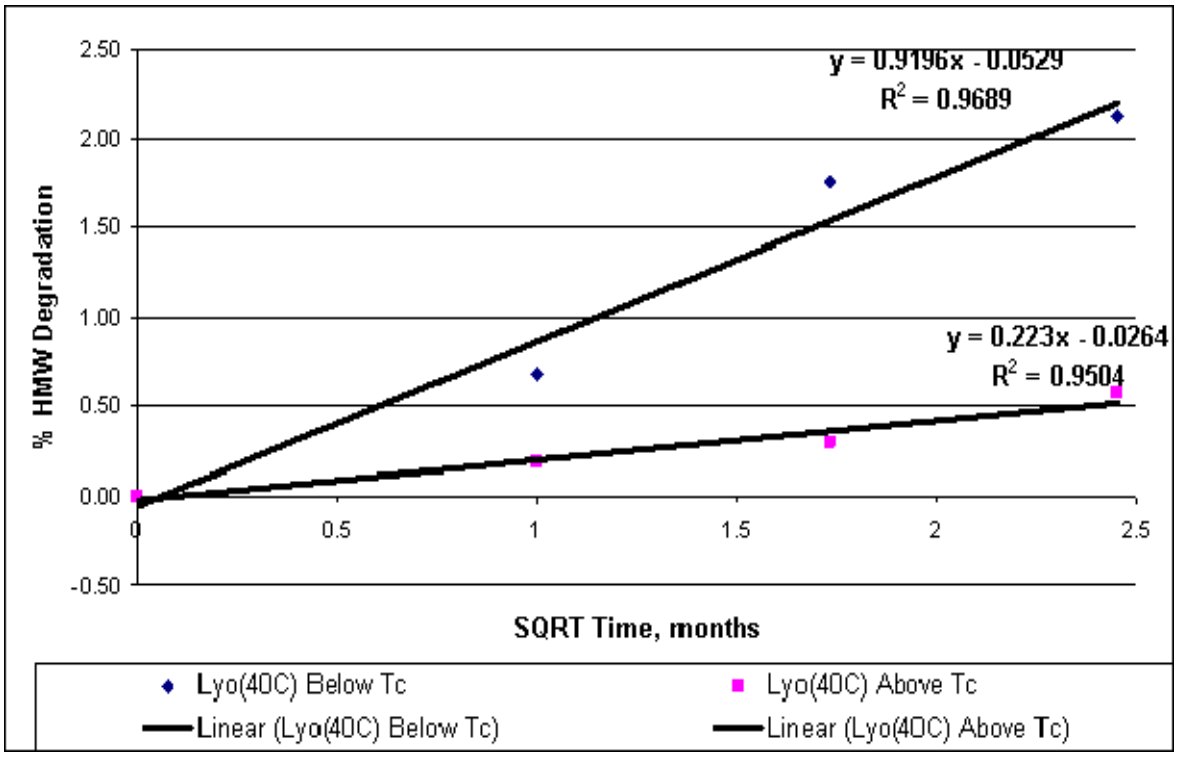

The blue points represent the rate constants calculated for the product freeze dried conservatively (below the collapse temperature) and the pink dots represent the rate constants calculated from the HMW degradation of product lyophilized above the collapse temperature. The black lines represent the linear best straight line calculated using excel, resulting in R^2 values of 0.9686 and 0.9504 respectively. The fit on figure 42 was found to be much more acceptable and shows that the model may be acceptable for analysis of the data.

Table 24 illustrates the complete set of rate constants calculated based on equations 11 through to 14 for 25°C 60% relative humidity and the 40°C 75% relative humidity stability storage conditions for the β peak high molecular weight for all formulations. The β peak eluted at approximately 7.1 minutes for protein X formulation and 8.6 minutes for all BSA based formulations.

Table 24: Rate Constants, *k*, for Storage Temperatures 2-8°C, 25°C and 40°C for up to 6 months stability for each formulation calculated using Arrhenius Kinetics calculated from actual high molecular β peak degradation

Time, months	Square Root Time	k (25°C)	k (40°C)	k (25°C)	k (40°C)
		Cycle 1		Cycle 2	
Protein X 4% Mannitol 1%Sucrose 10mM Tris (B2)					
0	0				
1	1	0.05	1.40	0.18	1.54
3	1.732050808	0.41	2.31	0.43	1.923
6	2.449489743	0.44	2.12	0.48	1.91
BSA 4% Mannitol 1%Sucrose 100mMNaCl 10mM Tris (B1)					
0	0				
1	1	0.10	0.14	0.18	0.83
3	1.732050808	0.11	0.18	0.24	0.76
6	2.449489743	0.09	0.20	0.29	0.74
BSA 4% Mannitol 1%Sucrose 10mM Tris (B2)					
0	0				
1	1	0.10	0.66	0.16	0.55
3	1.732050808	0.12	0.86	0.22	0.66
6	2.449489743	0.17	0.82	0.21	0.723
BSA 4% Glycine1%Sucrose 100mMNaCl 10mM Tris (B3)					
0	0				
1	1	0.10	0.57	0.53	0.48
3	1.732050808	0.10	0.478	0.36	0.39
6	2.449489743	0.08	0.37	0.27	0.31
BSA 4% Glycine1%Sucrose 10mM Tris (B4)					
0	0				
1	1	0.06	0.56	0.01	0.03

Table 24: Rate Constants, *k*, for Storage Temperatures 2-8°C, 25°C and 40°C for up to 6 months stability for each formulation calculated using Arrhenius Kinetics calculated from actual high molecular β peak degradation

Time, months	Square Root Time	k (25°C)	k (40°C)	k (25°C)	k (40°C)
		Cycle 1		Cycle 2	
3	1.732050808	0.13	0.978	0.01	0.09
6	2.449489743	0.12	0.79	0.06	0.12

As discussed in the previous chapters, that drying above the collapse temperature was not achieved in the Protein X formulation due to the high Tc and the difficulty in generating primary drying conditions to achieve the goal. Cycle 2 in this case dried very close to the collapse temperature so the focus is on the BSA formulations in support of the hypothesis. Note that the only formulation where the rate of degradation reduces over time was the BSA and buffer 3 formulation. This may indicate that the rate slows down as a function of time and was consistent for both cycles, indicating that the combination of Glycine and NaCl may improve stability over time.

The rate constant was not calculated for the storage conditions at 2-8°C as the rate of degradation was not found to be significant. All time 0 results indicated that the degradation was higher for the material generated from lyophilisation cycle 2 than from lyophilisation cycle 1, meaning the collapse has an initial affect on the degradation of the protein.

From examining the table 24, data to support the hypothesis proposed at the beginning of this project was available for certain formulations and at certain storage conditions. For example, for all glycine based formulations (BSA buffer 3 & 4) the rate of degradation was lower for the material processed above collapse for all storage conditions apart from the 25°C 65% humidity for BSA buffer 3. However as the 40°C condition generated stability degradation rate constant profiles proved to be in agreement with the hypothesis, it would be projected that if the stability storage profile was extended further than 6 months, the results for this particular formulation at

the conditions stated would also agree with the hypothesis that drying above the collapse temperature does not necessarily negatively affect stability of the protein. However, when focusing further on table 24, it is clear that for mannitol based formulations, the results are not as favourable. Further work is required to understand these data and concentrate on mannitol as an excipient. The only favourable result was at 40°C for BSA buffer 2, which showed a lower degradation profile for the material freeze dried above collapse, which shows some promise as 40°C 70% relative humidity is known as accelerated conditions (aggressive, worst case) in the pharmaceutical industry. Stability profiles at these storage conditions are better indicators than for lyophilized material at 2-8°C or 25°C 65% relative humidity. When examining the data further, BSA and buffer 1, which contains 100mM NaCl does not indicate and improvement on protein stability above collapse. Therefore, freeze drying above the collapse temperature during primary drying (while maintaining acceptable protein stability profiles) is dependent upon excipient selection. Excipient selection in the liquid bulk formulation is critical for optimum freeze drying (Jennings, 1999).

Table 25 illustrates the rate constants calculated for 25°C 60% relative humidity and the 40°C 75% relative humidity stability storage conditions for the γ peak high molecular weight for all BSA based formulations. The γ peak eluted at approximately 9.2 minutes for all BSA based formulations.

Table 25: Rate Constants, k, for Storage Temperatures 2-8°C, 25°C and 40°C for up to 6 months stability for each formulation calculated using Arrhenius Kinetics calculated from actual high molecular γ peak degradation (BSA formulations only as Protein X has only one degradative peak known as β)

Time, months	Square Root Time	k (25°C)	k (40°C)	k (25°C)	k (40°C)
		Cycle 1		Cycle 2	
BSA 4% Mannitol 1%Sucrose 100mMNaCl 10mM Tris (B1)					
0	0				
1	1	0.334	0.45	0.36	0.98
3	1.732050808	0.25	0.37	0.35	0.94
6	2.449489743	0.18	0.33	0.37	0.94
BSA 4% Mannitol 1%Sucrose 10mM Tris (B2)					
0	0				
1	1	0.51	1.34	0.17	0.91
3	1.732050808	0.42	1.42	0.25	0.98
6	2.449489743	0.40	1.22	0.32	0.94
BSA 4% Glycine1%Sucrose 100mMNaCl 10mM Tris (B3)					
0	0				
1	1	0.35	0.62	0.07	0.12
3	1.732050808	0.30	0.47	0.06	0.12
6	2.449489743	0.23	0.46	0.05	0.13
BSA 4% Glycine1%Sucrose 10mM Tris (B4)					
0	0				
1	1	0.09	0.67	0.03	0.19
3	1.732050808	0.09	0.99	0.06	0.17
6	2.449489743	0.14	0.92	0.12	0.22

As already discussed, it is common practise to trend and compare the degradation rate constant (k) relative to the storage condition as a function of the square root of time (Pikal et. al., 1991; Chang et. al., 2005; Wang et al., 2009). Using 25mg.mL^{-1} BSA in 4% Glycine 1% Sucrose 10mM Tris buffer as an example, the rate constant, k, for cycle 2 at 40°C was estimated at 0.222% whereas for cycle 1 it was 0.919%. From this information, it is possible to conclude that

there is evidence that the rate of degradation for the material processed above the collapse temperature is lower than that processed below the collapse temperature, based on the rate constant calculations. The finding agrees with some of the literature published (Lueckel et al., 1998; Wang et al. 2003).

Similar to the results presented in table 24, the strong argument supporting the initial hypothesis lies with the glycine based formulations and the mannitol based formulation without NaCl as an excipient (for the BSA based formulation only). The BSA formulation with NaCl and the protein X formulation (not containing NaCl but containing mannitol) shows results that do not support the hypothesis. However, the data indicates that excipient selection, as already stated, plays a key role in protecting the protein molecule when aggressively dried.

The data presented in section 7.7 supports the need for a more thorough examination around the concept of freeze drying above the collapse temperature from a high molecular weight degradative viewpoint. The two proteins selected allow a molecular weight span of 66kDa to 150KDa. From this study, both larger and smaller protein sizes should be examined, which would support this work and the work performed to date in the literature (Wang, 2000). However, to examine, in total, the effect on the protein, an investigation into the protein structure was performed. It has been shown in sample SEC chromatograms that the monomer for both proteins was present in the samples, and this was the case for all samples analysed. However, even though the monomer was evidently present, it was important to show that the tertiary structure remained in tact.

To complete the assessment, CD was used to examine changes in the tertiary structure of the protein in each formulation at time 0 and time 6 months lyophilized both below and above the collapse temperature.

7.8 CD

The circular dichroism method used may be seen in section 5.10 of this thesis and is reported by Kelly and Price, 2000. The tertiary structure of the protein molecule for each formulation

lyophilized using both cycles (section 8.6) was analysed at time 0 and time 6 months at the relevant storage conditions. Reconstitution was performed using a plastic syringe (0.5mL for the cycle 1 products and 2mL for the cycle 2 products) by injecting approximately 0.38mL (cycle 1) or 1.5mL (cycle 2) into each vial. A sample from each cycle-formulation-time point was analysed n=1 repeats to examine the tertiary structure of the protein.

Each vial from each lot was compared to the time 0 by plotting the tertiary structure on the same axis for all samples of the same formulation. It is important to know that absorbance of the liquid formulation to estimate the tertiary structure of the protein (Kelly & Price, 2000). In this case, the initial absorbance of the bulk formulation was used. There was a slight shift in the magnitude of the profile from 300nm to 250nm relative to each other, which is due to concentration differences between the samples as a result of reconstitution (Kelly & Price, 2000). As reconstitution was performed using a plastic syringe as opposed to a hamilton gas tight syringe for the purposes of this analysis, the amount of water used to reconstitute each lyophilized product may vary slightly, which likely lead to slight differences in the spectrum with respect to profile magnitude. Also, the use of the bulk A280 result as opposed to independently measuring the A280 value for each sample after reconstitution may generate variability in the profile.

For the purposes of this study, as long as the profile trended the same way, even if slightly shifted in magnitude, the tertiary structure was verified to be the same for each sample. Due to the nature of the reconstitution step, each sample may be slightly different in final concentration. The important output as part of this assay for the purposes of this project is to compare the topology of each spectrum. If there are any changes in the aromatic content and orientation of the proteins as well as the disulfide bond configuration, the topology will be different (Kelly & Price, 2000) indicating, in this case, structural differences between proteins subjected to different lyophilisation cycles and over storage time. However, the spectrum profiles replicated each other apart from this, which meant that the tertiary structure of the protein for each formulation was not affected by the change in lyophilisation cycle conditions. Importantly, this method focuses on the intact protein element and is not quantitative.

Figure 43 represents the near UV CD spectrum for protein X in TMS (buffer 2) freeze dried below the collapse temperature. It was expected that the profile would be the same for all protein X formulation samples, as drying above the collapse temperature was not achieved in this case due to the high collapse temperature and the fact that it was difficult to generate the conditions during primary drying to dry at a product temperature above the collapse temperature for this product.

Fig. 43: Near-UV CD Spectrum of 25mg/mL Protein X in 4% Mannitol 1% Sucrose 10mmM Tris Buffer at pH 7.0 from both lyophilisation cycles (Buffer 2)

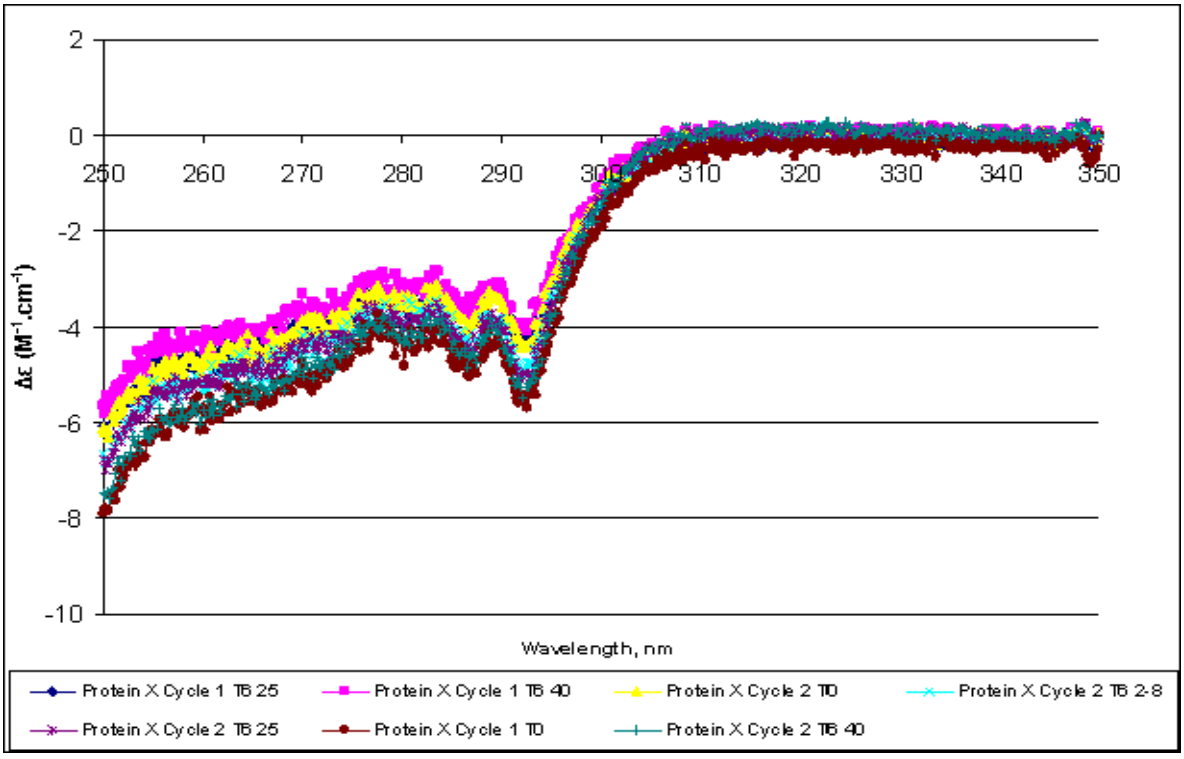

It is evident that a change in processing conditions (shelf temperature and vacuum pressure, resulting in primary drying even though both cycles were performed below the collapse temperature) during primary drying did not have an impact on the tertiary structure of the protein. This information, along with the degradation profile at 25°C and 40°C, the moisture content, reconstitution less than 1 minute and the acceptable cake appearance allows one to conclude that drying below collapse for this particular protein in this buffer matrix may not have

a negative impact on the stability of the protein post lyophilisation. In order to challenge this formulation, it would be a good idea to melt (gross collapse) the product as based on the data, drying above collapse in the virtis benchmark 1000 freeze dryer was not possible without generating conditions outside the freeze dryer capabilities.

Figure 44 illustrates all the spectra relevant to BSA in 4% Mannitol 1% Sucrose 100mM NaCl 10mM Tris buffer (Buffer 1). This spectrum represents a typical near UV BSA CR spectrum as found in the literature (Muller & Wollert, 1976).

Fig. 44: Near-UV CD Spectrum of BSA in 4% Mannitol 1% Sucrose 100mM NaCl 10mM Tris Buffer at pH 7.0 from both lyophilisation cycles (Buffer 1)

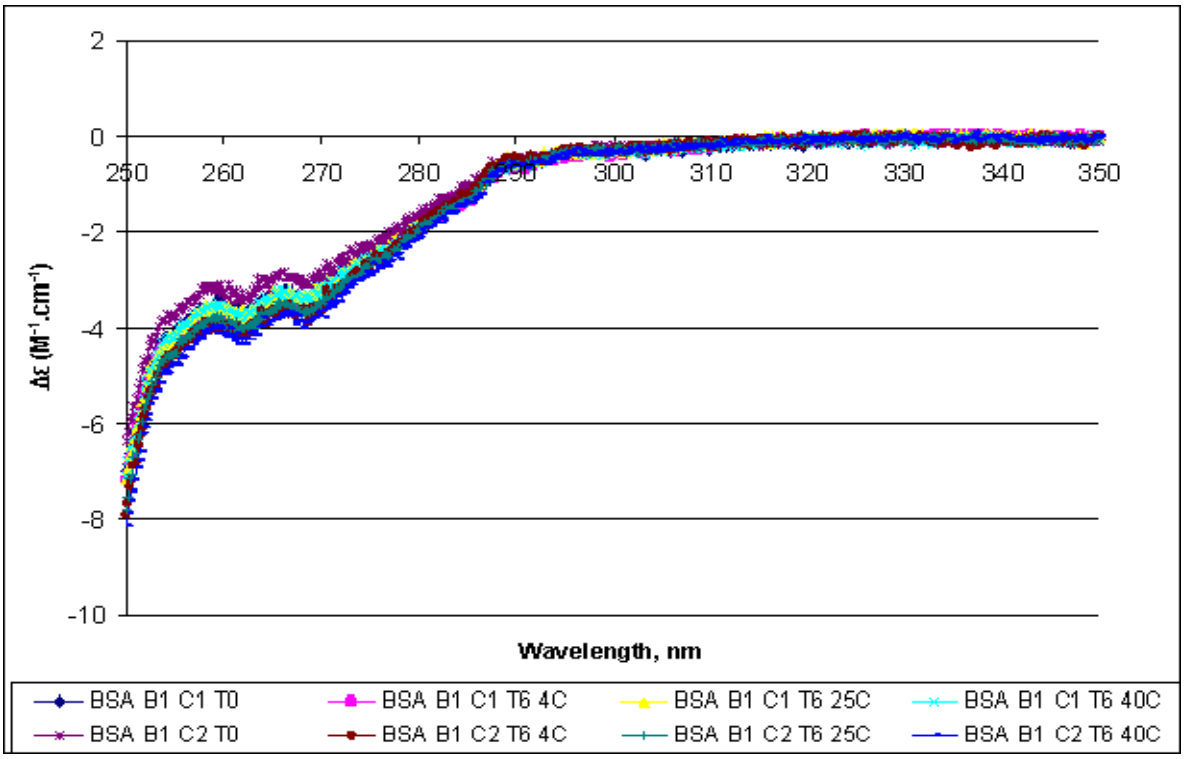

It is clear that the profile of each spectrum is consistent with each other. A slight shift in the profile was observed but each profile topology was consistent. It is evident that a change in processing conditions (shelf temperature and vacuum pressure, resulting in primary drying even though both cycles were performed below and above the collapse temperature) during primary

drying did not have an impact on the tertiary structure of the protein. This information, along with the degradation profile at 25°C and 40°C, the moisture content, reconstitution less than 1 minute and the acceptable cake appearance allows one to conclude that drying below and above collapse for this particular protein in this buffer matrix may not have a negative impact on the stability of the protein post lyophilisation.

Figure 45 illustrates all the spectra relevant to BSA in 4% Mannitol 1% Sucrose 10mM Tris buffer (Buffer 2).

Fig. 45: Near-UV CD Spectrum of BSA in 4% Mannitol 1% Sucrose 10mmM Tris Buffer at pH 7.0 from both lyophilisation cycles (Buffer 2)

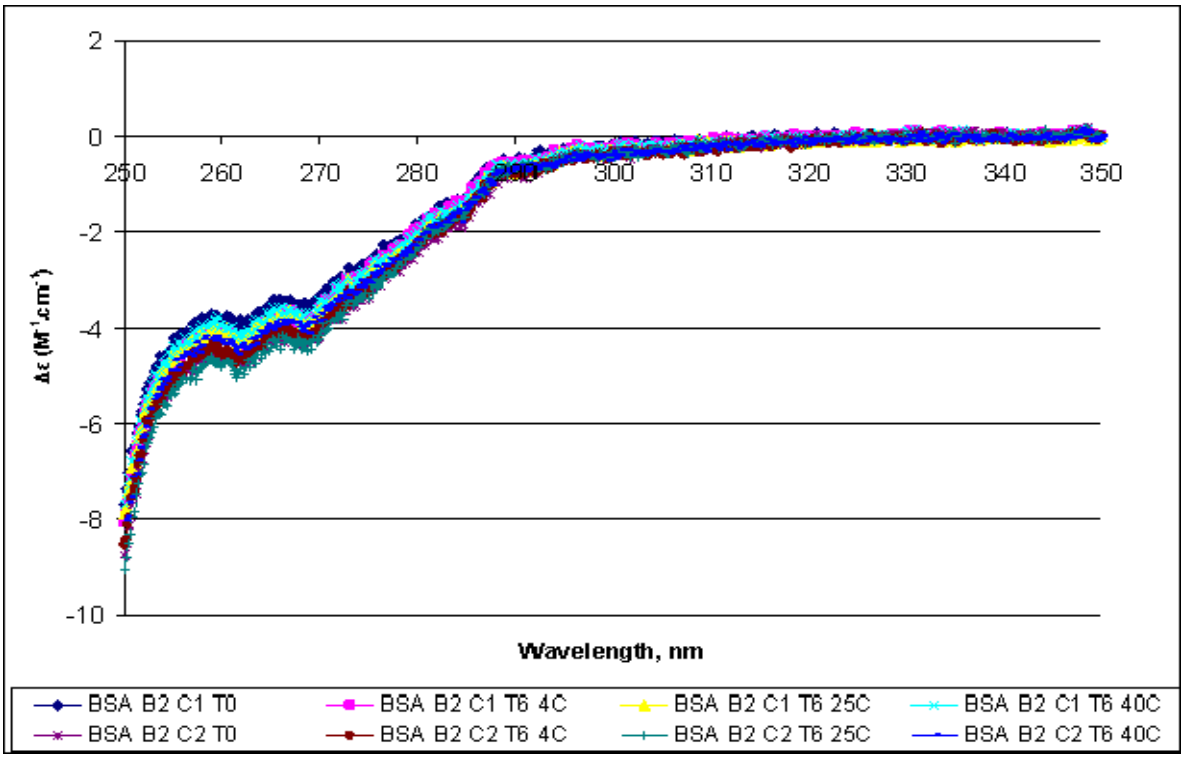

After examining the spectrum in figure 45, it is possible to arrive at the same conclusions as for figure 44.

Figure 46 illustrates all the spectra relevant to BSA in 4% Glycine 1% Sucrose 100mM NaCl 10mM Tris buffer (Buffer 3).

Fig. 46: Near-UV CD Spectrum of BSA in 4% Glycine 1% Sucrose 100mM NaCl 10mmM Tris Buffer at pH 7.0 from both lyophilisation cycles (Buffer 3)

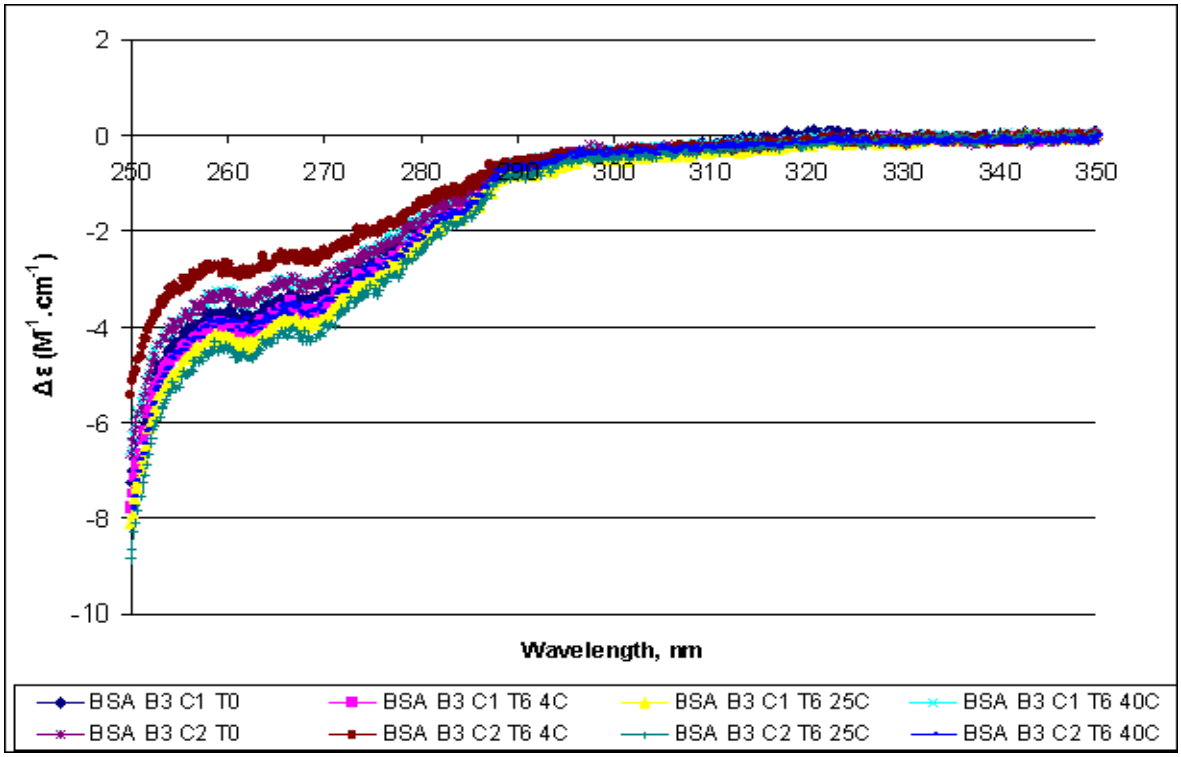

After examining the spectrum in figure 46, it is possible to arrive at the same conclusions as for figure 44.

Figure 47 illustrates all the spectra relevant to BSA in 4% Glycine 1% Sucrose 10mM Tris buffer (Buffer 4).

Fig. 47: Near-UV CD Spectrum of BSA in 4% Glycine 1% Sucrose 10mmM Tris Buffer at pH 7.0 from both lyophilisation cycles (Buffer 4)

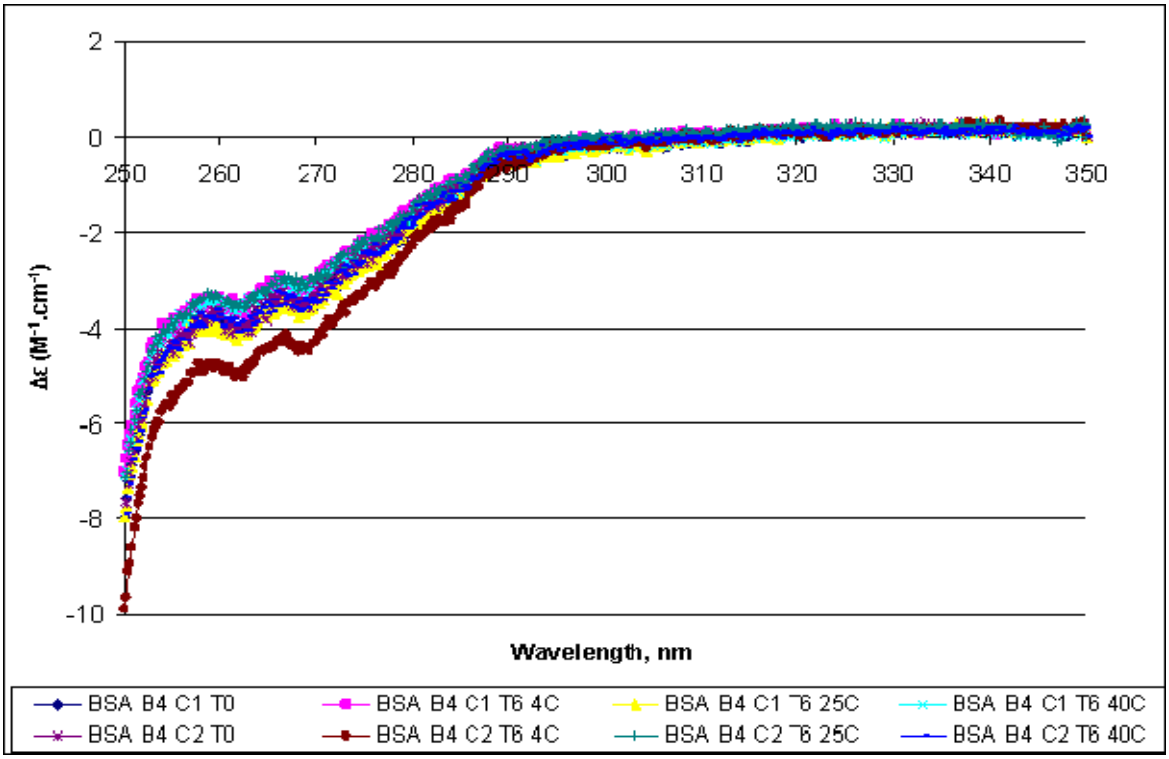

After examining the spectrum in figure 47, it is possible to arrive at the same conclusions as for figure 44.

Based on the entire set of CD results, there is no evidence of structural differences between any of the products irrespective of how they were lyophilized which means that for the two proteins in question, the aggressive lyophilisation cycle may be a possibility. This aside, drying above the collapse temperature allows companies to employ much more aggressive cycles once the characterization of the protein under these conditions has been robustly completed. The cycle time reduction on account of this allows an increase in productivity which will save and earn the company millions in the long term. The CD results show that the tertiary structure of each protein was not an issue and was not affected by primary drying conditions. Instead, the degradation rate constants are the main factors influencing the results. Therefore, across all

results for the duration of the stability profile, there is evidence that the presence of the excipient, glycine, improves the stability of the protein when freeze dried aggressively (above collapse).

8.0 AREAS FOR FURTHER INVESTIGATION

As part of this project, the initial intention was to examine the effect of collapse on the structure of the lyophilized cake other than using visual appearance and product thermocouple trending as the guide. BET (Brauner, Emmet & Teller – surface area analysis) and SEM (Scanning Electron Microscopy) were originally planned and employed but due to system issues with the BET and sampling methodology associated with SEM; these methods did not form part of the overall thesis. BET provides a quantitative measurement of surface area and SEM provides an image at the microscopic level to visually verify difference (if any). Going forward, it would be intended to use methods like BET and SEM to examine the effect of collapse on the lyophilized cake structure.

Secondly, another intention was to examine excipient crystallization in the dried powder state during stability and link these crystallization events (such as the crystallization of sucrose, NaCl, any remaining amorphous Glycine and mannitol) to the moisture change in the lyophilized cake over time and storage conditions. This would allow identifying the specific source of the moisture increase and differentiating between stopper moisture transfer and excipient crystallization as sources of moisture.

Thirdly, it was observed that foaming was a common occurrence after reconstitution of the protein product freeze dried above collapse. To examine this, protein activity and biological potency studies should be performed. The effect of protein activity or recovery was not studied as part of this project.

Lastly, it would be very beneficial to perform studies on protein freeze drying and the effect of melting on the degradation levels. To force melting, one could target drying above the gross collapse or melting temperature (which may be very difficult) or one could design a primary drying step with a time short of what would be required to effectively dry, thereby maintaining ice in the product into secondary drying.

9.0 CONCLUSION

In recent years, research has been conducted in the field of lyophilisation specific to freeze drying of protein formulations above the collapse temperature (Schersch et al., 2010; Passot et al., 2007; Wang et al., 2003; Lueckel et al., 1998; Pikal & Shah, 1990) and also in attempting to understand the impact of excipients on the ability to dry above the collapse temperature (Shalaev & Franks, 1996). As discussed in this thesis, drying above collapse has been shown to have a negative effect on protein stability (Wang et al., 2003). However, literature also suggests that this may not be true for all proteins along with the fact that excipient choice is a major factor in the ability to dry protein products aggressively (Passot et al., 2007; Schersch et. al., 2010). To examine drying above collapse and the associated variables, a project was designed allowing the examination performing primary drying at product temperatures below and above collapse temperature of protein drug products of a protein concentration of 25mg.mL^{-1}. SEC, CD, DSC and Karl Fischer were used to analytically examine the stability of five formulations consisting of 25mg.mL^{-1} protein and a combination of excipients, freeze dried below and above the specific collapse temperature of each formulation.

Freeze drying above and below the critical temperature was assessed using two model proteins consisting of either a mannitol or glycine based formulation in the presence of a variety of excipients. All bulking agents were crystallized using an annealing step during freezing, as crystalline bulking agents are known to act as structural support to lyophilized cake during the primary drying step (Shalaev & Franks, 1996). Protein X was lyophilized using only a mannitol based formulation. Protein B (Fraction V BSA, 66kDa) was lyophilized in one of four formulations which were either mannitol or glycine based.

Low temperature Differential Scanning Calorimetry and Freeze Drying Microscopy were used to characterize each liquid formulation to allow design of each lyophilisation cycle from a freezing step and primary drying step perspective. Visual appearance of the lyophilized cake and the thermal profile of the product during primary drying were used to identify any structural differences as a result of performing the primary drying step above the collapse temperature. Powder DSC was used to assess the Tg which was complemented with residual moisture data

measured by Karl Fischer. The protein tertiary structure was assessed using CD and the degradation profiles were investigated by applying SEC, where a rate constant was calculated using Arrhenius degradation kinetics by plotting the high molecular weight degradation versus the square root of time (square root kinetics). This allowed comparing the rate constant degradation of the material dried above collapse to the same product freeze dried below collapse.

A 6 month stability study was conducted, applying the majority of the above named analytical test methods, at storage conditions of 4°C, 25°C 60% Humidity, 40°C 75% Humidity along with ICH guidelines. All protein concentrations were targeted at 25mg.mL^{-1} throughout all formulations.

The majority of glycine based formulations lyophilized above the collapse temperature showed better initial time 0 degradation profiles than the product resulting form the lyophilisation cycles where primary drying was conducted below the collapse temperature. This information is significant and point to supporting the hypothesis that collapse may not negatively affect protein stability to the same effect as once thought (Schersch et al., 2010; Passot et al., 2007; Shalaev & Franks, 1996) for certain combinations of excipients in the presence of high protein concentrations. Interestingly, for the glycine based formulation in the presence of sodium chloride; the degradation rate seemed to improve as a function of time based on the calculated rate constants. All lyophilized products assessed for protein tertiary structure conformation using CD were consistent through all lyophilisation cycles and stability time points indicating that the effect of drying above collapse had no effect on the stability of the protein formulations in question used as part of this thesis.

A potential hypothesis for the ability to freeze dry above the collapse temperature may lie with the crystallization of the amorphous bulking agent during freezing. The crystalline excipient provides support to the dried matrix, allowing more aggressive drying without compromising stability (Pikal & Shah, 1990; Shalaev & Franks, 1996). The crystallization of the bulking agent during collapse could increase the local Tg temperature restricting mobility in amorphous phase that lead to degradation.

Consistent with literature data (Pikal & Shah, 1990), freeze-drying above collapse resulted in longer reconstitution time. The protein product generated from performing primary drying below the collapse temperature showed near immediate reconstitution of 2-4 seconds. However for material processed above the collapse temperature, depending on the formulation, reconstitution took up to 1 minute. All material that was lyophilized above the collapse temperature exhibited foaming. This may in fact be actual protein, which may lead to issues with the recovery of protein generated in this way. Future work needs to verify what protein recovery post lyophilisation would look like as a function of drying above collapse.

This data indicated that performing lyophilisation above the collapse temperature may not be as major an issue as first thought. These data generally supports current literature (Passot et al, 2007; Wang et al, 2003; Schersch et. al., 2010) at higher and more anticipated protein concentrations that would be common when dealing with parenteral products.

Further work that may be conducted to supplement this project may be in the form of an assessment of the effect of multiple bulking agents and excipients (both crystalline and amorphous) by investigating protein stability as a result of performing primary drying above the gross collapse or Tm. However, achieving this depends on heat transfer and the capability of the freeze dryer.

REFERENCES

Adams G. D. J. and Ramsay, J. R. 1996. Optimizing the Lyophilisation cycle and the Consequences of Collapse on the Pharmaceutical Acceptability of *Erwina* L-Asparaginase. J. Pharm Sci., 12: 1301-1305.

Akers, M. J., Milton, N., Byrn, S. R., Nail, S. L. 1995. Glycine crystallization during freezing: the effect of salt form, pH, and ionic strength. Pharm. Res., 12: 426-430.

ASTM. 1991. Standard Test Method for Assignment of the Glass Transition Temperatures by Differential Scanning Calorimetry or Differential Thermal Analysis. pp1356-1391

Atkins, P. 2009. Elements of Physical chemistry 5th Edition, Oxford University Press

Bam, L. N. et al. 1995. Stability of Protein Formulations: Investigation of surfactant effects by a novel EPR spectroscopic technique. Pharm. Res., 12: 2-11.

Bellows, R. J. & King, C. J. 1972. Freeze-Drying of aqueous solutions: Maximum allowable operating temperature. Cryobiology, 9: 559-561.

Bindschaedler, C. 1999. Lyophilisation process validation. [In: Rey, L., May, J. C. (Eds.), Freeze Drying/ Lyophilisation of Pharmaceutical and Biological Products, 1999], vol. 96. Marcel Dekker, New York, pp. 373-408.

Breen, E.D. et al. 2001. Effect of moisture on the stability of a lyophilized humanized Monoclonal Antibody Formulation, Pharm Res., 18: 1345-1353

Carpenter, J. F. et al. 1997. Rational Design of Stable Lyophilized Protein Formulations: Some Practical Advice. Pharmaceutical Research, 14(8): 969-975

Chatterjee, K e. al. 2005. Partially Crystalline Systems in Lyophilization: II. Withstanding Collapse at high Primary Drying temperatures and the impact on Protein Activity recovery. J. Pharm. Sci. 94(4), 809-820.

Colandene, J. et al. 2006. International Patent Classification A61K 38/17. Publication Number WO 2006/081320

Creighton, T. E. 1993. Proteins: Structures and Molecular properties, 2nd edition; W. H. Freeman and Company: New York

Dixon, D. et al. 2008. The Impact of protein Concentration on Mannitol and Sodium Chloride Crystallinity and Polymorphism upon Lyophilisation. J. Pharm. Sci., 98: 3419-3429

Dudde, S. P. & Dal Monte, P. R. 1997. Effect of Glass Transition Temperature on the Stability of Lyophilized Formulations Containing a Chimeric Therapeutic Monoclonal Antibody. Pharm. Res., 14(5): 591-595

Dushman, S. and Lafferty, J. M., 1962. Scientific foundations of vacuum technique, John Wiley and sons, Inc., New York, 2nd edition.

Franks, F. 1997. Freeze Drying of bioproducts: Putting principles into practice. European journal of Pharmaceutics and BioPharmaceutics., 45: 221-229.

Franks, F. 1991. Freeze Drying: From empiricism to predictability. The significance of glass transitions. Dev. Biol. Std., 74: 9-19

Franks F. 2008. Freeze-drying of Pharmaceuticals and Biopharmaceuticals: Principles and Practice. Royal Society of Chemistry.

Fransson, J.; Florin-Robertsson, E.; Alexsson, K.; Nyhlen, C. 1996. Oxidation of human insulin-like growth factor I in formulation studies: Kinetics of methionine oxidation in aqueous solution and in solid state. Pharm. Res., 13: 1252-1257.

Hageman, M. J. 1988. The role of moisture in protein stability. Drug. Dev. Ind. Pharm., 14: 2047-2070.

Hageman, M. J. 1992. Water sorption and solid-state stability of proteins. In *Stability of Protein Pharmaceuticals, Part A: Chemical and Physical pathways of protein degradation*. (Ahern, T. J., Manning, M. C., Eds.) Plenum Press. New York. pp. 273-309.

Hagen, S. J. et al. 1995. Protein reaction kinetics in a room temperature glass. Science, 269 : 959-962

Hunter, A. K. & Carta, G. 2001. Effects of bovine serum albumin heterogeneity on frontal analysis with anion-exchange media. J. Chromatography. A., 937: 13-19

Izutsu, K., Yoshioka, S., Terao, T. 1993. Decreased protein stabilizating effects of cryoprotectants due to crystallization. Pharm. Res., 10: 1232-1237

Jennings, T. A. 1999. Lyophilisation: Introduction and Basic Principles. Interpharm Press, Colorado, USA

Jennings, T. A., Duan, N. 1995. Calorimetric monitoring of Lyophilisation. J. Parent. Sci. Technol., 49 : 272-282.

Kelly, S. M. & Price, N. C. 2000. The use of Circular Dichroism in the Investigation of Protein Structure and Function Current Protein and Peptide Science. 1 : 349-384

Kuu, W. Y. et al. 1995. Determination of Mass Transfer coefficients during freeze drying using modeling and parameter estimation techniques. Int. J. Pharm., 124: 241-252.

Lai, M. C. and Topp, E. M. 1999. Solid-State Chemical Stability of Proteins and Peptides. J. Pharm. Sci., 88(5): 489-500.

Leuckel et al. 1998. Effects of Formulation and Process Variables on the Aggregation of Interleukin-6 (IL-6) after Lyophilization and on Storage, Pharm. Dev. Technol., 3(3): 337-346

Levine, K.; Slade, L. 1993. The glassy state phenomenon in food molecules. [In The glassy state in foods] Blanshard, J. M. V., Lillford, P. J., Eds.; Nottingham Press: Nottingham, pp. 35-101.

Li, S.; Patapoff, T. W.; Overcashier, D.; Hsu, C.; Nguyen, T. H.; Borchardt, R. T. 1996. Effects of Reducing Sugars on the chemical stability of Human Relaxin in the lyophilized state. J. Pharm. Sci., 85: 873-877.

Mackenzie, A. P. 1976. The Physico-Chemical basis for the Freeze-Drying Process. International Symposium on Freeze-Drying of biological products, Washington, D.C. Develop. Biol. Std., 36: 51-67.

Manning, M. C.; Patel, K.; Borchardt, R. T. 1989. Stability of Protein pharmaceuticals. Pharm. Res., 6: 903-918.

Meister, E. & Gieseler, H. 2009. Freeze Drying Microscopy of Protein/ Sugar Mixtures: Drying Behavior, Interpretation of Collapse Temperatures and a comparison to corresponding Glass Transition data. J. Pharm. Sci.98 (9): 3072-3087

Muller, W. E. & Wollert, U. 1976. Interaction of Benzodiazepine Derivatives with Bovine Serum Albumin – II. Circular Dichroism Studies. Bioch. Pharm., 25: 147-152

Nail, S. L et. al. 2002.Fundamentals of Freeze Drying [In Development and Manufacture of Protein Pharmaceutical]. Edited by S. Nail and M. Akers. Academic/ Plenum Publishers, New York, pp. 281-359.

Nail, S. L., Johnson, W. 1992. Methodology for in-process determination of residual water in freeze-dried products. Dev. Biol. Std., 74: 137-150

Nail, S. et al., 1994. An Improved Microscope Stage for Direct Observation of Freezing and Freeze Drying. Pharm. Res., 11 (8): 1098-1100

Nail, S.L. 1980. The effect of pressure on the heat transfer in the freeze-drying of parenteral solutions. J. Parenter. Drug Assoc., 34: 358.

Oliyai, C.; Patel, J.; Carr, L.; Borchardt, R. T. 1994. Solid-State stability of lyophilized formulations of an asparanaginyl residue in a model hexapeptide. J. Parenteral Sci. Technol., 48: 67-173.

Overcashier, D.E., Patapoff, T.W., Hsu C.H. 1999. Lyophilisation of Protein Formulations in vials: Investigation of the relationship between Resistance to Vapour Flow during Primary Drying and Small-Scale Product Collapse. J. Pharm. Sci., 88: 688-695.

Passot, S. et al. 2007. Effect of Product Temperature during Primary Drying on the Long-Term Stability of Lyophilized Proteins. Pharm. Dev. Technol., 12(6): 543-533

Patapoff, T. W. and Overcashier, D. E. 2002. The Importance of Freezing on Lyophilisation Cycle Development. BioPharm., 15(3): 16-21.

Patel, S. et al. 2010. Determination of End Point of Primary Drying in Freeze Drying Process Control. AAPS PharmSciTech. 11(1), 73-84.

Pikal, M. J. & Shah, 1992. S. Moisture transfer from stopper to product and resulting stability implications. Dev. Biol. Std. 74: 165-77, discussion 177-9.

Pikal, M. J.1990a. Freeze-Drying of proteins. Part I: process design. BioPharm., 3(8): 18-27.

Pikal, M. J. 1990b. Freeze-Drying of proteins. Part II: formulation selection. BioPharm., **1**3(9): 26-30.

Pikal, M. J., Dellerman, K., Roy, M. L. 1991. Formulation and Stability of Freeze Dried Proteins: Effects of Moisture and Oxygen on the Stability of Freeze-dried Formulations of Human Growth Hormone. [In International Symposium on Biological Product Freeze-Drying and Formulation]; May, J. C., Brown, F., Eds, Karger: Basel, Vol. 74, pp21-38

Pikal, M. J., Roy, M. L., Shah, S. 1984. Mass and Heat Transfer in vial freeze-drying of pharmaceuticals – the role of the vial. J. Pharm. Sci., 73: 1224-1237.

Pikal, M. J., Shah, S., Roy, M. L., Putman, R. 1990 The Secondary drying stage of Freeze Drying: drying kinetics as a function of temperature and chamber pressure. Int. J. Pharm., 72: 203-217.

Pikal, M. J., Shah, S., Senior, D., Lang, J. E. 1983. Physical Chemistry of freeze-drying: measurement of sublimation rates for frozen aqueous solutions by a microbalance technique. J. Pharm. Sci., 72: 635-650.

Pikal, M.J., Shah, S. 1990. The collapse temperature in freeze-drying: dependence on measurement methodology and rate of water removal from the glassy phase. Int. J. Pharm., 62: 165-168.

Pikal, M.J. 1985. Use of laboratory data in Freeze Drying process design: Heat and Mass Transfer coefficients and the computer simulation of Freeze Drying. J. Parent. Sci. Technol., 39 (3): 115-139.

Rambhatla, S., Pikal, M. J. 2003. Heat and Mass Transfer issues during Freeze Drying, I: Atypical Radiation and the vial edge effect. AAPS PharmSciTech., Article 14.

Rambhatla, S., Ramot, R., Bhugra, C., Pikal, M. 2004. Heat and Mass Transfer issues during Freeze Drying, II: Control and Characterization of the degree of supercooling. AAPS PharmSciTech., 5(4): Article 4.

Randolph, T. W., Searles, J. A. 2002. Freezing and Annealing Phenomena in Lyophilisation: Effects upon Primary Drying Rate, Morphology and Heterogeneity. Am. Pharm. Review., 5(4): 40-46.

Rey, L. C.; May, J. C. 1999. Freeze Drying/ Lyophilisation of pharmaceutical and biological products; Marcel Dekker, Inc. New York,

Roy, I., Gupta, M. N. 2004. Freeze-Drying of Proteins: Some emerging concerns. Appl. Biochem., 39: 165-177.

Schersch K. et. al. 2010. Systematic Investigation of the effect of Lyophilizate Collapse on Pharmaceutically Relevant Proteins I: Stability after Freeze Drying. J. Pharm. Sci., 99(5): 2256-2277

Searles, J. A., Carpenter, J. F., Randolph, T. W. 2001a. Annealling to Optimize the Primary Drying Rate, Reduce Freezing-induced Drying Rate Heterogeneity, and determine Tg' in Pharmaceutical Lyophilisation. J. Pharm. Sci., 90(7): 872-877.

Searles, J. A., Carpenter, J. F., Randolph, T. W. 2001b. The Ice Nucleation Temperature Determines the Primary Drying Rate of Lyophilisation for Samples Frozen on a Temperature-Controlled Shelf. J. Pharm. Sci., 90(7): 860-871.

Shalaev, E. Y.; Franks, F. 1996. Changes in the physical state of model mixtures during freezing and drying: Impact on product quality. Cryobiology., 33: 14-26

Tang, X., Pikal, M. J. 2004. Design of Freeze-Drying Processes for Pharmaceuticals: Practical Advice. Pharm. Res., 21(2): 191-200.

Tchessalov, S. 2008. Lyophilisation of Pharmaceuticals: Cycle Robustness and process tolerances transfer and scale up. Eur. Pharm. Rev., 3: 76-83

Tchessalov, S. 2010. LYOPHILIZATION ABOVE COLLAPSE - methods of lyophilizing a pharmaceutical substance involving a primary drying step executed at a product temperature at US Patent Application Number 20100041870

Tsourouflis, S et al. 1976. Loss of structure in Freeze dried Carbohydrates Solutions: effect of Temperature, Moisture Content and Composition. J. Sci. Fd Agric., 27: 509-519

Wang, B. et al. 2009. Impact of Sucrose level on Storage Stability of Proteins in Freeze Dried Solids: II. Correlation between Aggregation Rate with Protein Structure and Molecular Mobility. J. pharm. Sci., 98(9): 3145-3166

Wang, D.Q. et al., 2003. Effect of Collapse on the Stability of Freeze-Dried Recombinant Factor VIII and α-Amylase. J. Pharm. Sci., 93(5): 1253-1263

Wang, W. 2000. Lyophilisation and development of solid protein pharmaceuticals. Int. J. Pharm., 203: 1-60.

Xiang, J et al. 2004. Investigation of Freeze-Drying sublimation rates using a freeze-drying microbalance technique. Int. J. Pharm., 279: 95-105.

Xie, M. & Schowen, R. L. 1999. Secondary Structure and Protein Deamidation. J. Pharm. Sci., 88(1): 8 - 13